

**State Water Survey Division**  
ATMOSPHERIC CHEMISTRY SECTION  
AT THE  
UNIVERSITY OF ILLINOIS



SWS Contract Report 252

**STUDY OF ATMOSPHERIC POLLUTION  
SCAVENGING**

*Nineteenth Progress Report*  
*Contract Number DE - AC02 - 76EV01199*

*May 1981*

*Authors:*

Richard G. Semonin  
Van C. Bowersox  
Donald F. Gatz  
Mark E. Peden  
Gary J. Stensland

*Sponsored by:*  
*United States Department of Energy*  
*Pollutant Characterization and Safety Research Division*  
*Office of Health and Environmental Research*  
*Washington, DC*

*Richard G. Semonin*  
*Principal Investigator*



## TABLE OF CONTENTS

	<u>Page</u>
ABSTRACT-----	v
CHAPTER 1: Summary of Sulfate and pH for SCORE-79-----	1
INTRODUCTION-----	1
RESULTS AND DISCUSSION-----	1
CHAPTER 2: Reproducibility of Aerosol Samples Collected on Nuclepore Filters Under Inverted Funnel Rain Shields-----	7
INTRODUCTION-----	7
EXPERIMENTAL METHODS-----	7
RESULTS-----	8
DISCUSSION-----	12
REFERENCES-----	12
CHAPTER 3: Comparison of Two Sampling Methods for Medium-Volume Aerosol Sampling-----	15
INTRODUCTION-----	15
SAMPLER DESIGN-----	15
EXPERIMENTAL METHODS-----	17
RESULTS AND DISCUSSION-----	17
CONCLUSIONS-----	22
REFERENCES-----	23
CHAPTER 4: Comparison of Total Versus Soluble Data for Ambient Aerosol Filter Samples-----	24
INTRODUCTION-----	24
EXPERIMENTAL PROCEDURE-----	24
Technique to Determine Soluble Components-----	25
Technique to Determine Total Elements-----	25

	<u>Page</u>
RESULTS AND DISCUSSION-----	25
REFERENCES-----	29
 CHAPTER 5: Investigation of Multivariate Statistical Methods for Estimating Background Lithium in Precipitation Tracer Experiments-----	30
INTRODUCTION-----	30
THEORY-----	30
SELECTION OF A DATA SET FOR THE PREDICTION EQUATION-----	30
General Method Development-----	30
Prediction Using Subsets of Individual Experiments-----	35
Preliminary methods testing-----	35
Selection of subsets of collectors-----	40
CONCLUSION-----	46
REFERENCES-----	46
 CHAPTER 6: Design of a Feasibility Study to Assess the Impact of Pre- cipitation Quality on Soil Water Quality-----	49
INTRODUCTION-----	49
EXPERIMENT DESIGN-----	49
SUMMARY-----	52
REFERENCES-----	52
 CHAPTER 7: A New Search for Old Evidence to Identify Trends in the Chemistry of Precipitation in the Continental United States---	54
INTRODUCTION-----	54
SUMMARY OF SEARCH-----	54
REFERENCES-----	55

	<u>Page</u>
CHAPTER 8: Seasonal Precipitation Concentrations and Depositions for North American from the CANSAP/NADP Networks-----	56
INTRODUCTION-----	56
DATA SOURCES AND SAMPLING LIMITATIONS-----	56
CANSAP Network-----	56
NADP Network-----	57
SEASONAL AND ANNUAL DATA ANALYTICAL PROCEDURES-----	57
SEASONAL CONCENTRATION DISTRIBUTIONS-----	58
Calcium-----	58
Ammonium Concentration-----	63
Nitrate Concentration-----	63
Sulfate Concentration-----	63
Measured pH Distribution-----	75
Discussion of Concentration Distributions-----	75
SEASONAL DEPOSITION DISTRIBUTIONS-----	82
Calcium Deposition-----	82
Ammonium Deposition-----	86
Nitrate Deposition-----	86
Sulfate Deposition-----	94
Hydrogen Ion Deposition Distribution-----	101
Discussion of Deposition Distributions-----	101
ANNUAL CONCENTRATION AND DEPOSITION DISTRIBUTIONS-----	101
Precipitation Distribution-----	106
Calcium Concentration and Deposition-----	106
Ammonium Concentration and Deposition-----	106
Nitrate Concentration and Deposition-----	118
Sulfate Concentration and Deposition-----	118
pH and Hydrogen Ion Deposition-----	118
Discussion of the Annual Concentration and Deposition Distribution-----	119
REFERENCE-----	119

	<u>Page</u>
CHAPTER 9: A New Sequential Rainwater Sampler-----	120
INTRODUCTION-----	120
Description and Evaluation of the Instrument-----	120
PRELIMINARY SEQUENTIAL DATA RESULTS-----	123
Conclusion-----	123
Acknowledgements-----	126
APPENDIX, Reports, Reprints, and Preprints	

## ABSTRACT

The very dense SCORE network of samplers was used to analyze the spatial variability of sulfate concentration and pH in convective precipitation. All available data from each site for the 1979 field experiment were included in the analysis. The sulfate values varied between 0.5 and 15 mg/L or by more than a factor of 30. The range of median values for the data set was 1.7 to 4.7 mg/L or a factor of 2.8. The range of pH values was 3.3 to 7.4 for all data, but for heavier rainfalls the range was 3.4 to 7.1. The median pH for all data was about 4.3.

Fourteen pairs of aerosol samples were obtained to examine the reproducibility of sample collection and analysis. Good agreement was found for Si, S, K, Ca, Fe, and TSP and poorer agreement for Ti, Mn, Zn, Br, and Pb. However, statistical analyses reveals that the agreement is clearly less than desired. Some possible explanations for the discrepancies are offered, but additional experiments are needed to clarify this problem for addressing spatial variability problems.

A comparison was carried out between an inverted funnel aerosol collection method and an isokinetic sampler free to move with the wind. The data shows that the isokinetic sampler collects more aerosol for the 11 elements analyzed and TSP than the inverted funnel. The isokinetic/funnel ratio ranged from 1.05 for S to 1.32 for Si and Ti. This finding must now be placed in the context of its impact on scavenging ratio calculations.

An attempt was made to determine the soluble/insoluble ratio for Ca, K, and S of daily aerosol samples. The total concentration was found by ion-excited X-ray fluorescence while the soluble contribution was determined by flame atomic absorption and automated colorimetric methods. The results are inconclusive and a number of possible problems need to be explored before quantitative values will be available.

Statistical methods to estimate background lithium in tracer experiments were used to help predict the deposition patterns. The principle components regression did not yield a result useful to estimate scavenging efficiency. The primary useful result is that the background concentration of any tracer must be carefully assessed in designing future experiments and the methods development points the direction that such assessments must take.

Using combined data sets from the NADP and CANSAP networks, descriptive maps of calcium, ammonium, nitrate, sulfate and pH were prepared. Seasonal and annual distributions are shown for the data period July 1978 through September 1980.

The evaluation of a newly designed sequential sampler for precipitation chemistry was carried out in a field experiment in 1980. The results are quite promising although some minor changes will be made as a result of the evaluation prior to construction of additional units.

## CHAPTER 1

### SUMMARY OF SULFATE AND pH FOR SCORE-79

Gary J. Stensland

## INTRODUCTION

The field measurements for the Summer Chemistry Of Rain Experiment for 1979 (SCORE-79) began on 26 July and ended on 11 August, 1979. The major objective of SCORE-79 was to assess the surface rainfall chemistry variability. A second objective was to relate this variability to cloud parameters, air quality measurements on the ground and from airplanes, chemical source characteristics, and other meteorological measurements.

The location of the summer 1979 precipitation chemistry samplers is shown in Fig. 1, with the Pacific Northwest Laboratory (PNL) bulk samplers being operated only from 9 July to 28 July. The large square box in Fig. 1 encompasses the recording raingage network. In Fig. 1, the dense north-south line of wet/dry samplers (59-166) provided small time and space scale cases such as were sampled in SCORE-78. The rest of the precipitation chemistry sites in Fig. 1 were designed to provide data on larger scales of several kilometers in space and a few hours in time.

The wet-side of the wet/dry sampler was changed within 24 hours of the end of a precipitation event. The dry-side was changed much less frequently. Only wet-side data will be discussed in this chapter.

## RESULTS AND DISCUSSION

The SCORE-79 sulfate data for the wet/dry samples are summarized in Fig. 2. The top half of Fig. 2 includes the data from the dense sampling line in order of site location from north to south along the abscissa. On some rain days the dense line was serviced two or three times as the lines of showers would pass and then be separated from the next shower line by an hour or more. The remaining wet/dry sites were usually serviced only once on any given rain day and thus the total number of samples for the sites on the bottom half of Fig. 2 is generally lower than for the densely spaced sites.

The sulfate values on Fig. 2 vary from less than 0.5 mg/L to greater than 15 mg/L, or by more than a factor of 30. At site 148 the maximum value was 12 mg/L and the minimum value was about 0.5 mg/L for a variation of a factor of 24 at a site. The extremely high  $\text{SO}_4$  values were usually associated with very small volume samples.

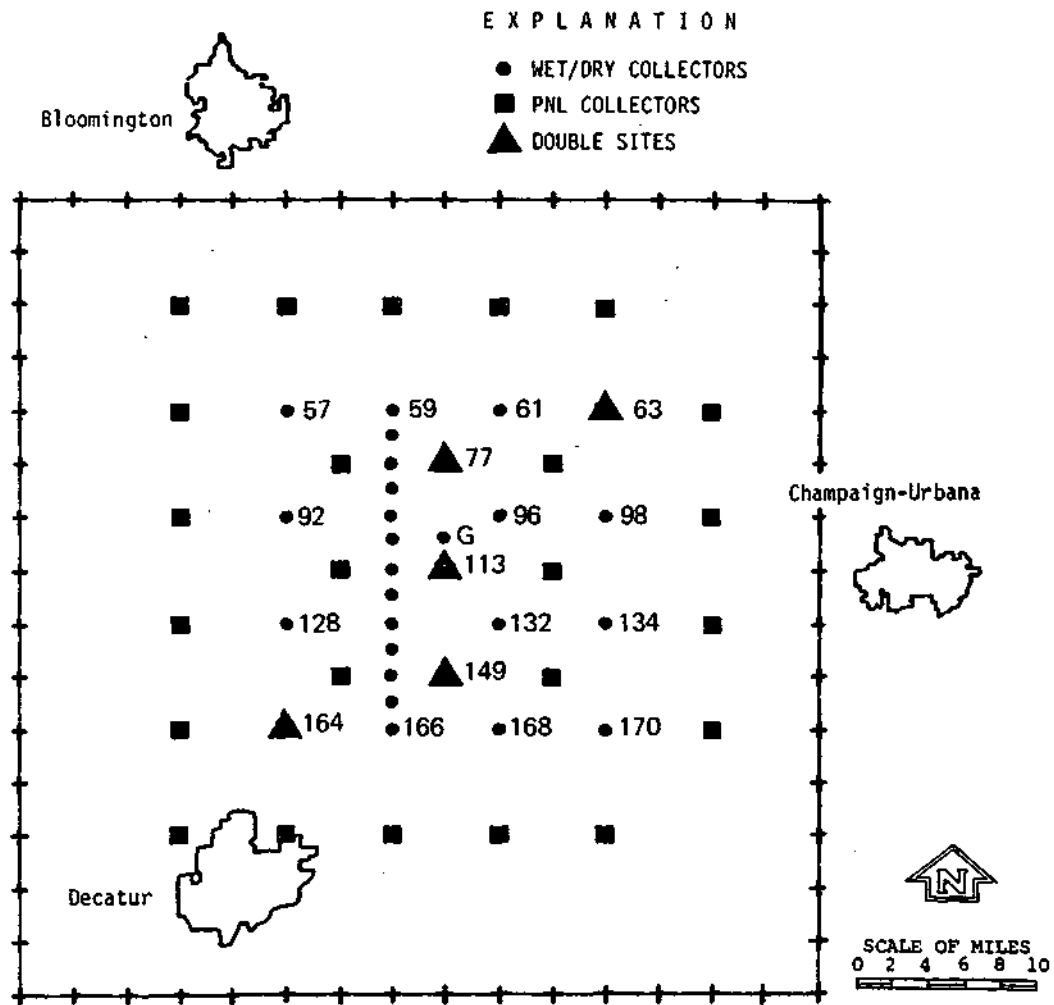


Figure 1. The network arrangement of wet/dry and bulk (PNL) precipitation collectors for the SCORE-79 experiment.



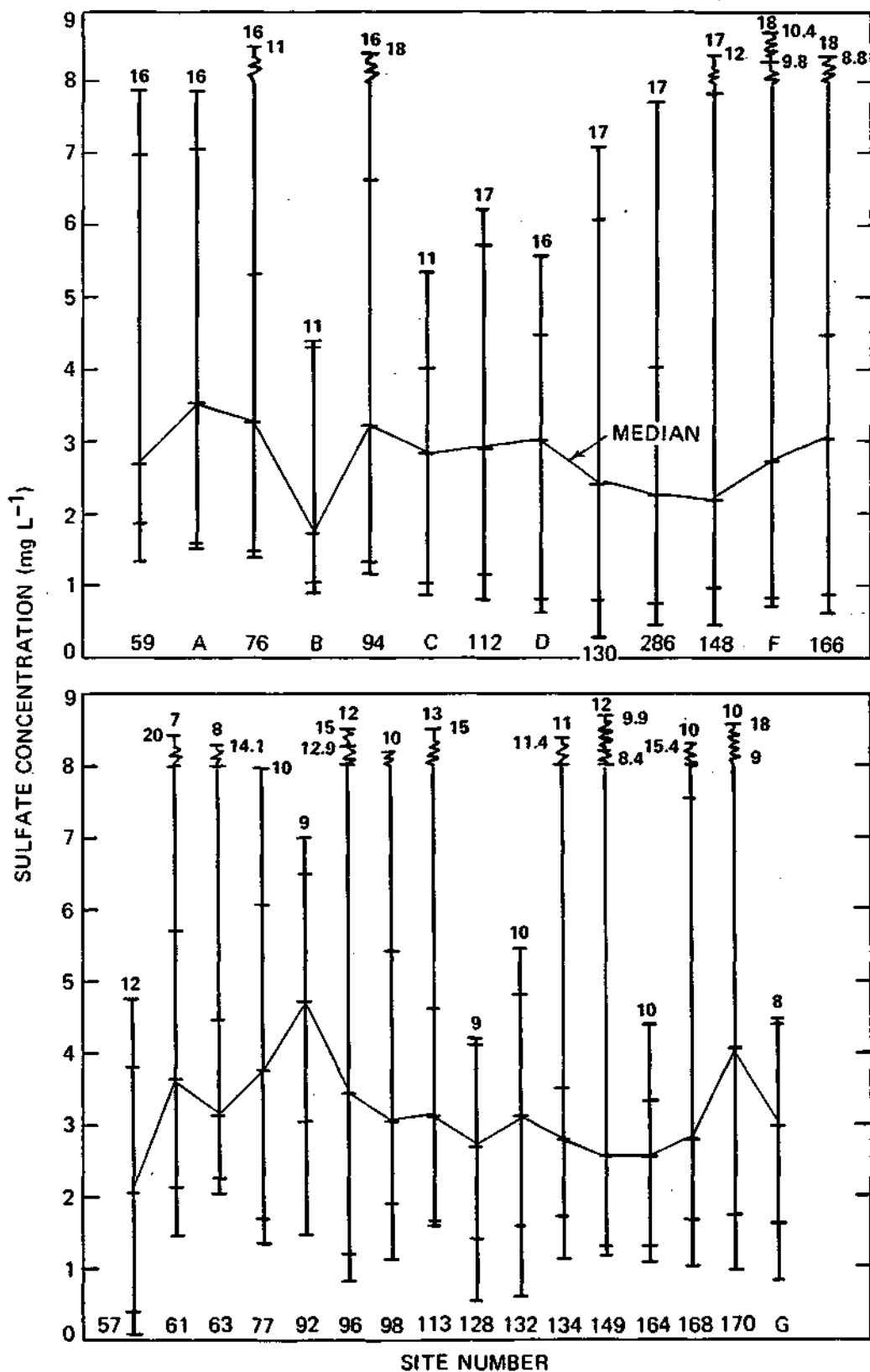


Figure 2. Sulfate data by site for SCORE-79 wet/dry samples. The dots on the vertical lines represent the highest, second highest, median, second lowest, and lowest sulfate concentrations at the site with the total samples number listed above the vertical line.

The solid lines in Fig. 2 connect the median site values. For cases with an even number of samples, indicated by an "I" in the figure, the median was calculated as an average of the two middle values. The lowest median value was 1.7 mg/L at site B and the highest median value was 4.7 at site 92, which gives a variation of a factor of 2.8 for the set of wet/dry sites.

The pH data for the wet/dry samples from SCORE-79 are summarized in Fig. 3. The format of Fig. 3 is like that of Fig. 2 except that the lab type is indicated in Fig. 3 for the samples which produced the maximum, minimum, etc. The four lab types have the following meaning:

- T Only a trace of water in the sample bucket such that only pH or pH and conductivity were measured.
- W The typical sample from the wet-side of the wet/dry sampler, with  $\geq 35$  mL of sample and thus enough volume for measurement of pH conductivity and all the ions.
- WA A sample with volume less than 35 mL but greater than 10 mL. After pH and conductivity were measured 50 mL of deionized water was used to dilute the sample such that all the ions could be measured.
- WC A sample with volume less than 10 mL and greater than about 3 mL. After pH was measured, the sample was diluted with 10 mL of deionized water and then the ions were measured.

For the buckets being used, 17.5 mL of water converts to 0.01 inch of rainfall. Thus the W samples were those corresponding to collected rainfall of 0.02 inch or more.

For the data in Fig. 3, only one median value corresponded to a small volume sample (T, WA, or WC). However, the maximum or minimum values at sites were frequently from small volume samples. For the 13 sites in the dense line (sites 59-166) the distribution is:

	Maximum pH	Minimum pH
No. of W samples	5	3
No. of WA samples	1	6
No. of WC samples	3	4
No. of T samples	4	0

Small volume samples are more likely to have experienced greater percent evaporative losses during the fall of the raindrops through the atmosphere or during the rather brief interval from the end of the rainfall until the closing of the wet/dry sampler. Such evaporative losses would cause the generally acid samples to become unusually high in acid concentration (very low pH). At the other extreme, the small volume samples are also most effected by dust that might be present during the brief rainfall event or by dust contamination of the buckets during non-rain periods. This explains the high frequency of small volume samples which are associated with high pH values. The sites in

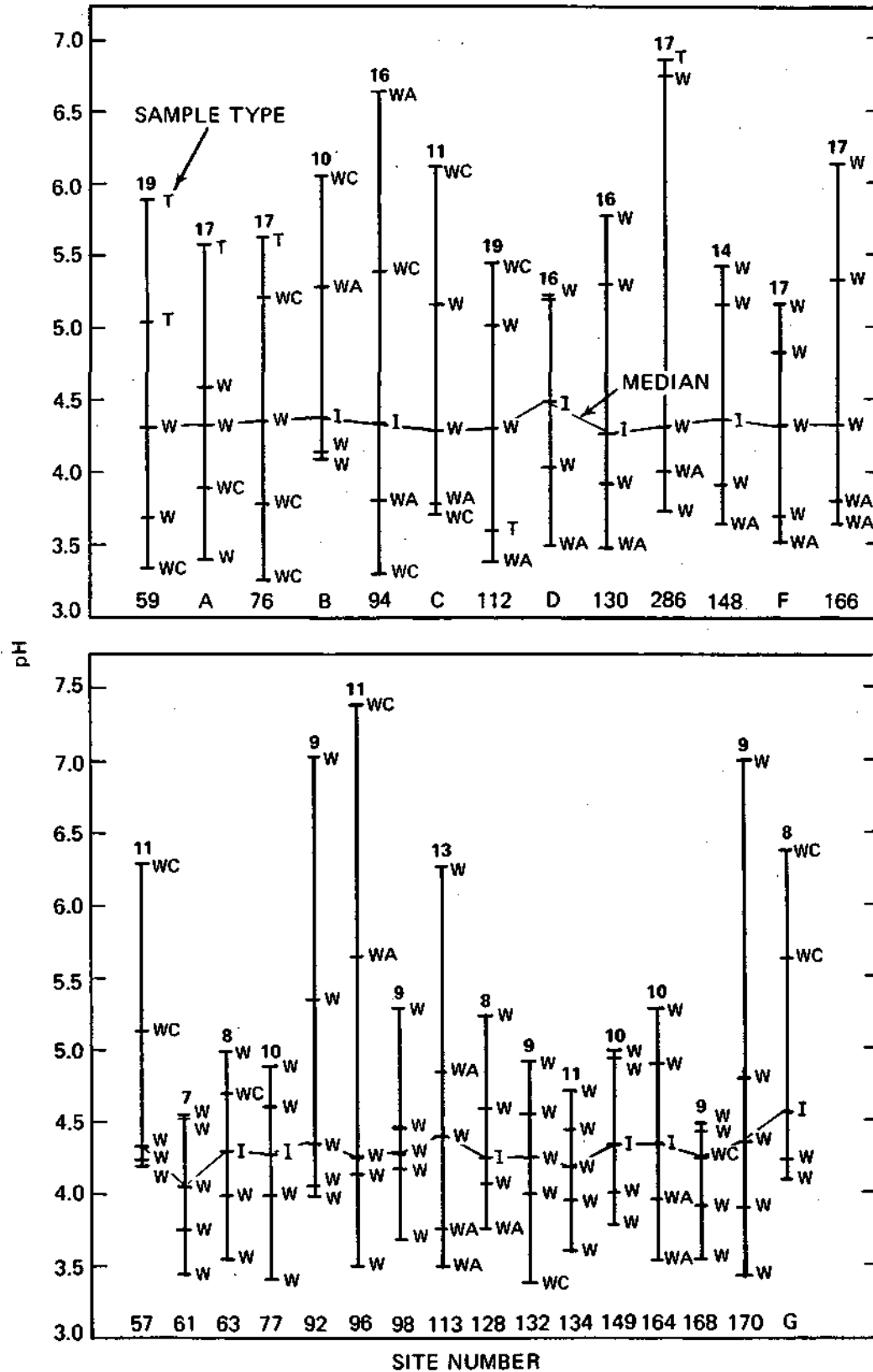


Figure 3. Values of pH for SCORE-79 wet/dry samples. The dots on the vertical lines have the same meaning as in Figure 2. The letters denote the laboratory sample types (described in text).

the bottom half of Fig. 3, off the dense line, have a lower occurrence of small volume samples since the collection periods for each sample were generally longer.

From Fig. 3, the lowest pH values is seen to be 3.25 (a WC sample), and the highest pH is 7.40 (also a WC sample). Considering only W samples, the pH extremes are 3.40 and 7.05. The extreme values for a site are 3.50 and 7.40 for site 96. If only W type samples are considered the extreme range was observed at site 170, with values of 3.45 and 7.02.

The median pH was generally about 4.3, with a range in the site medians of 4.05 to 4.55. From Fig. 2 the median  $\text{SO}_4$  concentration was about 3.0 mg/L or 62  $\mu\text{eq/L}$ . The  $\text{pH} = 4.3$  corresponds to 50  $\mu\text{eq/L}$ . Therefore for the wet/dry samples from SCORE-79 it appears that sulfate was slightly greater than the hydrogen ion concentration, on an equivalent basis.

## CHAPTER 2

### REPRODUCIBILITY OF AEROSOL SAMPLES COLLECTED ON NUCLEPORE FILTERS UNDER INVERTED FUNNEL RAIN SHIELDS

Donald F. Gatz

#### INTRODUCTION

We have used Nuclepore filters exposed face down under inverted rain shields to collect aerosol samples in a number of field observation projects related to precipitation scavenging of airborne particulate matter. These include extensive field projects such as METROMEX (Changnon et al., 1971) and SCORE-78, as well as weekly sampling at Whiteface Mountain, N.Y., Charlottesville, VA, and Champaign, IL, and daily sampling at Champaign. Data collected during Project METROMEX were used to identify aerosol sources in the St. Louis area (Gatz, 1978) as well as for precipitation scavenging research. To show the validity of these previous results it is desirable to know the uncertainty associated with element concentrations measured from a single filter sample. Therefore an experiment was carried out during the summer of 1977 in which pairs of samples were collected simultaneously on identically exposed filters. The filter pairs were then analyzed using the same method. This paper reports the reproducibility of the sampling method.

#### EXPERIMENTAL METHODS

Samples were collected in July, 1977, at about 1.5 m over grass at the University of Illinois Willard Airport, 8 km south of Champaign, Illinois. A little-used crushed limestone service drive is 25 m east of the sampling site, and the airport terminal and parking lot are 0.5 km to the southwest. Other parking lots covered with crushed limestone are also found within 0.5 km of the sampling site in a sector extending from south through west.

Nuclepore filters 37 mm in diameter with 0.8  $\mu\text{m}$  diameter pores were exposed in plastic holders face down under 25 cm diameter polyethylene funnels. Fourteen pairs of samples were collected over 12 hr periods from noon to midnight.

Further details of sample collection, analysis, and correction for filter collection efficiency were given previously (Gatz, 1978) and need not be repeated here.

## RESULTS

The results of comparing duplicate samples are presented in two ways. In the first, concentrations of each element and total suspended particles (TSP), measured under funnel 1, are plotted against those measured under funnel 2. The second comparison, in Table 1, is more quantitative. It gives, 1) mean ratios of element and TSP concentrations measured by the two samplers, 2) the probability that measurements of the two samplers were drawn from the same population, and 3) the overall uncertainty of a single measurement.

The comparison plots are shown in Fig. 1. Points were plotted only for sample pairs where both measurements were above detection limits. The straight lines represent perfect agreement between samplers.

Figure 1 shows that the best agreement between samplers was achieved for Si, S, K, Ca, Fe, and TSP. Poorer agreement, in the form of a greater scatter of points about the line of perfect agreement, was observed for Ti, Mn, Zn, Br, and Pb. The plot for Al contains only 5 points because of the frequent occurrence of upper limit measurements. The Al results are discussed in more detail later.

The statistical comparison of the two samplers presented in Table 1 has two main purposes. The first purpose is to compare concentrations measured by the two samplers, and the second is to present data on the uncertainty of a single measurement. In addition, the table shows mean concentrations of 10 elements and TSP. Al is not shown because it had only 5 valid sample pairs.

Comparison of the samplers is expressed first in terms of the mean ratio ( $\pm$  the standard error). The table shows ratios consistently (except for Mn) less than 1.0. Furthermore, the ratios are frequently more than two standard errors away from 1.0, which suggests that the differences are significant. The significance of the differences is also expressed in terms of the probability,  $P$ , that the respective samples were drawn from the same population, based on a paired T-test. Thus, with 95% confidence we can reject the hypothesis that the two samplers were sampling the same population for Si, S, K, Fe, Br, Pb, and TSP. The hypothesis cannot be rejected for Ca, Ti, Mn, and Zn.

The most readily apparent reason for a significant difference between samplers is an error in sampler flow rate calibration. Such an error was discovered and corrected after these samples were collected. It could possibly have caused a bias of 5-10% in the measured concentrations of a single sampler. The differences implicit in the mean ratios, which are concentrated in the range between 0.85 and 0.90, are consistent with bias of such a magnitude, but opposite in sign, by the respective samplers.

These results show an accuracy that is clearly less than what one would hope to achieve in filter sampling of atmospheric aerosols, but nevertheless, it represents what really occurred, and one may justifiably ask what confidence limits these results imply for an individual measurement, where it is not known which way the sampler might be biased from the mean.

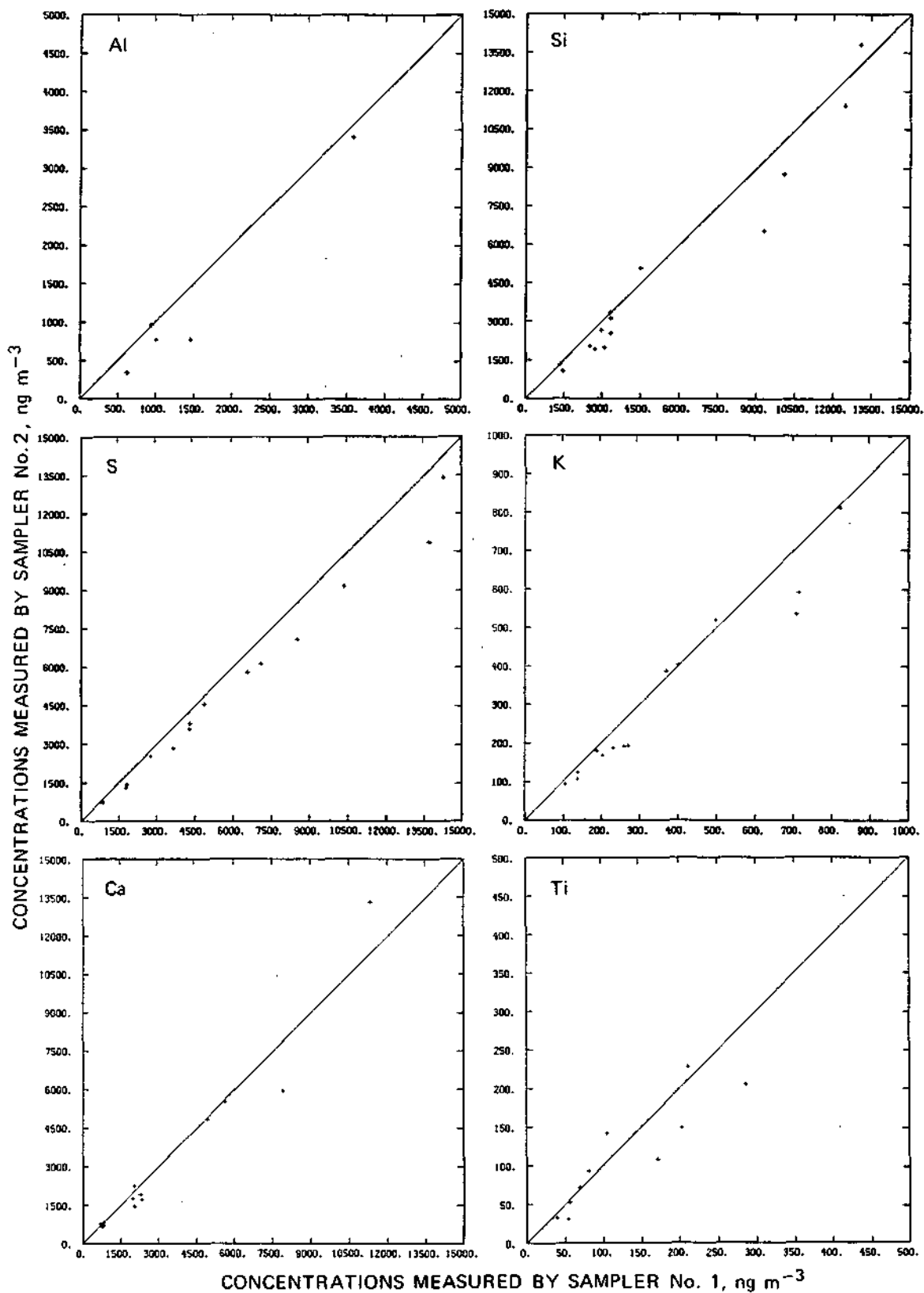


Figure 1. Comparison of concentrations measured from duplicate filter samples, Willard Airport, Champaign, Illinois, July, 1977.

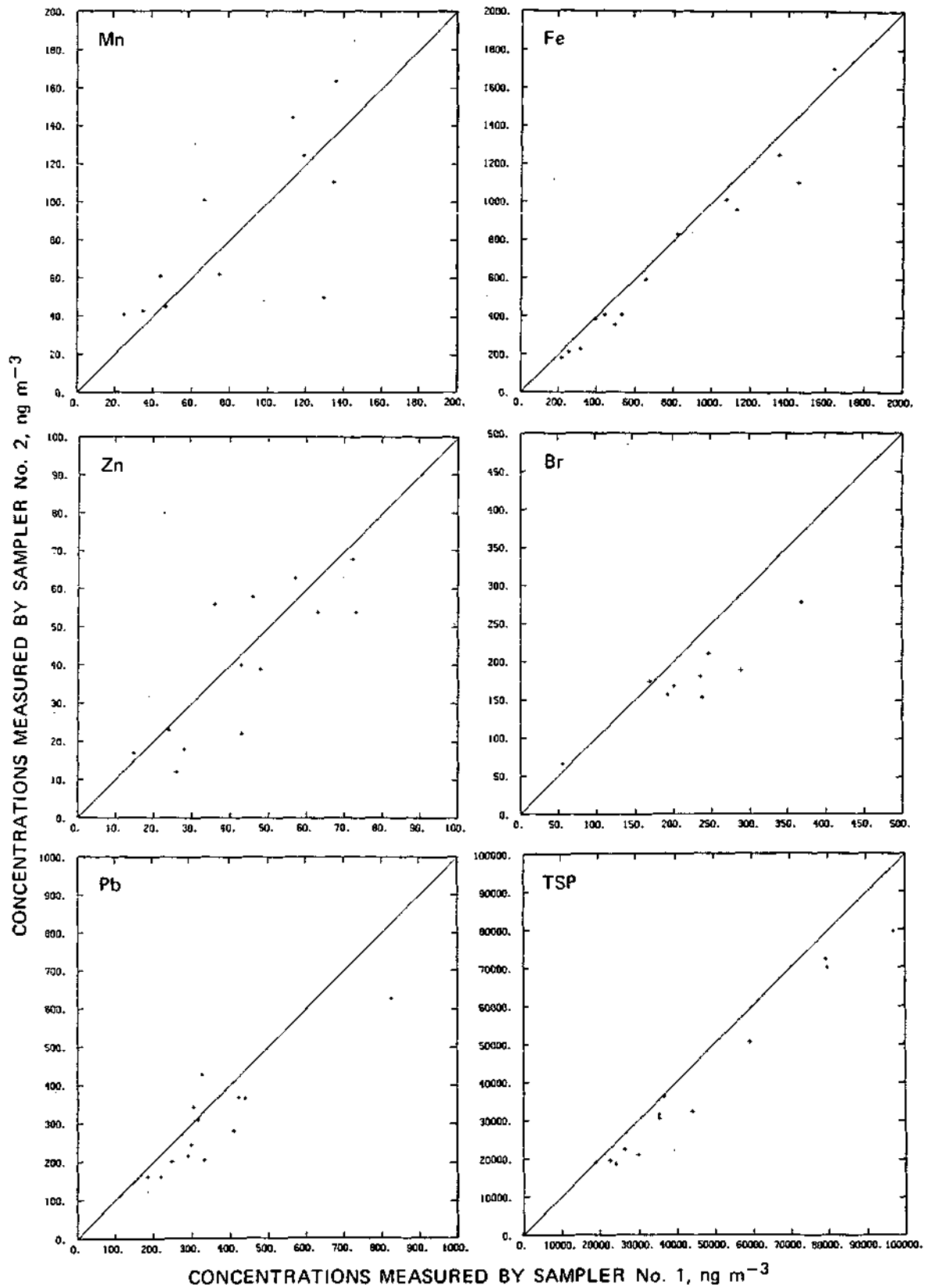


Figure 1. Comparison of concentrations measured from duplicate filter samples, Willard Airport, Champaign, Illinois, July, *Will.*



Table 1. Comparison of duplicate Nuclepore filter sampling and analysis, using the inverted funnel sampler.

	<u>No. of sample pairs</u>	<u>Mean concentration ng m<sup>-3</sup></u>	<u>Mean ratio Sa.2/Sa.1 + S.E.M.</u>	<u>p*</u>	<u>Uncertainty, %**</u>
Si	14	5,000	0.865 ± 0.039	0.029	± 9.6
S	14	5,670	0.844 ± 0.018	0.000	± 10.2
K	14	342	0.872 ± 0.031	0.015	± 9.4
Ca	14	3,115	0.904 ± 0.037	0.456	± 8.3
Ti	10	120	0.897 ± 0.078	0.192	± 15.4
Mn	11	85	1.118 ± 0.108	0.843	± 10.7
Fe	14	730	0.872 ± 0.028	0.008	± 8.6
Zn	13	42	0.916 ± 0.084	0.264	± 10.9
Br	9	199	0.838 ± 0.059	0.008	± 17.3
Pb	13	329	0.858 ± 0.052	0.023	± 13.6
TSP	14	39,100	0.867 ± 0.027	0.000	± 10.7

\*P = probability that sample pairs were from the same population, based on paired T-test.

\*\*95% confidence limits on the true concentration, expressed as a percent of the mean element concentration.

Assuming that the best estimate of the true concentration of a given element during any sampling period was the mean of the two measurements, I computed the deviation from the mean (one-half the difference,  $D$ , between the two samplers) for each pair of samples, and the mean and standard error of this deviation over all valid sample pairs. From these data I computed the upper one-tailed 95% confidence limit on the mean, assuming the  $D/2$  values to be normal. Normal plots of the  $D/2$  data were used to verify that this assumption was approximately true. The uncertainty given in Table 1 is this 95% confidence limit expressed as a percent of the mean concentration for each element for the 14 pairs of samples. The plus or minus sign attached to each uncertainty value expresses the fact that for a single sampler one would not know whether the observed concentration was above or below the true value.

## DISCUSSION

The results in Table 1 show overall uncertainties mostly less than 15% at 95% confidence. This includes uncertainties arising both from sampling and from analyses, but the analytical uncertainty (Flocchini *et al.*, 1972; 1976) appears to account for less of the overall uncertainty than sampling, at least for the present data set. With the present sampling error corrected, the two would be roughly equivalent.

The analytical results for Al invite a closer look because Al was detected in both samples only 5 times in 14 pairs. Individual filter measurements are shown in Fig. 2. In pairs 2, 5, 13, and 14, Al on one filter was well above the detection limit, while that on the second of the pair was reported as an upper limit. If such a result was caused by sampling problems, other elements should also be affected. This is not the case. The alternative is that the problem arises in analysis. Some samples where Al was questionable have been re-analyzed, with no change in results.

Thus, the nature of the problem has not been found, but one should be cautious in using Al concentrations from samples collected and analyzed as described earlier.

## REFERENCES

- Changnon, S. A., F. A. Huff, and R. G. Semonin, 1971: METROMEX: an investigation of inadvertent weather modification. Bull. Amer. Meteor. Soc., 52(10), 958-967.
- Flocchini, R. G., P. J. Feeney, R. J. Sommerville, and T. A. Cahill, 1972: Sensitivity versus target backings for elemental analysis by alpha-excited X-ray emission. Nucl. Instrum. Methods, 100, 379-402.

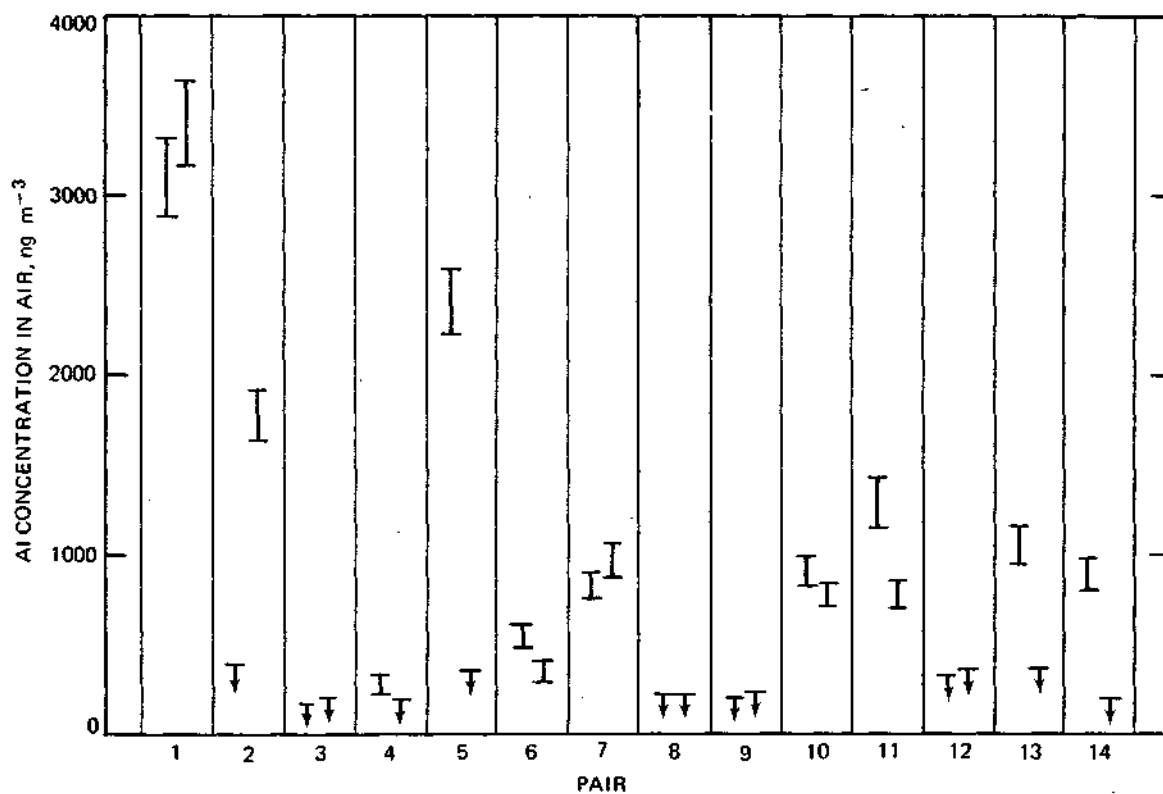


Figure 2. Detailed comparison of Al concentrations measured from duplicate filters.

Flocchini, R. G., D. J. Shadoan, S. J. Lange, R. A. Eldred, P. J. Feeney, and G. W. Wolfe, 1976: Monitoring California's aerosols by size and elemental composition. Environ. Sci. Techn., 10, 76-82.

Gatz, D. F., 1978: Identification of aerosol sources in the St. Louis area using factor analysis. J. Appl. Meteor., 17(5), 600-608.

## CHAPTER 3

### COMPARISON OF TWO SAMPLING METHODS FOR MEDIUM-VOLUME AEROSOL SAMPLING

Donald F. Gatz

## INTRODUCTION

It is well known that sampling of large ( $> 10 \mu\text{m}$  diameter) atmospheric particles is subject to substantial errors arising from particle momentum unless the sampling is done isokinetically. Thus, we were concerned that concentrations of individual elements and total suspended particles (TSP) measured on 37 mm diameter Nuclepore filters that were exposed face down under a polyethylene funnel rain shield might be seriously in error for some of the larger aerosol particles near ground level. Some of the large particles, because of their inertia, are probably unable to make the required  $90^\circ$  bend from their (mean) horizontal trajectory in the ambient wind that is required for them to be collected on the filter. Thus, a simple sampling device was designed to slow the air and allow it and the airborne particles to make the required bend before reaching the filter.

This report compares TSP and elemental concentrations measured in both new and old sampling configurations, operated simultaneously, side by side.

## SAMPLER DESIGN

The new sampler was designed to rotate about a vertical axis and was provided with a tail so it would always face into the wind. Details of the sampler's design are given in Fig. 1.

The air inlet has a cross-sectional area of  $20.3 \text{ cm}^2$ . Downstream from the inlet the tube flares out to a cross-sectional area of  $81.1 \text{ cm}^2$ . This decreases the air speed by a factor of 4.0, allowing airborne particles a greater chance to make the  $90^\circ$  bend without impacting on the wall. The dimensions were chosen so that air moving at the average annual wind speed of 3.0 m/sec would slow and approach the filter at approximately 75 cm/sec. The face velocity of air through the filter at the usual pumping rate is 70 cm/sec, so at the average wind speed, the sampler should sample a very slight excess of large particles.

Note that the sampler inlet has been provided with a shield to prevent rain from entering.

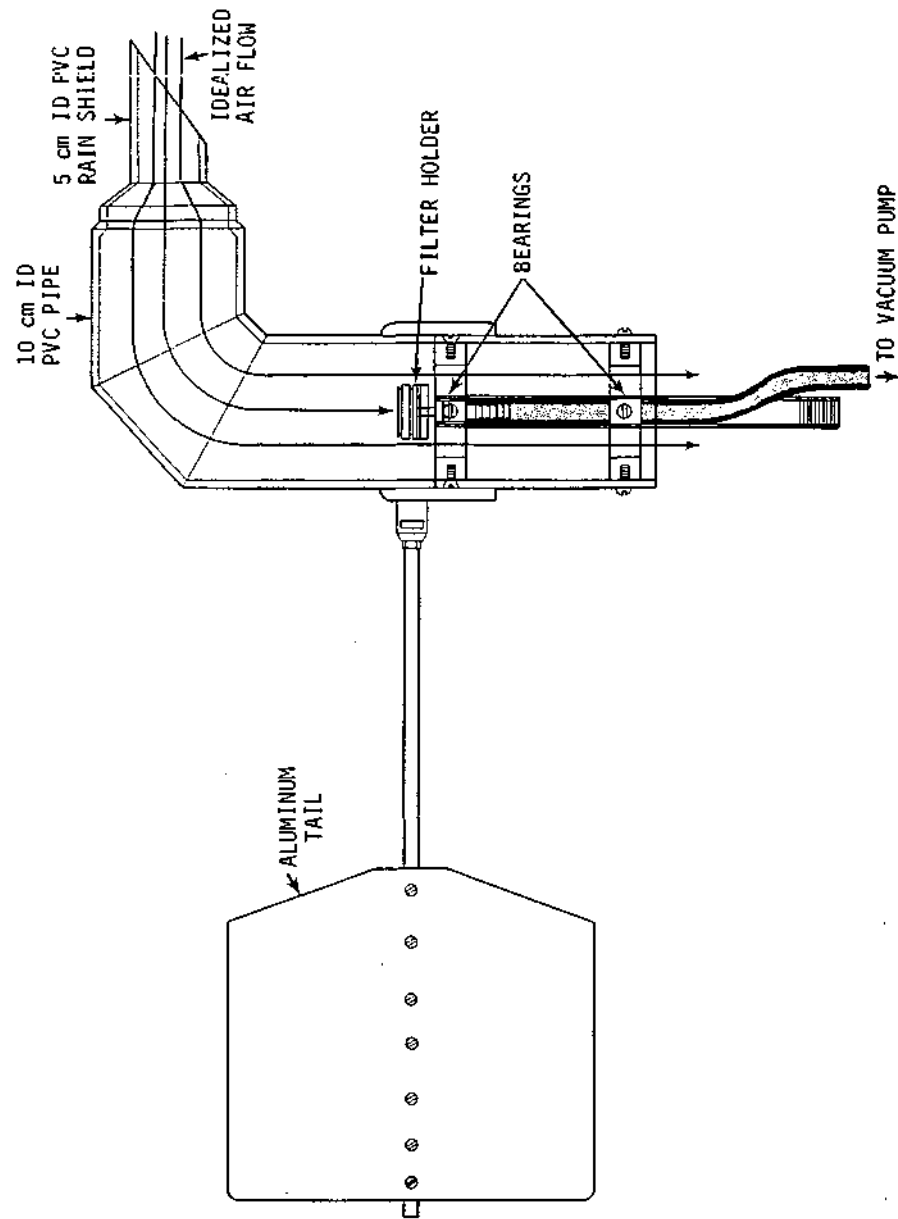


Figure 1. Detailed drawing of the vane sampler.

## EXPERIMENTAL METHODS

Aerosols for elemental analysis were collected on pre-weighed 37 mm diameters Nuclepore polycarbonate membranes with 0.8  $\mu$ m diameter pores, face down under an inverted polyethylene funnel rain shield at about 1.5 m over grass. Samples were collected over 12-hr periods from noon to midnight.

Filters were weighed to the nearest hundredth of a milligram on a micro-balance, using a radioactive source to dissipate static charge. No humidity conditioning was necessary before pre-weighing since the polycarbonate membranes do not absorb moisture. After sample collection, the filters were conditioned for at least 24 hr at 47% relative humidity to allow moisture absorbed on the collected particulate matter to come to equilibrium. Filters were then reweighed.

Elemental analysis of the filters was carried out at Crocker Nuclear Laboratory, University of California-Davis, using ion-excited X-ray fluorescence. Absolute error limits of  $\pm 10\%$  in most cases to as high as  $\pm 30\%$  near detection limits are quoted by the laboratory (Flocchini *et al.*, 1972; 1976). Further details of the filter sampling and analysis procedures were given by Gatz (1978).

Results are presented below for two field comparisons of the two types of samplers. The first was carried out at the University of Illinois Willard Airport in October and November, 1977. Twenty-six pairs of samples were collected and analyzed. The second comparison was done at our Bondville Road field site, a 7.5 acre grassy plot surrounded, in summer, by corn and soybean fields, about 10 km southwest of Champaign. Twenty-four sample pairs were collected at this site.

## RESULTS AND DISCUSSION

Element and TSP concentrations measured on the filter under the funnel are plotted against those from the filter in the vane sampler in Fig. 2. The straight line is the line of perfect agreement between samplers.

A considerable scatter points on both sides of the line is shown for Al. This relatively large scatter is probably the result of the same unexplained problem with Al measurements noted in Chapter 2 of this report. The plots in Fig. 2 for Si, K, Ca, Ti, Mn, Fe, and Pb show a definite tendency for higher concentrations for the filter exposed in the vane sampler.

The plot for TSP also shows a strong tendency for higher concentrations in the vane samples, but a greater scatter in the points may be seen, as compared to the element plots.

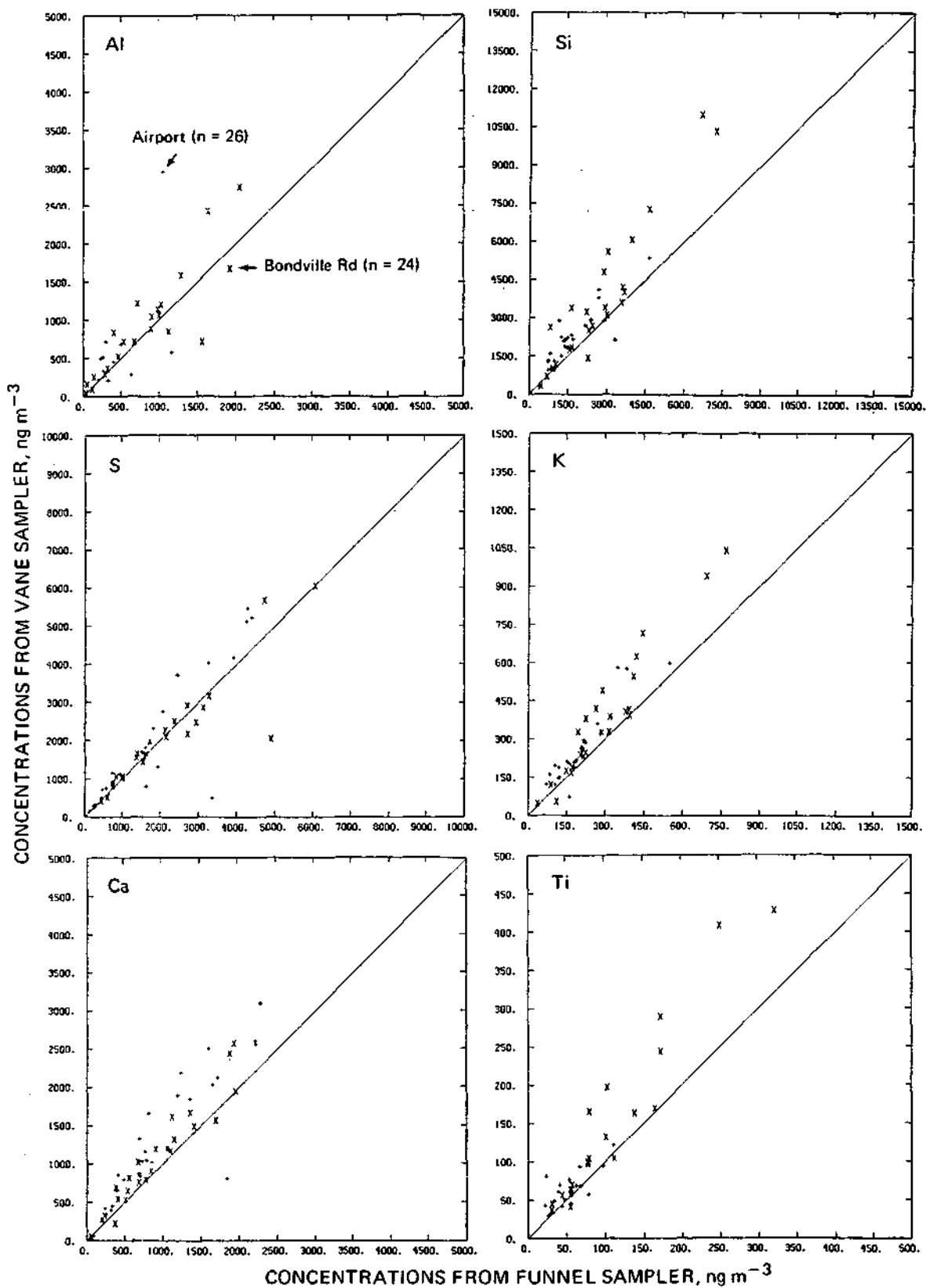


Figure 2. Comparison of airborne elemental and TSP concentrations as measured by funnel and vane samplers.



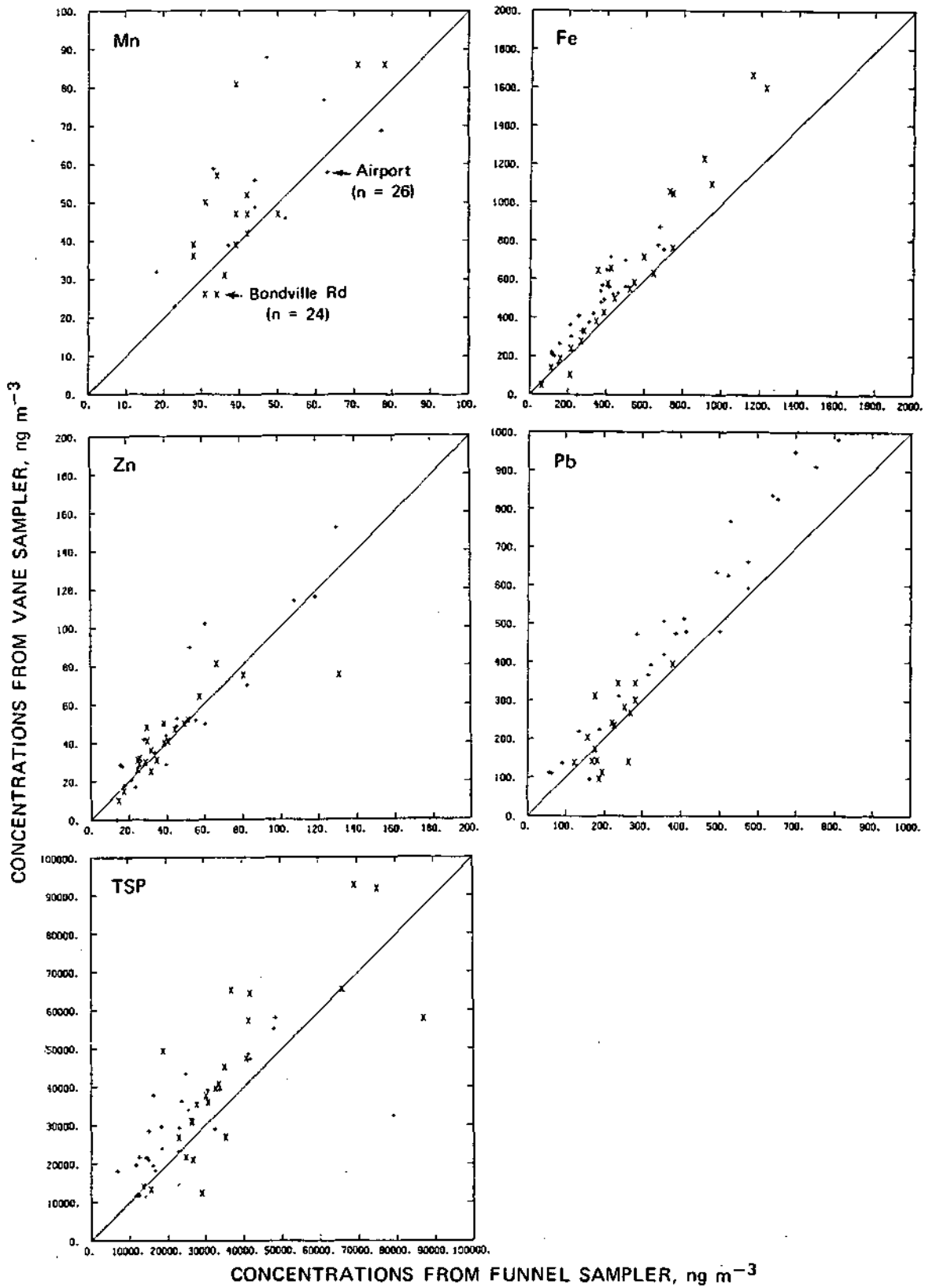


Figure 2. Comparison of airborne elemental and TSP concentrations as measured by funnel and vane samplers.

The plots for S and Zn show a better agreement between the two samplers than was the case for the other elements and TSP. Of these two elements, Zn has the greater scatter in the points.

In the case of S, Ca, Zn, and TSP there are one or two anomalous points where the funnel sample concentration was much higher than that of the vane sample. In the case of the anomalous sample pairs on the S, Ca, and Zn plots, each was collected on a day with dense fog (visibility less than 1/2 mi) during some portion of the time when the sample was being collected. Less dense fogs had no apparent effect, or affected both filters proportionately. These occurrences are interpreted as being caused by fog water blowing into the vane sampler (since it always faces the wind), collecting on the filter, and dissolving a portion of the accumulated deposit, which was subsequently removed from the filter as the water drained off, or was drawn off in droplets into the stream of air passing through the filter. Apparently the fog droplets were too large to be collected by the filter under the funnel; at least that filter was less affected. The elements affected have previously been observed to be among the most soluble in rain water, whereas the unaffected elements are generally expected to occur in less soluble or insoluble compounds.

The two major anomalous points on the TSP comparison were not caused by fog leaching. Examination of original data for one of these points strongly suggests an error in weighing the filter. The data for the other anomalous point do not suggest any particularly error, but such a large anomaly seems unlikely to have occurred naturally.

The comparison between vane and funnel results is expressed quantitatively in Table 1, where ratios of vane to funnel concentrations are summarized. Mean ratios and the standard error of the mean, are given for each element in several data sets. Ratios are given separately for the Fall 1977 set, the Summer 1978 set, and for these two sets combined.

A comparison of sampling variability in two duplicate funnel collectors, as presented in Chapter 2 of this report, shows the random and systematic sampling and analysis errors can cause uncertainties up to about  $\pm 15\%$  (95 confidence) for single samples. The 20% and 35% differences between the vane and funnel samplers exceed even that extreme value. Moreover, there is evidence in the comparison of S concentrations, that no such systematic error occurred in the vane/funnel comparison.

The vane/funnel ratios for S, which is known to occur primarily on sub-micrometer particles in the atmosphere, are close to 1.0. Since submicrometer particles should be only minimally influenced by deviations from isokinetic sampling, the S ratio of 1.0 is evidence that there was no systematic errors due to calibration, as occurred in the comparison of funnel samplers.

The vane/funnel ratios given in Table 1 were calculated from data for all samples plotted in Fig. 2. This includes the several anomalous points discussed above. These tend to decrease the vane/funnel ratio and increase the standard error, so that results presented in Table 1 can be viewed as conservative.

Table 1. A comparison of vane/funnel ratios for 11 elements and TSP.

	Fall, 1977 Airport			Summer, 1978 Bondville Road			Combined data sets		
	<u>n</u>	<u>Mean</u>	<u>S.E.</u>	<u>n</u>	<u>Mean</u>	<u>S.E.</u>	<u>n</u>	<u>Mean</u>	<u>S.E.</u>
Al	12	1.38	0.22	22	1.21	0.10	34	1.27	0.10
Si	26	1.36	0.07	24	1.28	0.11	50	1.32	0.06
S	26	1.11	0.06	24	0.99	0.03	50	1.05	0.04
K	26	1.29	0.05	24	1.24	0.06	50	1.26	0.04
Ca	26	1.39	0.07	24	1.17	0.05	50	1.29	0.05
Ti	17	1.33	0.15	20	1.30	0.07	37	1.32	0.08
Mn	11	1.26	0.11	16	1.21	0.09	27	1.23	0.07
Fe	25	1.39	0.05	24	1.18	0.06	49	1.28	0.04
Zn	20	1.16	0.07	22	1.05	0.05	42	1.10	0.04
Pb	26	1.29	0.05	17	1.02	0.08	43	1.18	0.05
TSP	26	1.36	0.09	24	1.17	0.09	50	1.27	0.06

The results of the combined data sets indicate that on the average the vane filter collected significantly more than the funnel for every element except S, and possibly Zn. The same may be said for the Fall 1977 data set, but in the Summer 1978 set the ratios of the additional element Pb and TSP, and possibly Al were not significantly different from 1.0

The elements Si, K, Ca, Ti, Mn, and Fe consistently showed significantly greater concentrations as measured by the vane sampler. In central Illinois these airborne elements come predominately from blowing soil or road dust, and reside on relatively large particles ( $> 3 \mu\text{m}$  diameter). The remaining elements, which were always or sometimes sampled as well by the funnel sampler as the vane sampler, are known to occur predominately on smaller particles ( $< 1 \mu\text{m}$ ) and are thus more likely to be correctly sampled by the funnel sampler because they follow the streamlines of the air being drawn into the face-down filter.

Thus, the results are consistent with the known particle size characteristics of the various elements, and with the hypothesis that the face-down filter might be under-sampling the ambient aerosol because it is anisokinetic for the larger particles.

Previous concentration measurements using the funnel sampler will be too low by 0 to 35% depending on the element, but analysis based on relative values, such as those done by Gatz (1978), will not be affected.

## CONCLUSIONS

The results show that a face-down medium-volume filter will under-sample the larger particles in the ambient aerosol. A simple quasi-isokinetic sampler was found to measure 20% to 35% higher concentrations, on the average, for various airborne elements, and TSP. Elements found predominantly on sub-micrometer particles, including S and Zn, were adequately sampled on the face-down filter, although some tendency was seen for under-sampling at the higher concentration levels.

The vane sampler used in this comparison was rather simple and inexpensive to build. It has been shown to be better than a face-down filter for general aerosol sampling, but should be further tested for absolute accuracy. A wind-tunnel comparison against known isokinetic samplers is required.

The vane sampler was found to give invalid results if dense fog occurred during the sampling period. However, rain, even accompanied by strong winds, did not have the same effect.

REFERENCES

- Flocchini, R. G., P. J. Feeney, R. J. Sommerville, and T. A. Cahill, 1972: Sensitivity versus target backings for elemental analysis by alpha-excited X-ray emission. Nucl. Instrum. Methods, 100, 379-402.
- \_\_\_\_\_, D. J. Shadoan, S. J. Lange, R. A. Eldred, P. J. Feeney, and G. W. Wolfe, 1976: Monitoring California's aerosols by size and elemental composition. Environ. Sci. Techn., 10, 76-82.
- Gatz, D. F., 1978: Identification of aerosol sources in the St. Louis area using factor analysis. J. Appl. Meteor., 17(5), 600-608.

## CHAPTER 4

### COMPARISON OF TOTAL VERSUS SOLUBLE DATA FOR AMBIENT AEROSOL FILTER SAMPLES

Gary J. Stensland and Donald F. Gatz

#### INTRODUCTION

Since May 1977, daily aerosol filter samples have been collected at two field sites near Champaign, Illinois. Results from these studies have been discussed in the two previous Progress Reports for this contract. The purpose of this chapter is to compare data for calcium, potassium, and sulfur for two analysis techniques, namely a total versus a soluble procedure. The comparison is important since both procedures have been used in our field experiments. The data will show that conclusions can be made for calcium and magnesium but that the methodology of the experiment prevents a conclusion at this time with respect to sulfur.

The aerosol sulfur is usually in the form of readily soluble compounds and thus is frequently determined with wet chemical measurements after extraction in water. The alkali and alkali earth elements are associated with compounds that are not so readily soluble. In our research we have switched from water to a pH 3 hydrochloric acid extraction procedure in order to more closely simulate the manner in which the aerosols will be extracted in very acid precipitation solutions. A chapter in the 18th Progress Report compared these two soluble extraction procedures for calcium and magnesium (Bartlett and Stensland, 1980). Usually the differences were small but in the extreme case, the calcium concentration was 25% higher in the pH 3 solution compared to the water (pH ~ 5.6) solution. Certainly the term "soluble" is a relative term, with the results depending on the type of extraction procedure. On the contrary "total" is an absolute term since there is only one total value.

#### EXPERIMENTAL PROCEDURE

The main field site was located about ten kilometers southwest of Champaign-Urbana in east-central Illinois and is called the Bondville site. The surrounding area is rural farmland. The low-volume aerosol sampling system consisted of a Gast piston-type vacuum pump with an inverted polyethylene funnel serving as a weather shield housing the filter unit. The filter unit consisted of a Nuclepore™ filter, with a diameter of 37 mm and a pore size of 0.8  $\mu$ m diameter, mounted in a Millipore Field Monitor filter holder. The unit was mounted face down with the filter surface 2 cm above the funnel's rim and 2 meters above the ground.

#### Technique to Determine Soluble Components

After the collection period, the filters were stored in sterilized petri dishes at room temperature. Storage time before analysis was typically 2 months but ranged from several days to 5 months.

The filters were extracted in 25 mL of deionized water by vigorous agitation (wrist-action shaker) for 20 minutes at room temperature. The solutions were immediately filtered with Millipore HA filters to remove insoluble particles.

The analytical method for the  $\text{SO}_4$  was methylthymol blue automated on the Technicon Autoanalyzer II. Calcium and potassium ions were determined by flame atomic absorption using an Instrumentation Laboratories AAES 353.

#### Technique to Determine Total Elements

Elemental analysis of the filters was carried out at Crocker Nuclear Laboratory, University of California-Davis, using ion-excited X-ray fluorescence. Absolute error limits ( $\pm 3$  standard deviations) of  $\pm 10\%$  in most cases to as high as  $\pm 30\%$  near detection limits are quoted by the laboratory (Flocchini *et al.*, 1972; 1976). Corrections for X-ray absorption as a function of aerosol particle size were applied during processing of the raw data by the analytical laboratory. However, no corrections were applied to S, since it was assumed that sulfur was on particles essentially less than 1  $\mu\text{m}$  diameter.

### RESULTS AND DISCUSSION

During SCORE-78 two identical aerosol filter samples were collected at the Bondville site on 24 days in June and July. The comparative data are presented in Table 1, with the subscript t in the column headings indicating "total" and the subscript w indicating "soluble" in water. The tabulated data, if multiplied by 100, indicate the percent increase (for positive numbers) of the element when determined by the total method versus the water soluble method. For example, for the filter removed on June 30, the total calcium was 13.2% greater than the water soluble calcium; potassium was 220% greater; and sulfur was 31.7% less. Actually sulfate was measured in the wet chemical procedure and was divided by 3.0 to convert to sulfur. Notice in Table 1 that 22 of the 24 sulfur values are negative, all the potassium values are positive and the calcium values are about half and half.

The data are summarized at the bottom of each column in Table 1 with various statistical parameters. For calcium the median value indicates that total calcium was 13.3% greater than soluble calcium. The mean difference was  $19.3 \pm 90\%$ , with the  $\pm$  value being the standard error (standard deviation  $\div$  square root of sample number) which suggests that there is a statistical difference between the two techniques.

Table 1. Solubility for calcium, potassium and sulfur for 24 daily aerosol samples from the Bondville, IL site for 1978.

<u>Date off</u>	$\frac{C_t - C_w}{C_w}$	$\frac{K_t - K_w}{K_w}$	$\frac{S_t - S_w}{S_w}$	
June 13	0.635	2.128	1.118	
15	0.047	3.415	-0.343	
16	-0.026	3.290	-0.463	
17	-0.042	0.344	-0.262	
18	-0.059	2.052	-0.347	
19	0.239	1.000	-0.310	
20	-0.098	1.013	-0.295	
21	0.416	0.324	-0.178	
22	0.371	1.306	-0.404	
23	0.158	2.232	-0.339	
24	-0.013	2.094	-0.193	
25	0.010	1.022	-0.142	;.
26	0.134	2.384	-0.219	
27	-0.010	2.140	-0.314	
28	0.553	3.563	-0.084	
29	0.212	4.870	-0.278	
30	0.132	2.200	-0.317	
July 1	-0.022	1.419	-0.114	
25	1.954	0.600	-0.214	
26	-0.329	0.500	1.437	
27	0.221	0.880	-0.068	
28	0.268	1.117	-0.268	
29	0.169	1.297	-0.088	
30	-0.289	0.956	-0.636	
Standard Deviation	0.440	1.148	0.457	
Standard Error	0.090	0.234	0.093	
Mean	0.193	1.756	-0.138	
Median	0.133	1.362	-0.265	
Maximum	1.954	4.870	1.437	
Minimum	-0.329	0.324	-0.636	



For potassium the median value indicates that total potassium is 136% greater than soluble potassium; the mean value is  $175 \pm 23\%$ . Generally, for the water soluble extraction solution of an aerosol filter or of a rainwater solution, the potassium concentrations are about 5-10 times lower than those for calcium.

The surprising result in Table 1 is that total sulfur was less than soluble sulfur, with a median difference of -26.5% and a mean difference of  $-13.8 \pm 9.3\%$ . Before discussing possible explanation for this result, the data in Table 2, for the Willard Airport site which is about 8 kilometers southeast of the Bondville site, are considered.

For the airport site the sampling apparatus, the water soluble extraction procedure, and the chemical measurement procedure were identical to those used at the Bondville site. For calcium, the median differences from Table 2 was 70.3%, with the positive value indicating that the airport values were larger. This result is very likely due to the unpaved service road about 30 meters east of the airport site and an unpaved parking lot about 50 meters south of the site. The potassium difference was lower, with a median of only 5.9%. This result is consisted with assuming the unpaved areas caused the elevated calcium since such sources are rich in calcium compared to potassium. For sulfur the airport had larger values than the Bondville site, with a median difference of 7.6% and mean difference of  $9.4 \pm 6.6\%$ . The unpaved sources could likely explain the somewhat elevated potassium and sulfur values at the airport site. However, the Bondville sulfur and potassium values might be low in Table 2 due to a systematic error due to pump calibration errors. However, this effect is not large enough to account for the difference in the total and soluble sulfur at the Bondville site (Table 1). Therefore, we think the sulfur difference in Table 1 is probably due to the total sulfur measurements being too low. Some points to consider in explaining the reason for the sulfur difference are the following:

1. The suggestion that a significant portion of the sulfur was not sulfate, and thus not measured by the wet chemistry method, would produce an error in the opposite direction to that observed.
2. The particle beam used in the PIXE measurements could volatilize some of the sulfur compounds. Although this has been found to be true for some PIXE setups, it has been shown to be absent at the U. C. Davis setup where these measurements were done (T. Cahill, personal communication, 1981).
3. The sulfate measurements by the wet chemical method could be enormously high. Very recent results by our analytical laboratory group have established that high phosphate levels (present in a small percentage of rain samples) can result in enormously high sulfate measurements (F. McGurk, personal communication, 1981). If soluble phosphate is present in the aerosol extraction samples, then this could explain the sulfur difference in Table 1.
4. No particle size connection was made for sulfur in the PIXE measurements because sulfur particle size information was not available. It

Table 2. Comparison of 22 daily aerosol filters for calcium, potassium, and sulfur for the Bondville site (e.g.  $Ca_w$ ) versus the Willard Airport site (e.g.  $Ca_w^*$ ).

<u>Date off</u>	$\frac{Ca_w^* - Ca_w}{Ca_w}$	$\frac{K_w^* - K_w}{K_w}$	$\frac{S_w^* - S_w}{S_w}$
June 13	0.697	-0.446	0.505
15	0.208	-0.188	0.069
16	0.667	0.024	-0.062
17	0.392	-0.317	-0.023
18	0.455	0.094	-0.117
19	4.005	0.173	0.154
20	1.149	0.520	-0.019
21	1.563	-0.032	0.101
22	0.358	-0.153	0.222
23	0.907	0.181	-0.117
24	1.519	-0.165	-0.109
26	0.633	0.224	0.116
27	0.392	0.545	0.083
28	1.348	0.540	0.300
29	0.709	0.740	-0.193
30	1.102	-0.111	-0.052
July 1	1.359	0.086	0.297
26	-0.703	0.092	0.176
27	1.282	0.032	0.105
28	0.959	-0.156	0.061
29	-0.139	0.472	1.108
30	0.001	-0.113	-0.535
Standard Deviation	0.095	0.310	0.308
Standard Error	0.192	0.066	0.066
Mean	0.857	0.092	0.094
Median	0.703	0.059	0.076
Maximum	4.005	0.740	1.108
Minimum	-0.703	-0.446	-0.535

is generally believed that atmospheric sulfur particles are  $< 1$  micron, and thus the connection would not be important. However, if the sulfur is in larger particle sizes, then a connection is necessary and could explain the sulfur difference in Table 1 (T. Cahill personal communication, 1981). For example, if all the sulfate were known to be from sea spray, then the total sulfur PIXE measurements would be increased by +31%. If all the sulfate particles are in the 10-15 micron range, then the connection is + 60%.

Preliminary data for X-ray diffraction measurements on some filters from the Bondville site have shown the presence of significant amounts of gypsum. This might be the real form of some of the sulfur aerosol particles or it could be a result of conversions on the filter during the sample collection interval, which was 3 days for those filters analyzed by X-ray diffraction.

5. Filter handling procedures can result in the loss of those elements found in the larger particles which do not stick to the filter as well as smaller particles.

Additional research is needed to establish why the total sulfur measurements for the Bondville aerosol samples are lower than the soluble measurements.

#### REFERENCES

- Bartlett, J., and G. J. Stensland, 1980: Ambient air filter extraction procedures. In Study of Atmospheric Scavenging, by R. G. Semonin et al. C00-1199-60. 18th Progress Report to the Dept. of Energy, Pollutant Characterization and Safety Research Division, Contract EY-76-S-02-1199, 76-81.
- Cahill, T., personal communication, 1981.
- Flocchini, R. G., P. J. Feeney, R. J. Sommerville, and T. A. Cahill, 1972: Sensitivity versus target backings for elemental analysis by alpha-excited X-ray emission. Nucl. Instrum. Methods, 100, 379-402.
- \_\_\_\_\_, D. J. Shadoan, S. J. Lange, R. A. Eldred, P. J. Feeney, and G. W. Wolfe, 1976: Monitoring California's aerosols by size and elemental composition. Environ. Sci. Technol., 10, 76-82.
- McGurk, F. F., personal communication, 1981.

## CHAPTER 5

### INVESTIGATION OF MULTIVARIATE STATISTICAL METHODS FOR ESTIMATING BACKGROUND LITHIUM IN PRECIPITATION TRACER EXPERIMENTS

Donald F. Gatz

#### INTRODUCTION

The first known tracer experiments on precipitation systems were carried out in the USSR in 1964 (Burtsev et al., 1970), and additional experiments of this type were performed in the USSR between 1965 and 1968 (Shopauskas et al., 1970; Shopauskas et al., 1971; Preobrazhenskaia, 1968). All of these experiments were done as part of the Russian hail prevention program. Thus, anti-hail rockets were used to place the tracer into the cloud, where it was dispersed by explosives. Tracer experiments in the United States began in 1967 with the successful recovery of tracer released from an airplane into a thunderstorm updraft in Oklahoma (Gatz et al., 1969; Dingle et al., 1969). Since then more than 100 precipitation tracer experiments have been carried out worldwide (Gatz, 1977), including those performed as part of the METROMEX project at St. Louis.

Groups from the Battelle Pacific Northwest Laboratories and the Illinois State Water Survey carried out an extensive series of precipitation tracer experiments at St. Louis between 1971 and 1975 (Semonin, 1972; Gatz, 1974; Young et al., 1973, 1974, 1975, 1976, 1977). The Battelle group used as tracers the elements Eu, Ru, Ir, Re, Au, and Ta, while the Water Survey group used Li, In, and Cs.

Assessment of the results of their experiments by the Battelle group (Young et al., 1976, 1977) indicated in a number of cases that more tracer was deposited by the rain system than had been released into it. Initial results of the Water Survey's Li tracer experiments showed similar results. In the case of Li, it was discovered that a substantial natural background was present in the rain, and some means of correcting for that background would be necessary in order to assess the total mass of exclusively tracer Li that was deposited by each storm tagged with the tracer.

A variety of methods have been used to estimate the correction for background tracer material in individual rain events. Gatz and Schickedanz (1975) used the median deposition at sampling sites where the rain stopped before the tracer release began. Because of the strong dependence of deposition on rainfall amount, however, this method would not be generally applicable unless it could be shown that the distribution of rainfall amounts was the same for the group of samplers used to estimate background as for the group of samplers to which the estimate was applied.

The relationship between deposition and rainfall amount was the basis of other attempts to estimate background tracer. Vogel (1975) plotted dry-deposition-corrected (DDC) Li deposition against the amount of rain that fell

after the tracer release began, and subjectively identified one group of samplers where the Li deposition could be considered "background" and another that appeared to contain tracer Li. Gatz and Schickedanz (1975) and Schickedanz and Gatz (1975) tried a similar approach, plotting DDC Li deposition against rainfall separately for samplers where the rain had already stopped before the tracer release began and for samplers where it rained after the release began. These attempts were not successful in showing significantly different relationships between Li deposition and rainfall at the two groups of samplers; thus there was no basis for estimating background tracer depositions.

A similar approach was attempted by Gatz (unpublished). The idea was to identify samples containing tracer by their significant departure (95% confidence, one-tailed test) from the deposition expected (as a function of rainfall) in background rain. Expected values were derived from 32 non-tracer rain events in which soluble Li was measured.

The variation of background Li deposition with rainfall is shown in Fig. 1. The open circles are mean depositions, corrected for dry deposition, grouped according to rainfall. The vertical bars show the 95% confidence intervals for the samples grouped according to rainfall. That is, there is only a 5% chance that a sample in one of these groups would exceed the limit shown. The least-squares regression line (the "critical value" line) through the tops of the error bars (omitting the high values at 37 mm and 84 mm of rainfall) was used as the minimum criterion for identifying samples containing tracer. The "natural deposition" line through the mean values was used as the natural background to subtract from the total deposition to obtain the net tracer deposited in a given sample. Net tracer values were summed over all collectors to obtain the total tracer deposition in an event. Unfortunately the results suggested deficiencies in the method. Five of 11 tracer experiments analyzed in this way gave scavenging efficiencies ranging from 110 to 300%. One probable deficiency in this approach was the failure to identify those 5% of background samples that would naturally meet the criterion.

Since background Li is thought to come at least partially from the earth's crust, other attempts (Gatz and Schickedanz, 1975; Schickedanz and Gatz, 1975) at background estimation were based on a comparison of Li/K ratios in the rain with those of soil. No samples were found in which the Li/K ratio significantly exceeded that of soil. Furthermore, the location of the sites where the highest ratios occurred showed no consistent relationship to the area where meteorological considerations would have predicted that the tracer should have been deposited.

Sometime later, Gatz (1980) showed that the deposition patterns of soluble Li in a series of individual storms were very similar to those of other soluble soil-derived elements, such as Ca, Mg, K, and Na. This suggested that background soluble Li might be predicted from the deposition of these other elements. The statistical technique of principal components regression was selected as a means of predicting Li deposition from the deposition of Ca, Mg, K, and Na, as well as that of water (i.e., rainfall).

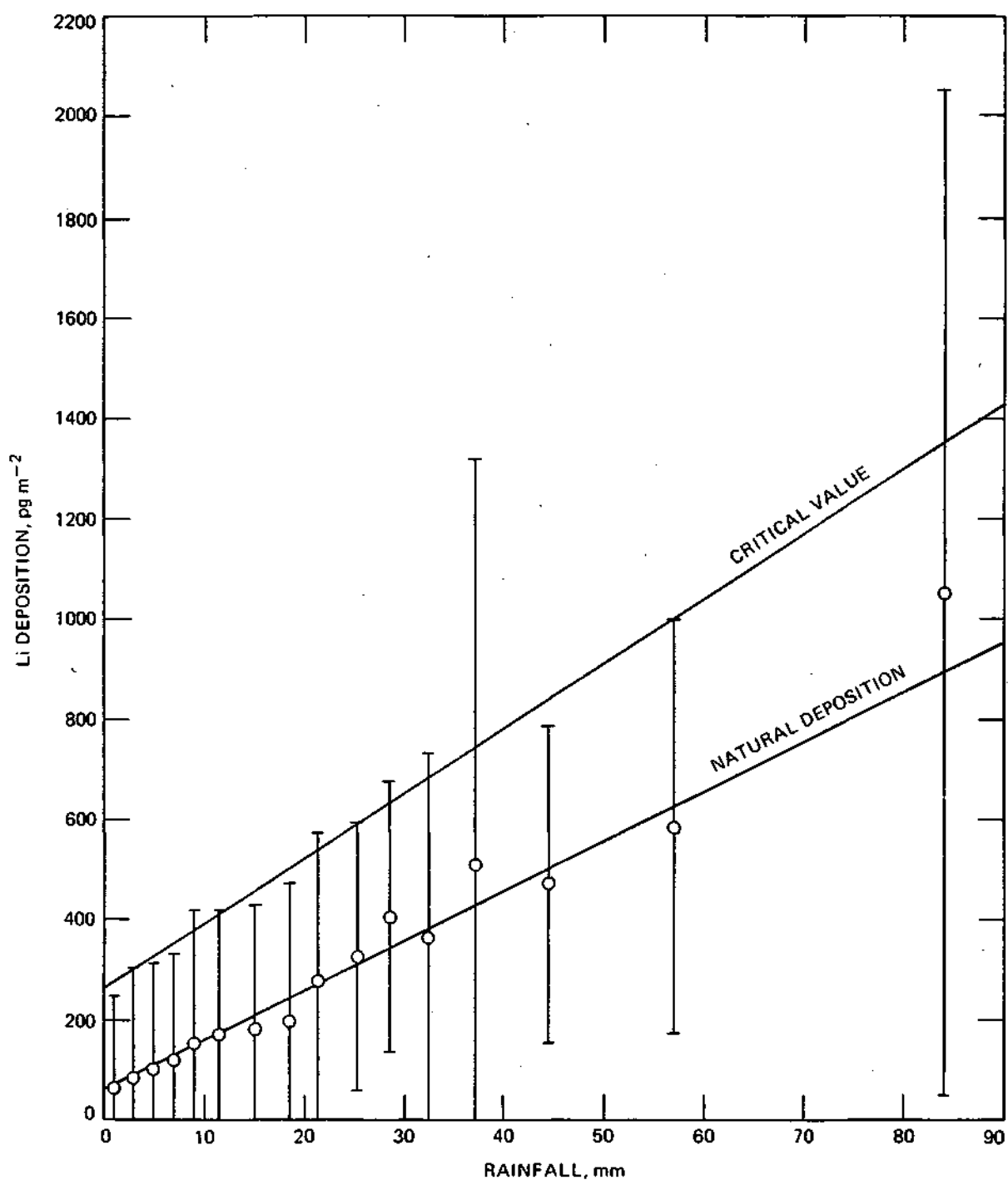


Figure 1. Variation of natural background Li deposition with rainfall amount. See text for details of regression lines shown.

## THEORY

Principal components regression is similar to ordinary multiple regression. That is, there is a dependent variable (in this case Li deposition) and a number of independent variables (in this case rainfall and the depositions of Ca, Mg, K, and Na). The idea is to develop an equation which expresses the dependent variable in terms of the independent variables and their respective coefficients,  $a$ , as in where  $D$  is the dependent variable,

$$D = C + I_1 a_1 + I_2 a_2 + \dots + I_n a_n \quad (1)$$

the  $I$ 's are the independent variables, and  $C$  is a constant. In ordinary multiple regression, problems arise when the  $I$ 's are correlated with each other, which is usually the case with meteorological variables. In principal components regression we avoid this problem, because we use principal components analysis to transform the original variables into new "variables" that are linear combinations of the original variables, and orthogonal to each other (i.e., not correlated). Also, the "new variables" are chosen so that they account for more of the variance in fewer terms than the original variables. For more detailed information on principal components regression, see Massy (1965).

The principal components regression program used was from the BMDP package of statistical computer programs (Brown, 1977). The program performs a principal components analysis and a regression upon the principal components (factor scores). The results are normally expressed as an equation such as Eq. (1), above, where the  $I$ 's are now factor scores. Since, however, the factor scores may be expressed as linear combinations of the original variables, the equation may be transformed into a sum of terms involving the original variables by making the appropriate changes in the values of the coefficients.

## SELECTION OF A DATA SET FOR THE PREDICTION EQUATION

To use principal components regression for estimation of background Li deposition in tracer experiments, methods must be determined for selecting the data set to be used to develop the prediction equations. The procedures followed in this case are described next in two subsections. The first deals with the first broad calculations that led to the realization that it was necessary to use separate prediction equations for each individual experiment studied. The second deals with tests on data from individual rain events that led to the selection of the specific method used for the remainder of the research.

### General Method Development

Three separate tests were performed, each using different data sets, in a step by step approach toward a reasonable method for selection of a prediction data set. The results of all three trials are shown in Table 1.

Table 1. Results of general method development trials.

<u>Predictor set</u>	<u>No. of components entered</u>	<u>Variance explained, %</u>
10 background experiments, all collectors	2	31
10 background experiments, 4 collectors only, from grid "box"	3	45
Single experiments, all collectors		
Expt. 102	4	83
Expt. 206	3	93



As a first trial, it seemed reasonable to use a data set consisting of all valid wet deposition data from all collectors and for all available background experiments (i.e., those where no tracer was released) for which the soluble portions of Ca, Mg, K, and Na were determined. There were 10 such experiments from 1972 to 1975. As shown in Table 1, the principal components regression results explained only 31% of the variance of the data after entering two components, and showed almost no further improvement when additional components were entered. This was not adequate for a prediction set.

Since the data set including all network sites and 10 separate rain events showed little suitability for prediction, the next step was to narrow the data set. For the next trial, the spatial domain was constricted by using data from a few collectors from the same small area of the network. Four collectors from the corners of a grid "box" were selected, and their data from the same 10 background experiments as used in trial 1 were used as the prediction set. Table 1 shows the result; after entering three components, the variance explained had improved to 45%. That was better, but the data set was still not adequate for use as a prediction set.

Since the first two trials using 10 background experiments were not successful, the next step was to constrict the time domain by using data from an individual experiment to predict background Li deposition in the same experiment. Preliminary experiments using all network collectors confirmed, as shown in Table 1, that much higher percent variance explained could be attained. As the table shows, use of all valid collectors from experiments 102 and 206 gave regression equations that explained 83% and 93% of the original variances, respectively.

#### Prediction Using Subsets of Individual Experiments

Preliminary methods testing. Although it was clear at this point that predictions of background Li depositions for individual experiments would have to come from subsets of data from the same experiments, a number of preliminary tests were necessary to establish the sensitivity of the results to various choices regarding the input data. The first choice centered around the independent variables to be used.

Using Experiment 206 (the rain of 9 August 1974), for which Zn was also measured in the soluble portions of the samples and 7 elements were measured in the insoluble portions, in addition to soluble Li, Na, Mg, K, and Ca, I tested the effects of adding additional variables to the data set. The results are shown in Table 2. Data set 1 included rainfall and the set of soluble soil-derived elements which factor analysis had shown (Gatz, 1980) to be deposited in rain in similar patterns to that of soluble Li. As presented previously in Table 1, these variables, with 3 components entered, gave a regression equation that explained 89% of the variance in the data. Data set 2 consisted of the same variables as set 1, plus soluble Zn. Table 2 shows no change in the resulting variance explained. Data set 3 consisted of the same variables as set 2, plus insoluble Li, Na, Mg, K, Ca, Fe, and Zn. Table 2 shows a slight reduction in the variance explained using these additional variables. Thus, there was no benefit from using additional variables beyond those used in data set 1.

Table 2. Effects of adding other measured elements to the principal components regression data set. Experiment 206, rain of 9-10 August, 1974.

<u>Data set</u>	<u>Independent variables used</u>	<u>No. of components entered</u>	<u>Variance explained, %</u>
1	Soluble Na, Mg, K, Ca; rainfall	3	89
2	Set 1, plus soluble Zn	3	89
3	Set 2, plus insoluble Li, Na, Mg, K, Ca, Fe, and Zn	3	85

No matter what method of choosing a prediction set was eventually selected, we would want to be able to estimate the accuracy of a background Li deposition prediction when applied to a tracer experiment. It seemed possible that the accuracy of a Li prediction might be gauged by the accuracy achieved by predictions of some of the other elements in the same experiment, for which predicted and observed values could be compared. Thus, the next test was to compare the accuracies of predicted depositions of soluble Li with those of Na, Mg, K, and Ca in the same background experiment. For prediction of Na, K, Mg, and Ca, the independent variables included rainfall and the remaining elements. Li was not used as an independent variable, so as not to compromise the validity of the non-Li deposition predictions as indicators of the accuracy of the Li prediction.

Three sets of about 20% of the collectors were selected at random from Experiment 206 as the prediction sets, and the predicted depositions were compared against observed depositions in the remaining collectors. The results are given in Table 3 in terms of relative accuracies; i.e., the difference between the predicted values summed over all independent collectors and the same sum for the observed values, expressed as a percent of the observed sum. The results show a substantial variation in accuracy between data sets for each element. Moreover, the highest correlation between accuracy values (not shown) for Li and any other element was 0.75 (56% variance explained) for Ca, not high enough, based on only three values, to pursue further at this time, but high enough to suggest that further investigation could be fruitful.

A third preliminary test was performed to test the sensitivity of the results to the number of components selected for entering in the regression equations. The usual procedure is to select only as many components as have significant F-values to enter, as computed by the BMDP program. In some cases, however, when the F-value is very close to the critical value, it would be helpful to know how sensitive the result is to the choice of the number of components to enter. A test of the effects of adding additional components was performed using Experiment 178, a background rain that fell on 8-9 August 1973. About 50% of the collectors, specifically the first 37 to have the rain stop, were chosen as the predictor set. Results are shown in Table 4 in terms of the relative accuracies of prediction for Li, Na, Mg, K, and Ca, as each additional component is entered, up to a maximum of 4. Triple asterisks (\*\*\*) mark the values that resulted from the normal selection process for components to enter. The table shows that in general, adding additional components does not increase accuracy; in fact, accuracy decreased for three of the five elements as an additional component beyond the conventional number was added. Overall, however, the accuracies showed relatively minor variations as components were successively entered. Thus, it appears that the results are not greatly sensitive to the choice of the number of components to enter.

The results thus far indicate there is no benefit to using additional independent variables beyond those available in most of our experiments, namely soluble Na, Mg, K, Ca, and rainfall. The results do not appear to be overly sensitive to the number of components entered in the regression equation. Finally, it has not been demonstrated that one could use the accuracy of prediction of one of the other available elements to predict the accuracy of the background Li prediction in a tracer experiment.

Table 3. Comparison of predicted and observed deposition for Experiment 206, rain of 9-10 August 1974. For other details of the calculations, see the text.

Data set	N <sub>p</sub> *	N*	Relative accuracy of prediction, %, (R <sup>2</sup> , %)**				
			Li	Na	Mg	K	Ca
1	18	52	2.1 (0.85)	17.1 (0.43)	-15.5 (0.54)	----- (0.21)	2.0 (0.57)
2	15	55	12.2 (0.82)	-21.2 (0.88)	11.7 (0.36)	-5.4 (0.92)	36.6 (0.94)
3	16	54	-18.4 (0.95)	-18.7 (0.76)	2.8 (0.66)	-10.4 (0.93)	2.4 (0.94)

\*N<sub>p</sub> = no. of collectors used to develop prediction equation, each set chosen at random.

N = no. of independent collectors used to verify the prediction.

\*\*Relative accuracy = 100 (sum of predictions - sum of observed)/sum of observed; R<sup>2</sup> is variance explained.

Table 4. Sensitivity of the relative accuracy of deposition prediction to the choice of the number of components to enter in the regression equation. Results are for Experiment 178, rain of 8-9 August 1973.

Component added	$N_p^*$	$N^*$	Relative accuracy, %**				
			Li	Na	Mg	K	Ca
1	37	33	-15.4	.0.6	-8.8	9.1	-2.9
2	37	33	-14.6***	0.1***	-9.4***	9.8***	-1.5
3	37	33	-17.0	1.9	-3.3	9.0	-4.5***
4	37	33	-17.5	2.4	-2.9	9.1	-5.0

\* $N_p$  = no. of collectors used to develop prediction equations; first 37 gages to have rain stop.

$N$  = no. of independent collectors used to verify the prediction.

\*\*Relative accuracy =  $100 (\text{sum of predictions} - \text{sum of observations}) / \text{sum of observations}$ .

\*\*\*Relative accuracy values obtained using prediction equations where the number of components entered was based on having a significant F-value to enter.

The remaining task is to develop a strategy for selecting the subset of collectors from an individual experiment to use as the prediction set. This subject is treated next.

Selection of subsets of collectors. Three different methods of selecting a subset of collectors as the prediction set was tried. The three methods involved the use of 1) "low collectors," 2) the first collectors to have rain stop, and 3) randomly-selected collectors.

The idea for "low collector" method arose from test calculations involving the use of data from all collectors in a given experiment to "predict" the results of the experiment. Comparison of predicted and observed depositions at individual collectors always gave a range of results in which some collectors received more deposition than predicted and some less. The thought occurred that perhaps it would be reasonable to assume that those collectors that showed an excess of observed over predicted Li deposition actually received tracer Li, and the remaining "low" collectors could be used as the prediction set. Results are given in Table 5. The results show that use of the "low collectors" consistently underpredicted Li deposition in three background experiments. The differences between predicted and observed values were, moreover, significant at the 95% confidence level for both parametric and non-parametric tests. Thus, use of the "low collectors" as a way to obtain the prediction set was abandoned.

The next thought was to use as predictors only those collectors where the rain stopped before the tracer release began. Such a group of collectors would have received rain from the same rain system as the rest, but could not have received any tracer Li, and thus would be ideal collectors to use as a prediction set. The idea was quite reasonable, but not always practical, since if the tracer release started as soon as the rain entered the network, which was often the case, the prediction set would be empty. However, by choosing as the prediction subset a certain portion of the collectors at which the rain stopped first, one would ensure that any collectors at which the rain stopped before the tracer release began would be included in the prediction subset. Results are shown in Table 6 for three background experiments. For two of the experiments, subsets of two different sizes were used to test whether the results were dependent on the size of the subset. The results show some improvement over the previous method. For Experiments 172 and 178, one of the selected data subsets predicted depositions that were not significantly different from those observed. However, the results were also somewhat inconsistent. The difference between predicted and observed deposition appears to vary with the exact subset chosen as the prediction set. For example, the subset of 20 from Experiment 178 gave results which were not significantly different from those observed, while in the same experiment the subset of the first 37 collectors to have rain stop estimated deposition significantly less than what was observed at the independent collectors. Therefore, the use of the first collectors to have rain stop as the prediction subset was also abandoned.

The remaining option was to choose a random selected fraction of the collectors to serve as the prediction set. For later use on tracer experiments, the fraction should be kept as small as possible to minimize the

Table 5. Summary of results of principal components regression method for estimating background tracer deposition using "low collectors" as the prediction set.

Exp. no.	No. of collectors		No. of components entered	Variance explained, %	Li deposition, g	
	Prediction set	Evaluation set			Predicted	Observed
172	20	15	1	83	451	684
178	43	27	2	70	1132	1898
206	38	32	3	96	269	651

Exp. no.	Difference* in deposition		Difference significant at 95% confidence level?	
	Mass,g	Relative,**%	T test	Wilcoxon test
172	-233	-34	yes	yes
178	-766	-40	yes	yes
206	-382	-142	yes	yes

\*Predicted minus observed.

\*\*100 (predicted-observed)/observed.

Table 6. Summary of results of principal components regression method for estimating background tracer deposition using the first collectors to have the rain end as the prediction set.

Exp. no.	No. of collectors		No. of components entered	Variance explained, %	Li deposition, g	
	Prediction set	Evaluation set			Predicted	Observed
172a	13	22	5	98	627	638
172b	17	18	4	97	481	528
178a	20	50	3	94	2227	2308
178b	37	33	3	79	1465	1765
206	20	50	4	81	1323	1187

Exp. no.	Difference* in deposition		Difference significant at 95% confidence level?	
	Mass, g	Relative, **%	T test	Wilcoxon test
172a	-47	-8.9	no	no
172b	-11	-1.7	yes	no
178a	-81	-3.5	no	no
178b	-300	-17.0	yes	yes
206	136	11.4	yes	yes

\*Predicted minus observed

\*\*100 (predicted-observed)/observed.



chance that a collector with tracer in it would be included in the prediction set. Experience with the data had shown that prediction accuracy seldom improved as the number of collectors in the prediction set increased beyond about 20. Since a full network data set consisted of about 80 collectors, the method chosen was to select randomly about 25% of the collectors for the prediction set.

Previous background predictions had been made only for the independent collectors, i.e., those not used in the prediction set, so as to provide a valid test of the prediction equation. It was also realized at this point, however, that for use in tracer experiments the predicted total background Li deposition would have to cover the entire network. Therefore, the predictions made and discussed in this section, while based on prediction sets of about 20 collectors, predict deposition at all network collectors with valid data.

Since previous results had shown that the difference between predicted and observed Li deposition in background experiments varied, sometimes quite markedly, from one randomly-chosen prediction set to another, some information on the uncertainty in an individual prediction was needed. Thus, for each of the three background experiments, 10 separate prediction sets were chosen at random from the collectors with valid data. For each prediction set a principal components regression equation was developed and used to predict background Li deposition over the whole network. This prediction was compared against the observed network deposition, and relative errors were computed for each prediction. Results are shown in Table 7. For the three experiments combined, the errors ranged from -48.9% (i.e., predicted Li deposition was less than observed) to +64.8% (i.e., predicted Li deposition was greater than observed). The median error was +5.0%.

A normal probability plot of the relative errors was made to check for a normal distribution, but normality could not be verified. Therefore, confidence intervals are expressed non-parametrically. The 95% confidence interval ranged from -22.8% to +22.9% relative error, and about 50% of the values, centered on the median, were in the range -8% to +14%.

Thus, for a single randomly-chosen set of predictor collectors, we may expect the prediction to be within roughly 10% of the observed deposition about 50% of the time, and within 20% about 95% of the time, for background experiments.

To assess the usefulness of such a background prediction method, we must translate these uncertainties to Li masses in a typical experiment and see what they imply for the accuracy of measuring the actual tracer Li deposited. Table 8 shows the observed Li deposition in three background experiments, along with 10% (50% confidence) and 20% (95% confidence) uncertainties.

Tracer Li mass released from an airplane in 9 experiments ranged from 90 g to 710 g. It is instructive to calculate the resulting uncertainties assuming that 710 g of Li had been released into each of these tracer experiments, and all of it had been deposited in the sampling network. Table 9 shows the results of such a series of calculations for both 50% and 95% confidence limits. For example, in Experiment 172, if all 710 g of tracer had been

Table 7. Comparison of observed and predicted deposition using ten different randomly-selected sets of about 20 collectors as prediction sets, in each of 3 background experiments.

Exp. no.	Prediction set	No. of predictor collectors	$R^2$	Li deposition, g		$\frac{P-0}{0}(100)$
				Observed	Predicted	
172	1	19	0.802	1220	1454	19.2
	2	24	0.920	1220	1276	4.6
	3	21	0.961	1220	1381	13.2
	4	19	0.890	1220	1416	16.0
	5	22	0.890	1220	1135	-7.0
	6	17	0.958	1220	1499	22.9
	7	19	0.833	1220	1346	10.4
	8	14	0.907	1220	1165	-4.5
	9	16	0.793	1220	1391	14.0
	10	19	0.924	1220	1412	15.7
178	1	26	0.813	3218	2868	-10.9
	2	17	0.868	3218	2922	-9.2
	3	19	0.916	3218	3244	0.8
	4	11	0.885	3218	3695	14.8
	5	20	0.768	3218	3771	17.2
	6	19	0.729	3218	3161	-1.8
	7	25	0.853	3218	3392	5.4
	8	19	0.838	3218	2484	-22.8
	9	22	0.703	3218	5304	64.8
	10	21	0.638	3218	2618	-18.6
206	1	28	0.907	1494	1258	-15.8
	2	18	0.993	1494	1748	17.0
	3	21	0.902	1494	764	-48.9
	4	18	0.867	1494	1551	3.9
	5	24	0.969	1494	1219	-18.4
	6	17	0.916	1494	1639	9.7
	7	15	0.976	1494	1591	6.6
	8	19	0.989	1494	1692	13.2
	9	21	0.936	1494	1518	1.6
	10	17	0.949	1494	1174	-21.4

Table 9. Illustration of effects of uncertainty in tracer background estimates on scavenging efficiency calculations.

Exp. no.	"Predicted" background deposition, g	"Observed" deposition, g	Tracer "released," g	50% Confidence limits on "background" upper, lower, g		50% Confidence limits on "scavenging efficiency" upper, lower, %	
172	1220	1930	710	1342	1098	117	83
178	3218	3928	710	3540	2896	145	55
206	1494	2204	710	1643	1345	121	79

Exp. no.	95% Confidence limits on "background" upper, lower, g		95% Confidence limits on "scavenging efficiency" upper, lower, %	
172	1464	976	134	66
178	3862	2574	191	9
206	1792	1196	142	58

deposited in the network, and if we had predicted the background exactly (but only knew with 95% confidence that it was between 976 g and 1464 g), then the calculated net tracer deposition would be (with 95% confidence) between  $1930 - 1464 = 466$  g and  $1930 - 976 = 954$  g. This corresponds to a 95% confidence interval for the scavenging efficiency of  $100 (466/710) = 66\%$  and  $100 (954/710) = 134\%$ . The other two background experiments show even wider 95% confidence intervals. The 50% confidence intervals are narrower, of course, but the chances that the true value is in that interval are only 50%.

Moreover, these confidence intervals are very likely conservative estimates, since, 1) the calculation used the maximum tracer released, 2) it is likely that less than 100% of the tracer would be deposited in the network, even if all of it reached the ground, and 3) because there is an additional uncertainty associated with a deposition estimate from a network of discrete samplers in an area, the "observed deposition" value will also have an uncertainty, and this will increase the total uncertainty of the scavenging coefficient estimate.

#### CONCLUSION

There are both positive and negative aspects to this result. The negative aspect is the most apparent: principal components regression has not been shown to provide a method of predicting background Li with an accuracy sufficient to yield useful estimates of the scavenging efficiency. Thus, to date no method has been found which will allow an accurate estimate of net tracer Li deposition in tracer experiments.

The positive aspects of the result center around the obvious conclusion that background must be carefully assessed in designing any future experiments of this kind. This analysis has improved our knowledge about how to do it. This assessment should, of course, include sampling and analysis of the same kind of rain events (i.e., convective or non-convective, heavy or light rain) in the same location where the tracer experiments will take place. However, even if the background levels of the tracer material are found, from such sampling and analysis, to be less than detectable, an analysis like that made in this paper must still be done, using detection limit values to assess potential uncertainties. Furthermore, the overall assessment must take account of the uncertainty in the "observe" deposition from a network of discrete samplers, and its effect on the feasibility of the experiment.

#### REFERENCES

Brown, M. B., Editor, 1977: BMDP-77 Biomedical Computer Programs, P-Series, University of California Press, Berkeley, 880 pp.

- Burtsev, I. E., L. V. Burtseva, and S. G. Malakhov, 1970: Washout characteristics of a P-32 aerosol injected into a cloud. Atmospheric Scavenging of Radioisotopes, Symposium Proceedings. Palanga, USSR, June 7-9, 1966, pp. 242-250. Israel Program for Scientific Translation, Jerusalem.
- Dingle, A. N., D. F. Gatz, and J. W. Winchester, 1969: A pilot experiment using indium as tracer in a convective storm. J. Appl. Meteor., 8, 236-240.
- Gatz, D. F., 1974: METROMEX: Air and rain chemistry analyses, Bull. Amer. Meteor. Soc., 55, 92-93.
- \_\_\_\_\_, 1977: A review of chemical tracer experiments on precipitation systems. Atmos. Envir., 11, 945-953.
- \_\_\_\_\_, 1980: Associations and mesoscale spatial relationships among rain water constituents. J. Geophys. Res., 85 (C10), 5588-5598.
- \_\_\_\_\_, and P. T. Schickedanz, 1975: Complex lines of 13 August 1973. In: Changnon, S. A., and R. G. Semonin, Editors, Studies of Selected Precipitation Cases from METROMEX. Report of Investigation 81, Illinois State Water Survey, pp. 269-321.
- \_\_\_\_\_, A. N. Dingle, and J. W. Winchester, 1969: Detection of indium as an atmospheric tracer by neutron activation. J. Appl. Meteor., 8, 229-235.
- Huff, F. A., and S. A. Changnon, 1975: Storms of 11 August 1972. In: Changnon, S. A., and R. G. Semonin, Editors, Studies of Selected Precipitation Cases from METROMEX. Report of Investigation 81, Illinois State Water Survey, pp. 11-67.
- Massy, W. F., 1965. Principal components regression in exploratory statistical research. Amer. Statis. Assoc. Journ., 60, 234-256.
- Morgan, G. M., G. L. Achtemeier, and H. T. Ochs, 1975: Squall line of 12 August 1973. In: Changnon, S. A., and R. G. Semonin, Editors, Studies of Selected Precipitation Cases from METROMEX. Report of Investigation 81, Illinois State Water Survey, pp. 232-267.
- Preobrazhenskaia, E. V., 1968: Detection of copper traces in precipitation in cases of cuprous sulfide modification of convective clouds. Glavnia Geofisicheskaiia Observatoriia, Trudy, No. 224, 169-175.
- Schickedanz, P. T., and D. F. Gatz, 1975: Severe storms of 23 July 1973. In: Changnon, S. A., and R. G. Semonin, Editors, Studies of Selected Precipitation Cases from METROMEX. Report of Investigation 81, Illinois State Water Survey, pp. 91-126.
- Semonin, R. G., 1972: Tracer chemical experiments in Midwest convective clouds. Reprints, Third Conference on Weather Modification, Rapid City SD, June 26-29, Amer. Meteor. Soc., Boston, pp. 83-87.
- \_\_\_\_\_, 1973: METROMEX chemical tracer studies. In: Huff, F. A., Editor, Summary Report of METROMEX Studies, 1971-1972. Report of Investigation 74, Illinois State Water Survey, pp. 125-129.

Shopauskas, K., B. Styra, and E. Vebra, 1971: Spreading and rainout of passive admixture injected into a cloud. Symposium Proceedings, Prague, Czechoslovakia, and Vienna, Austria, Sept. 18-24, 1969, pp. 340-346. Supplement Volume of the Proceedings of the 7th International Conference on Condensation and Ice Nuclei, Academia, Prague.

\_\_\_\_\_, \_\_\_\_\_, B. K. Vebrene, S. S. Shalaveyus, and D. A. Shopauskene, 1970: Washout of radioisotopes injected into a cloud from data of ground observations. Atmospheric Scavenging of Radioisotopes, Symposium Proceedings, Palanga, USSR, June 7-9, 1966, pp. 233-241, Israel Program for Scientific Translations, Jerusalem.

Vogel, J. L., 1975: Airmass storms of 10 August 1973. In: Changnon, S. A., and R. G. Semonin, Editors, Studies of Selected Precipitation Cases from METROMEX Report of Investigation 81, Illinois State Water Survey, pp. 192-231.

Young, J. A., T. M. Tanner, C. W. Thomas, and N. A. Wogman, 1973: Tracer and pollution studies during METROMEX. Annual Report to the U.S. Atomic Energy Commission, Division of Biomedical and Environmental Research, Vol II, Part I, pp. 98-100, Battelle Pacific Northwest Laboratory, BNWL-1751 PT1.

\_\_\_\_\_, \_\_\_\_\_, and \_\_\_\_\_, 1974: The entrainment of tracers near the sides of convective clouds. Annual Report to the U.S. Atomic Energy Commission, Division of Biomedical and Environmental Research, Part 3, pp. 146-147, Battelle Pacific Northwest Laboratory, BNWL-1850 PT3.

\_\_\_\_\_, \_\_\_\_\_, and \_\_\_\_\_, 1975: The entrainment of tracers near the sides of convective clouds. Pacific Northwest Laboratory Annual Report for 1974 to the USAEC Division of Biomedical and Environmental Research, BNWL-1950 PT3, UC-11, pp. 140-142.

\_\_\_\_\_, \_\_\_\_\_, and \_\_\_\_\_, 1976: The entrainment of tracers near the sides of convective clouds. Pacific Northwest Laboratory, Annual Report for 1975 to the USERDA Division of Biomedical and Environmental Research, Part 3, Atmospheric Sciences, BNWL-2000 PT3, pp. 179-184.

\_\_\_\_\_, \_\_\_\_\_, and \_\_\_\_\_, 1977: The entrainment of tracers into convective clouds at 10,000 to 13,500 feet near St. Louis. Proceedings of Precipitation Scavenging Symposium (1974), Champaign, IL, Oct. 14-18, 1974, U.S. Energy Research and Development Administration, ERDA Symposium Series 41, CONF-741003, available for \$10.50 from National Technical Information Service, U.S. Department of Commerce, Springfield, VA 22161.

## CHAPTER 6

### DESIGN OF A FEASIBILITY STUDY TO ASSESS THE IMPACT OF PRECIPITATION QUALITY ON SOIL WATER QUALITY

Van C. Bowersox

#### INTRODUCTION

Available wet deposition data for the last 5 years in the eastern United States have shown conclusively that incident rains and snows are acidic with respect to the  $\text{CO}_2$  equilibrium (i.e., pH 5.6). A central issue in studies of precipitation quality relates to the impact of this relatively acidic precipitation on terrestrial and aquatic ecosystems. Most attention has been drawn to the potentially deleterious effects of acid precipitation on the aquatic life of sensitive freshwater lakes (Schofield, 1976). Due to the complicated dynamics of drainage basins and the difficulty in obtaining representative measurements, little is known about the effects of acid precipitation on the fishlife of streams and rivers (Arnold, Light, and Dymond, 1979). Perhaps even less is known about the effects on soils, except to identify soil regions most likely to be sensitive to acid inputs (McFee, 1980).

#### EXPERIMENT DESIGN

Given the dearth of available information on the interactions of precipitation water quality on soils, a study has been designed to address the feasibility of tracing the contribution of precipitation chemistry to soil water chemistry in unsaturated soils (i.e., in soil generally above the water table). This investigation will be limited to the suite of anions and cations that constitute the major inorganic ions in precipitation; i.e., sulfate, nitrate, chloride, calcium, magnesium, sodium, potassium and H ion (measured as pH). Titrations will also be performed to measure total acidity/alkalinity. Complementary analyses will be performed of the soil matter to determine the soil buffering capacity and the soil ion exchange capacity. It is hoped that information about precipitation chemistry, soil water chemistry, and soil chemistry can then be integrated in such a way as to assess the impact or potential effects of rainfall quality on soil chemistry. Changes in soil chemistry, of course, could either enhance or degrade the agricultural productivity of soils for certain crops.

The experimental design requires two measurements of time dependent or event dependent quantities, precipitation chemistry and soil water chemistry, and one (presumably) secular quantity, soil chemistry. All of these measurements are to some extent site specific; and so the study will be performed at

a well defined site, the Bondville site operated under this contract. The chemistry of Bondville soils will be measured under laboratory conditions. Wetfall chemistry will be determined on samples collected on daily, weekly, and monthly time intervals with wet/dry deposition collectors (after the HASL design), routinely operated as part of the Bondville site measurements program. For purposes of this study, the measurement of soil water chemistry involves a little tested application of soil water sampling instrumentation. Much of the effort in this feasibility study will be directed toward developing a routine soil water sampling methodology which will yield results appropriate for adjudging the impact of precipitation quality on soil chemistry.

Soil water will be extracted from unsaturated (above the water table) soils using a lysimetric device buried in the soil at several pre-chosen depths. The lysimeter has two structural components, a 1 7/8 inch O.D. PVC pipe, for containing collected water, and a rounded-bottom, porous, ceramic cup, 2 inches in length and 1 7/8 inches in diameter, for collecting water. This cup is fixed to one end of the pipe and the other end of the pipe is sealed (see Fig. 1). The porous cup is a non-vitreous ceramic porcelain, fired from kaolin clay, ball clay, and alumina. These materials are relatively stable and inert, though trace quantities of exchangeable calcium (CaO), magnesium (MgO), sodium (Na<sub>2</sub>O), and potassium (K<sub>2</sub>O) are present (Leonard, Meyer and Wilkinson, 1979). Entrainment of solids by soil water percolating into the system is limited by the 1-2 micron pore size of the cup material. Collected water is removed from the buried lysimeter through access tubes which are exposed at the soil surface. Installation of the lysimetric sampler is effected by auguring a 3 inch hole to the desired depth, inserting the apparatus (porous cup down), then backfilling the hole with the removed soil (see Fig. 1). Once in place, sampling is initiated by drawing a vacuum of about 15-20 inches of mercury on the system. This vacuum is maintained by clamping the access tubes. Soil water migrates toward the evacuated chamber and through the cup, against the soil moisture and gravitational forces, affecting its natural percolation through the soil. The rate at which the collection proceeds is very dependent on soil moisture content. At least 24 hours is needed for an appreciable water volume to be collected (Leonard, Meyer, and Wilkinson, 1979).

Collected samples will receive the same care in handling as precipitation samples (Peden, Skowron, and McGurk, 1979).

Sampler operation will be evaluated at several depths at a single site (Bondville). Since most chemical and biological activity related to crop growth occurs in the A horizon, that soil layer will be emphasized. Pairs of samplers will be installed at plow layer depth (~ 8") and at the full A horizon depth (~ 15") for Bondville soils. These paired values will be intercompared to get some measure of point variability and intercompared to address the question of soil water changes with depth. In addition, one sampler will be located in the B horizon and one in the C horizon beneath, to further identify any depth dependence and, in particular, to ascertain whether inputs from precipitation are traceable to those depths.



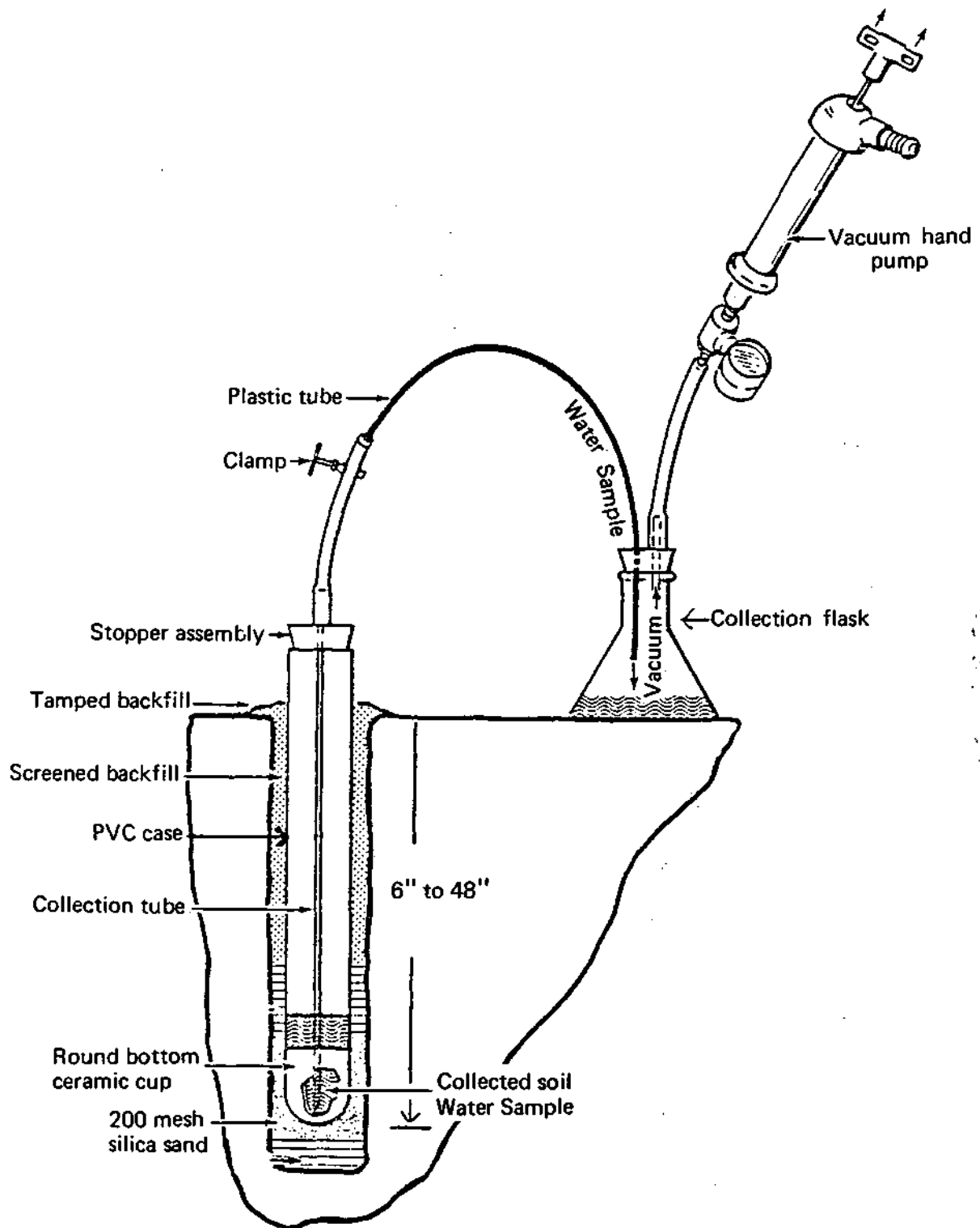


Figure 1. Typical Field Installation of Lysimeter Assembly for Soil Water Sampling

(Source: Soilmoisture Equipment Corp., Santa Barbara, CA)

## SUMMARY

A summary of the tasks and objectives of this feasibility study include:

- (1) measuring the chemistry of incident precipitation on time scales of days, weeks, and months;
- (2) assaying the soil chemistry of Bondville soils, e.g., soil exchange capacity and pH;
- (3) collecting soil water and measuring the chemistry of these samples at several depths; this involves (a) defining a requisite cleaning protocol for soil water samples, e.g., acid wash (recommended by Johnson and Cartwright, 1980), (b) assessing potential for systems or handling errors from contamination, i.e., determining chemical 'blank' levels, (c) determining optimum sampling protocol to obtain usable results for comparison with precipitation chemistry, (d) identifying constituents, if any, which are little affected by contact with soils and can be used as tracers of precipitation, and (e) developing a depth profile of soil water chemistry from which to infer depth dependence; and
- (4) integrating data for the chemistry of precipitation, for the chemistry of soils, and for the chemistry of soil water, to ascertain whether the impacts of precipitation quality on soil chemistry can be measured by this technique.

## REFERENCES

- Arnold, D., R. Light, and V. Dymond, 1979: Probable Effects of Acid Precipitation on Pennsylvania Waters. Report No. B0835NAEX to the U.S. EPA, Corvallis Env. Lab. by the PA Coop. Fishery Res. Unit, 328 Mueller Lab., University Park, PA 16802, 24 pp.
- Johnson, T., and K. Cartwright, 1980: Monitoring of Leachate Migration in the Unsaturated Zone in the Vicinity of Sanitary Landfills. IL Institute of Natural Resources, State Geological Survey Division, Urbana, IL, Circular 514, 82 pp.
- Leonard, R., A. Meyer, and M. Wilkinson, 1979: Soil Water Quality Studies with Ceramic Cup Lysimeters. Report No. KS-5824-M-1, Calspan Corp., P.O. Box 400, Buffalo, NY 14225, 37 pp.
- McFee, W., 1980: Sensitivity of Soil Regions to Acid Precipitation. Report No. B0531NAEX to the U.S. EPA, Corvallis Env. Lab. by the Dept. of Agronomy, Purdue Univ., West Lafayette, IN 47907, 179 pp.

Peden, M., L. Skowron, and F. McGurk, 1979: Precipitation Sample Handling, Analysis, and Storage Procedures. Research Report 4 to the U.S. DOE, Pollutant Characterization and Safety Research Division, Office of Health and Environmental Res. by the Illinois State Water Survey, University of Illinois, Urbana, IL, 71 pp.

Schofield, C., 1976: Acid Precipitation: Effects on Fish. Ambio, 5, 228.

## CHAPTER 7

### A NEW SEARCH FOR OLD EVIDENCE TO IDENTIFY TRENDS IN THE CHEMISTRY OF PRECIPITATION IN THE CONTINENTAL UNITED STATES

Van C. Bowersox

#### INTRODUCTION

Trend analyses of the record of precipitation chemistry in the United States have, for the most part, focused on two short-duration (< 5 yrs.) nationwide networks, one in the mid-1950's (Junge and Gustafson, 1956) and one in the mid-1960's (Lodge et al., 1968), and on data collected in the 1970's at various local and regional scale sampling networks (Cogbill, 1976). Spatially summarized data from the mid-1950's and mid-1960's data sets have suggested a dramatic increase in the extent of areas (mostly in the Midwest) where incident rains exhibited a net acidity with respect to the CO<sub>2</sub> equilibrium. These apparent changes served as the basis for interpreting the increased combustion of fossil fuels as the cause for decreased precipitation quality (Likens, Bormann, and Johnson, 1972). Another interpretation of these ~~same~~ data rests on the decreases in dissolved calcium as the effector of lowered pH from the 1950's to the 1960's in the Midwest (Stensland, 1979).

A basic assumption in the first argument is that the differences between 1950's and 1960's data reflect a smoothly varying change in precipitation quality over that decade; and that a cause/effect relationship existed between the gradual increase in SO<sub>x</sub> and NO<sub>x</sub> emissions and the increase in precipitation acidity over the eastern U.S. Testing the validity of this assumption requires a more complete record of precipitation chemistry data covering the time prior to the mid-1950's and the periods intervening the 1950's, the 1960's, and the 1970's data sets. This information can be compared to the more complete record for emissions to discern the nature of the relationship between trends in emissions and long term changes in deposition. Such information could be used to determine whether regional-scale acid rain is a recent phenomenon (post-1950) of the eastern U.S. or whether its history extends to earlier times and to other places.

#### SUMMARY OF SEARCH

To obtain additional data for the chemistry of precipitation in the U.S., abstracted literature and bibliographies are being searched for referred articles and other publications which may contain data in either interpreted or raw form. The search entails meteorological, chemical, and agricultural sources. Articles and other literature cited are further researched for possible unpublished sources of information, and this information is then solicited from the appropriate individuals and/or organizations.

Data that are obtained from this search are being composited by decades so that 10-year summaries of the chemistry of precipitation over large areas can be developed. This tack is being pursued because few sampling efforts at a given location have extended beyond about 5 years. It is necessary, therefore, to composite information from various locations over some rather arbitrarily defined time period (e.g., 10 yrs.). Results reported for essentially all inorganic ions are being considered in these summary analyses and displays. In addition, evaluations of potential biases and of data representativeness are being made, based on the following factors:

- location of sampling effort (e.g., urban, remote)
- siting criteria (i.e., proximity to potential biasing sources such as power plants, shorelines, etc)
- sample collection and sample handling equipment and procedures (i.e., sampling protocol)
- laboratory and analytical techniques
- extraneous contamination sources (e.g., "sampling equipment provided an inviting perch for birds")

The 10-year data summaries will be interpreted in retrospect to climatologic records, distribution of known natural and anthropogenic sources, land use patterns, and trends in fossil fuel consumption.

To date, new sources of old data have been uncovered for the 1920's and 1930's for the states of Illinois, Indiana, Iowa, and Minnesota in the Midwest, for the states of Tennessee, Kentucky, and Virginia in the Southeast, for New York in the Northeast, and for Texas.

#### REFERENCES

- Cogbill, C, 1976: The History and Character of Acid Precipitation in Eastern North America. Mater, Air, and Soil Pollution, 6, 407-413.
- Junge, C, and P. Gustafson, 1956: Precipitation Sampling for Chemical Analysis. Bull. Amer. Meteor. Soc, 37, 244-245.
- Likens, G., F. Bormann, and N. Johnson, 1972: Acid Rain. Environment, 14, 33-40.
- Lodge, J., et al., 1968: Chemistry of U.S. Precipitation. National Center for Atmospheric Research, Boulder, CO, 66 pp.
- Stensland, G., 1979: Calculating Precipitation pH with Application to the Junge Data. Chapter 8 of the Seventeenth Progress Report to the U.S. DOE, Pollutant Characterization and Safety Research Division, Contract EY-76-S-02-1199, pp. 79-108.

## CHAPTER 8

### SEASONAL PRECIPITATION CONCENTRATIONS AND DEPOSITIONS FOR NORTH AMERICAN FROM THE CANSAP/NADP NETWORKS

Richard G. Semonin

#### INTRODUCTION

There are two major North American precipitation chemistry networks currently in operation with a total of 126 stations. The first of these is the Canadian Network for Sampling precipitation (CANSAP) which began operations in the spring of 1977 and currently has 49 stations. The second is the National Atmospheric Deposition Program (NADP) network which began operations in later summer 1978 and currently has 79 stations providing samples for analysis. There are other networks for specific research purposes, notably the MAP3S (Multi-State Atmospheric Power Production Pollution Study), SURE (Sulfate Regional Experiment), and others that have varying sampling protocols, different sampling equipment, and separate analytical facilities for analysis. In addition, these research networks are localized in a region as opposed to the national CANSAP and NADP networks.

In this chapter, we shall describe the differences between the two network operations regarding sampling protocol and analysis procedures. We will then present the first results from combining the data sets to describe the seasonal variation of precipitation chemistry and the resulting annual picture.

#### DATA SOURCES AND SAMPLING LIMITATIONS

##### CANSAP Network

The Canadian stations are typically located at weather observing stations at airports in relatively rural settings. The sample collection is carried out by the duty personnel at these stations. The wet-only sampler inhibits the collection of dust and other foreign matter since it is only open during periods of precipitation. The collected sample is changed usually once per month although many factors may alter the schedule by a few days in extreme cases. The samples are analyzed by the Inland Waters Directorate Water Quality Laboratory at the Canada Center for Inland Waters in Burlington, Ontario.

The analyses include pH, conductivity, sulfate, nitrate, chloride, ammonium, sodium, potassium, magnesium, and calcium. Two measures of precipitation are reported. The first of these is the volume of the sample in the collector bucket and the second is the derived rainage volume associated with the sample collection interval.

### NADP Network

In contrast to the CANSAP network, the NADP stations are typically located at Agricultural Experiment Stations, in National Parks, or Forest Experiment Stations. Nearly all of the sites are relatively free from nearby point or areal sources of pollution. The samples are collected through the use of employees of the various institutions supporting the sampling effort. The wet-dry sampler also inhibits the collection of dust and other foreign matter into the precipitation since a rain switch, similar to that employed in the CANSAP network, is utilized to uncover one side of a 2-bucket collector. The sampling protocol dictates that the dry side of the equipment be removed once each 8 weeks for analysis at a central laboratory. The sample is changed each Tuesday of every week throughout the year and only rarely are there exceptions to this schedule.

The samples are shipped to a central laboratory at the Water Survey for analysis. The analysis includes the same items listed for the CANSAP network.

### SEASONAL AND ANNUAL DATA ANALYTICAL PROCEDURES

The monthly Canadian data were obtained on magnetic tape and converted to map coordinates for eventual objective plotting by computer methods. In order to blend the United States and Canadian data together the NADP samples had to be composited on a monthly basis to simulate the Canadian data. The very simple approach was taken to accumulate 4 weeks (occasionally 5) of NADP data corresponding to individual months through precipitation weighing of the samples collected in that interval. The result of this calculation produced a data set of monthly data (plus or minus 2 days) which corresponded to the monthly data in Canada.

The next step was to perform the same calculation using the monthly or simulated monthly data to acquire a seasonal average. The seasons are the climatologically defined periods of December-January-February for winter, March-April-May for spring, June-July-August for summer, and September-October-November for fall. The three monthly values were combined through precipitation weighing and then divided by three to get a monthly mean representative of each of the seasons.

The annual mean was obtained in much the same way as the seasonal values but extended throughout the each 12-month period (or fraction thereof) and then averaged for the 2+ years since the networks were in operation. One should be cautioned, however, that not all stations in the NADP have equal numbers of samples to incorporate in the averaging process. Some sites, particularly in the northeast, have been in operation since the fall of 1978 whereas certain sites in the middle west and west have only been in operation for less than a year. However, we have taken the liberty to incorporate all data into this analysis.

With the data set described above, the computer program which has been used extensively in the past to analyze scalar fields (Achtemeier et al., 1977) was used to objectively analyze the various precipitation chemistry constituents. In the following, the seasonal maps for calcium, ammonium, nitrate, sulfate, and pH will be shown. The annual distribution of each of these variables as well as the average precipitation volumes collected will also be shown.

## SEASONAL CONCENTRATION DISTRIBUTIONS

### Calcium

The major features of the calcium concentration shown in Fig. 1 include a sizable maximum over lower Alberta and Saskatchewan extending into the northern Great Plains with secondary maxima located in the southwest U.S. and in lower Ontario paralleling Lakes Erie and Ontario. The Midwest and Southeast are relatively featureless as can be seen in Fig. 1.

The winter calcium concentration distribution (Fig. 2) shows a number of maxima of calcium concentration all centered in Canada but close to the U.S. border. The major fall maximum in Alberta is still present in winter as is a secondary maximum along and parallel to the St. Lawrence River valley. A distinct maximum shows up north of Lake Superior which almost suggests a relationship to the famous Sudbury INCO smelter stack. The entire southern half of the United States from the east coast to the west coast is rather featureless in terms of calcium concentrations.

The spring pattern in Fig. 3 is similar although not as intense as the winter pattern with again a major maximum in western Canada extending into the upper Great Plains and a secondary maximum extending from lower Ontario to northeast Quebec. A maximum in south Texas also appears in spring, but this is probably an artifact of sampling and should not be interpreted as a meaningful feature of the pattern.

In Fig. 4, the summer concentration distribution maintains the primary features that have been shown for the previous three seasons, that is, a maximum in Saskatchewan with a secondary maximum through southern Ontario along Lake Erie and Lake Ontario. This summer distribution is very similar to that obtained for the fall season shown in Fig. 1.

The relatively high concentrations that appear in the seasons in the west may be easily rationalized as due to agricultural practices and the potential source of dust in that semi-arid region. However, of more interest, and some significance, is the relative maximum observed in each of the four seasons along the Lake Erie-Lake Ontario-St. Lawrence River valley area of southern Ontario and Quebec. It is difficult to imagine that this feature is associated with agriculture. One would certainly expect that an equal well-defined maximum should appear over the great agricultural areas of the Midwest



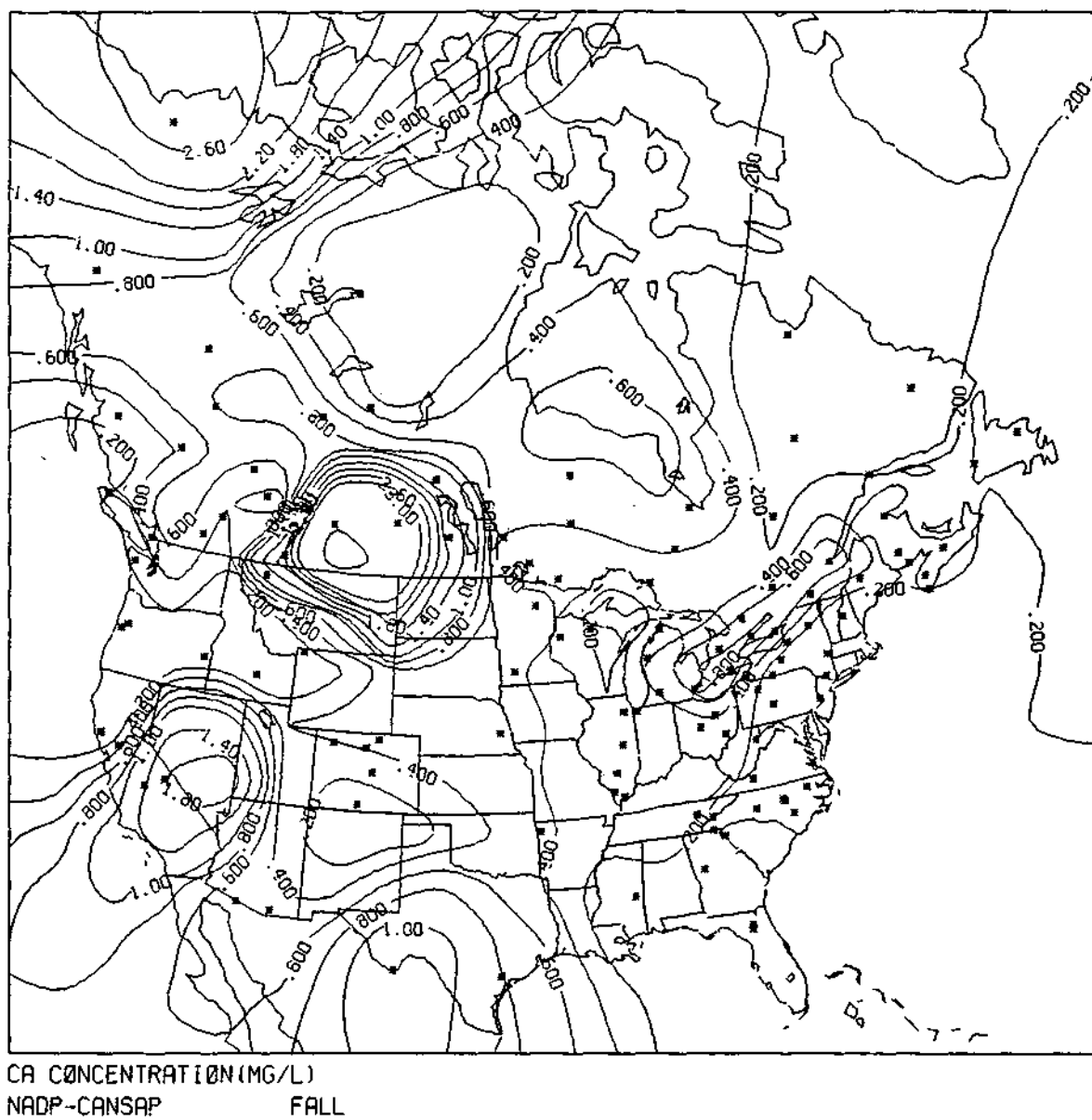
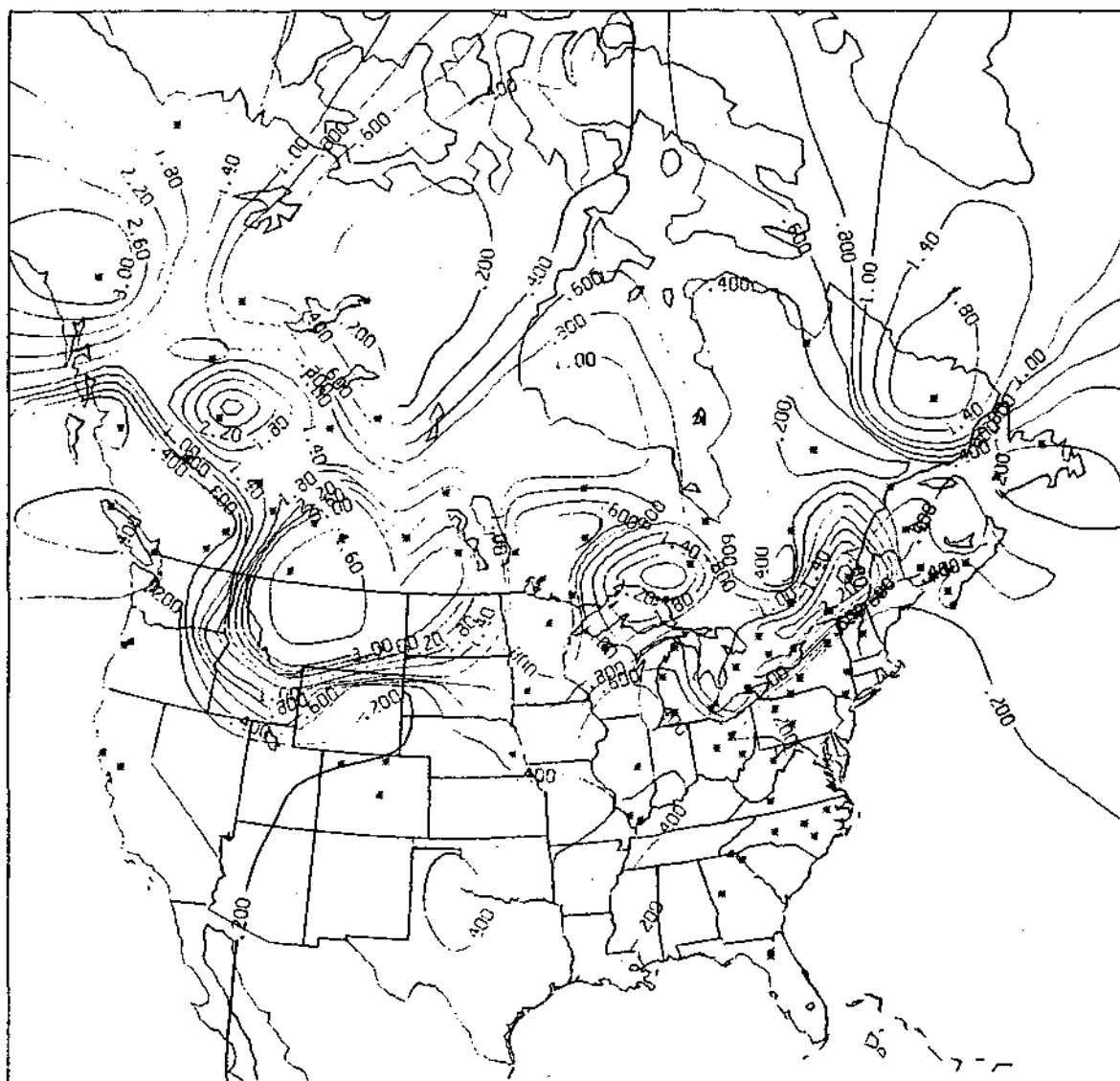


Figure 1. The North American average calcium concentration (mg/L) distribution for the Fall season obtained from the CANSAP and NADP networks.



CA CONCENTRATION(MG/L)  
NADP-CANSAP WINTER

Figure 2. The North American average calcium concentration (mg/L) distribution for the Winter season obtained from the CANSAP and NADP networks.

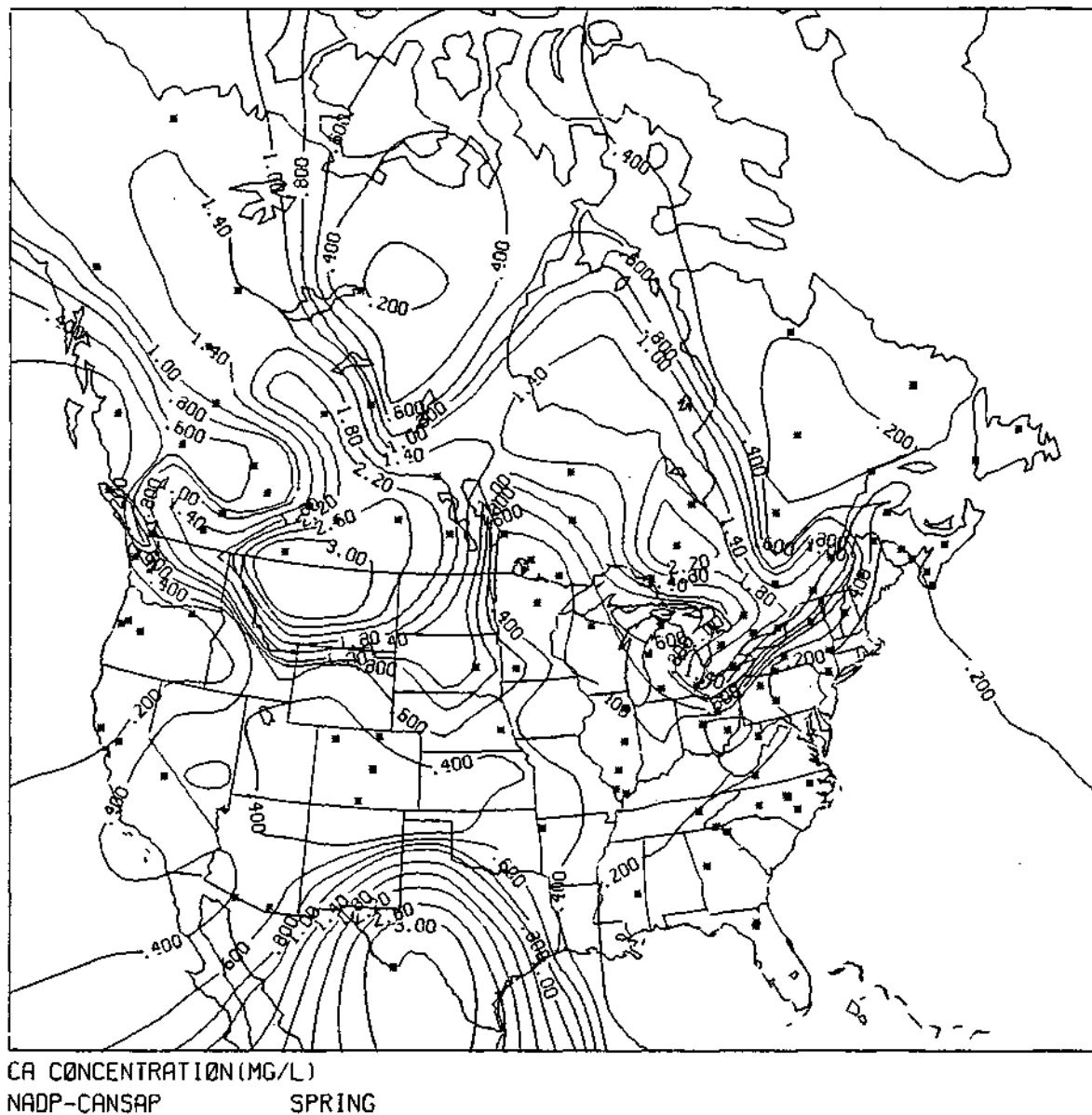


Figure 3. The North American average calcium concentration (mg/L) distribution for the Spring season obtained from the CANSAP and NADP networks.

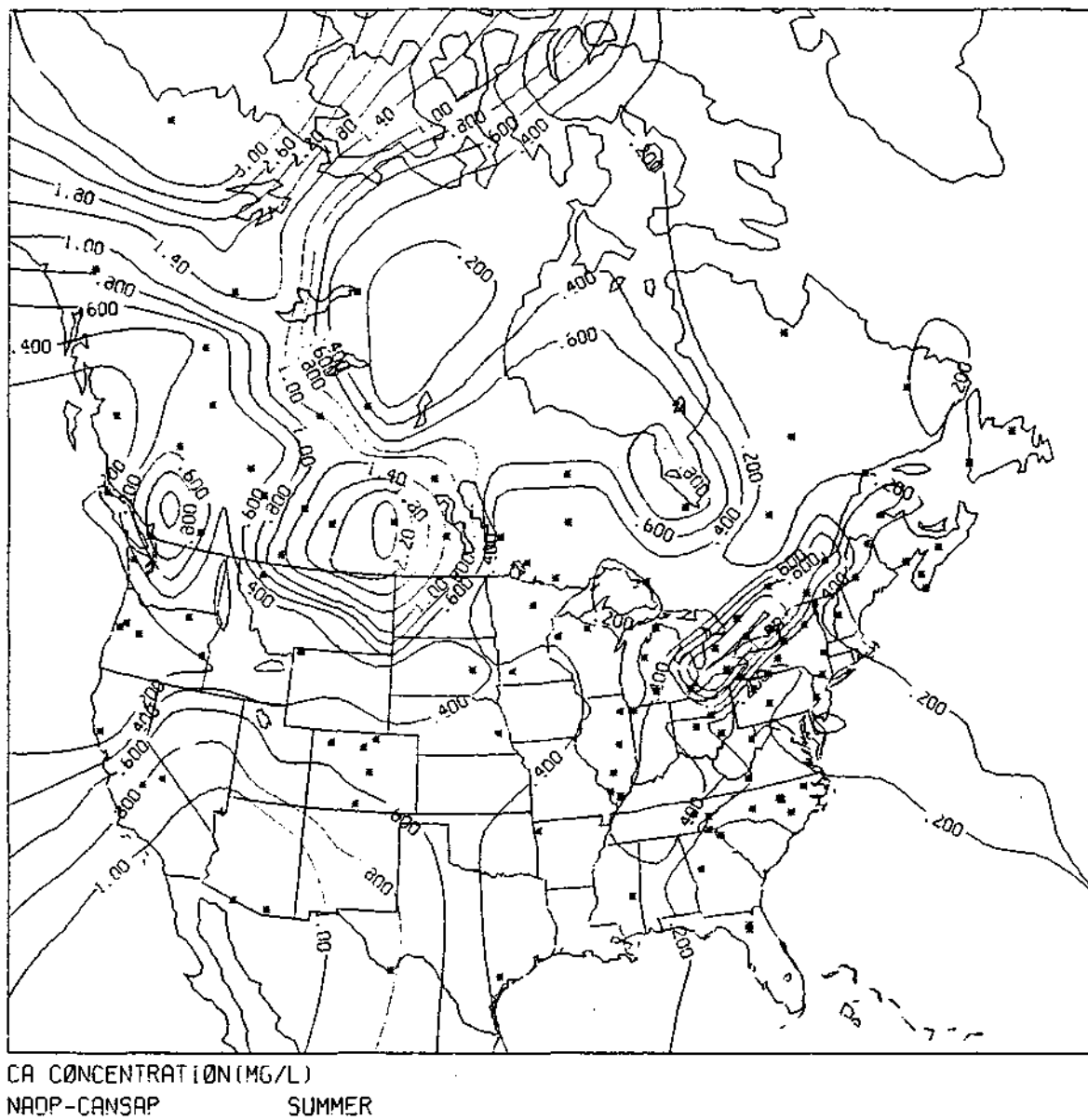


Figure 4. The North American average calcium concentration (mg/L) distribution for the Summer season obtained from the CANSAP and NADP networks .

extending from Ohio westward to western Iowa. However, the Illinois stations and those in southern Ohio do not reflect a maximum that might be associated with agricultural land management practices.

At this point it may be risky to attempt explanations of the patterns produced but they do serve to show the variability of chemical constituents in precipitation in all 4 seasons of the year.

#### Ammonium Concentration

A major feature to be noticed for the fall ammonium concentration distribution shown in Fig. 5 is the relative maximum over the western states particularly through the Great Plains from north to south and over the Great basin. The maximum in the Great Plains is quite visible in all four seasons whereas the Great Basin maximum over Nevada is only apparent in the summer and fall. Interestingly, in fall there is also a secondary maximum located in the southern Ontario region near Lakes Erie and Ontario similar to the maximum observed for calcium.

Qualitatively, there appears to be less variability in space during the winter season (Fig. 6) as contrasted to the maximum variability, as reflected by the number of maxima and minima, in the summer season (Fig. 8). The seasons of fall and spring (Figs. 5 and 7) seem to reflect the transition between the cyclonic storm regime of winter and the convectively modulated precipitation patterns of summer.

#### Nitrate Concentration

The nitrate concentration distribution is shown in Figs. 9-12 for the four seasons. An important feature of these seasonal distributions is the persistent maximum in the lower Ontario region north of Lakes Erie and Ontario. It appears that since this region of southeast Canada has shown a maximum or secondary maximum for calcium, ammonium, and now nitrate, there is a peculiar circumstance in that region that needs to be investigated. There are few other striking features of the concentration distribution for nitrate in any of the seasons in other parts of North America with a random number of maxima and minima scattered across the continent.

#### Sulfate Concentration

The fall season sulfate concentration shown in Fig. 13 shows a double maximum located in lower Ontario and in the central Tennessee region which may be associated with the Tennessee Valley Authority network of fossil fuel plants. The winter season, however, does not show a persistence of the Tennessee maximum and in fact shows a broad area of maximum concentration straddling the border between the United States and Canada extending from Alberta eastward to Maine (Fig. 14). In Fig. 15, the spring transition season shows a disappearance of the relatively well-ordered winter pattern with a

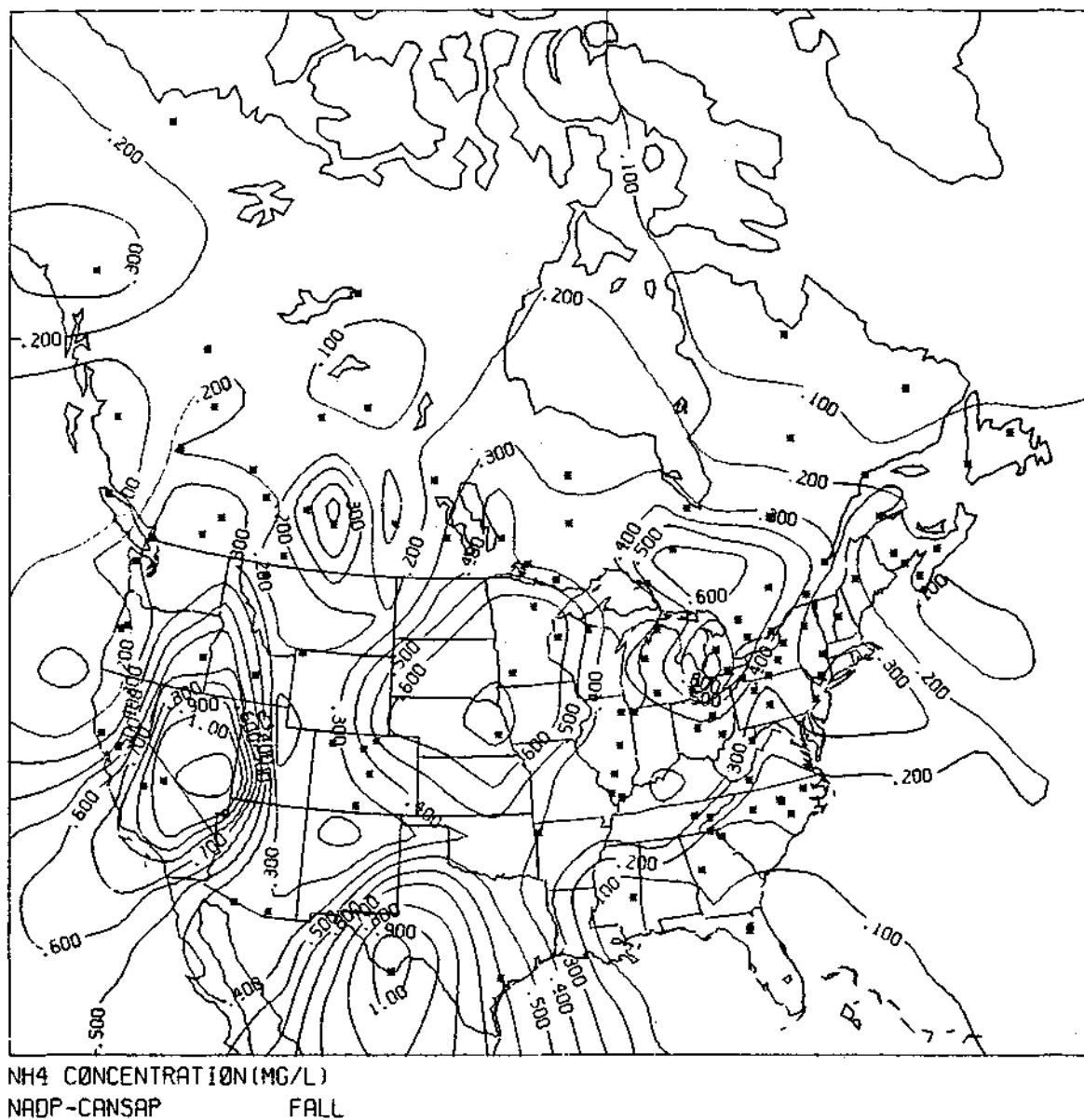


Figure 5. The North American average ammonium concentration (mg/L) distribution for the Fall season obtained from the CANSAP and NADP networks.



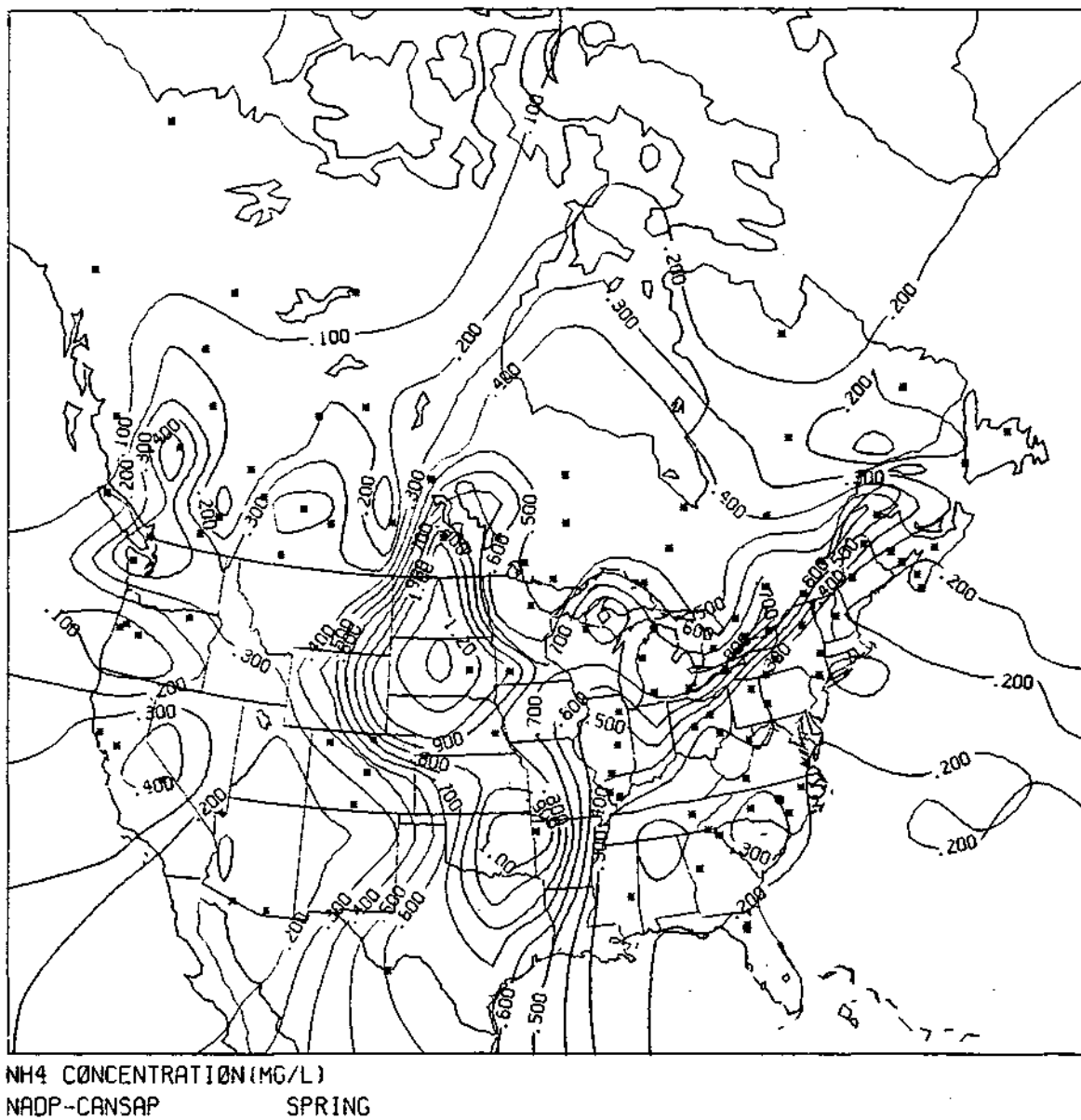


Figure 7. The North American average ammonium concentration (mg/L) distribution for the Spring season obtained from the CANSAP and NADP networks.



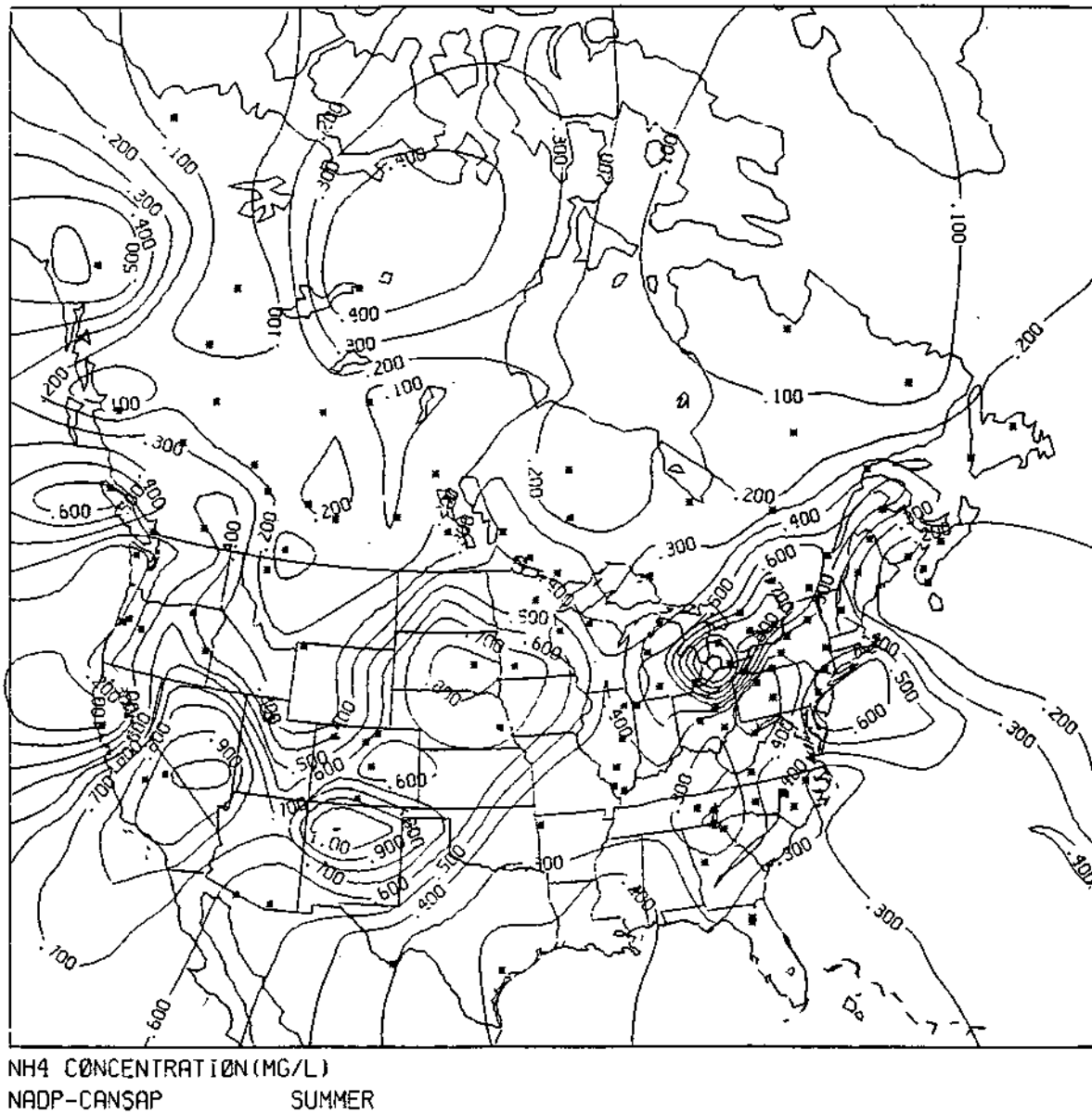
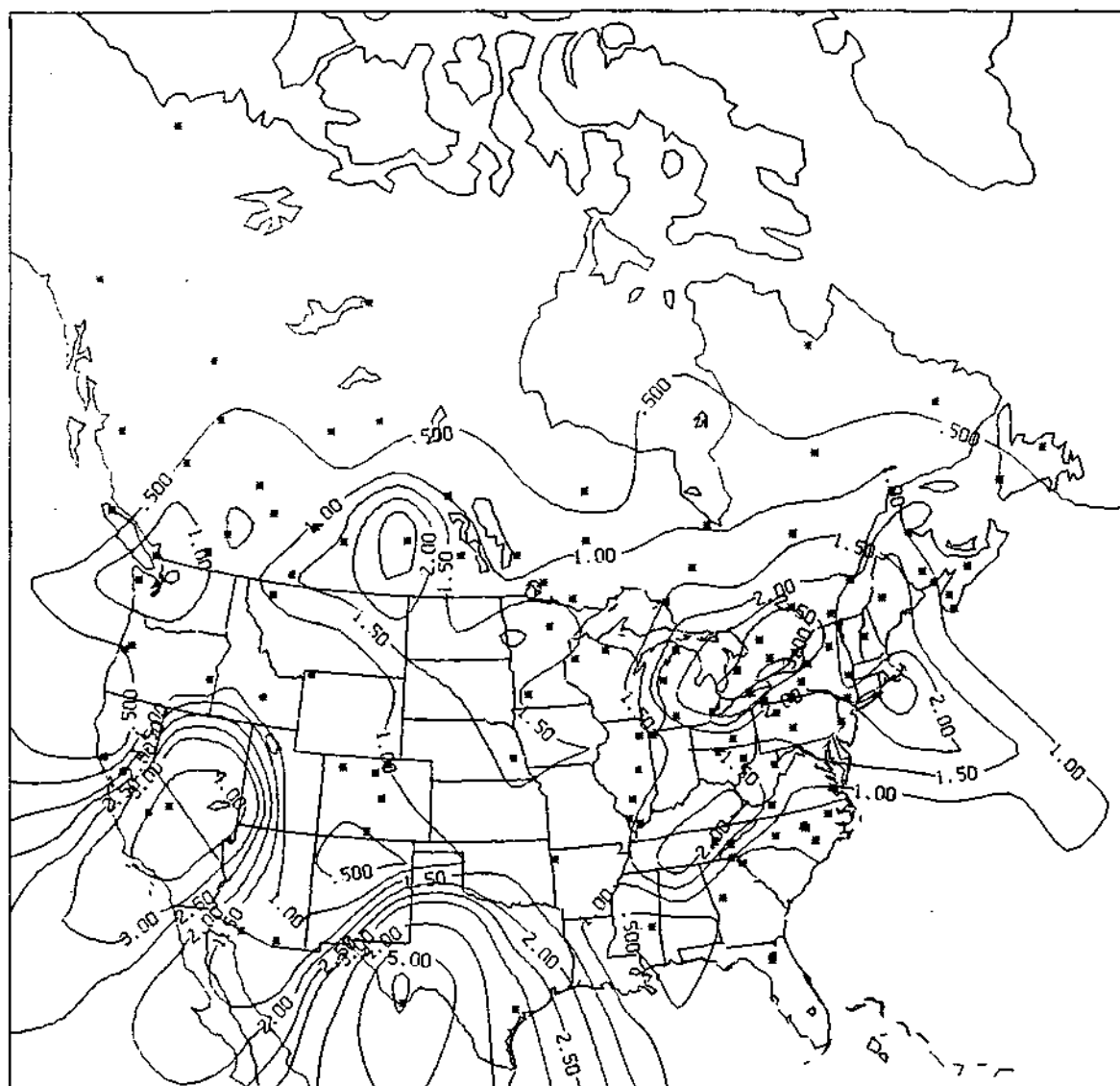
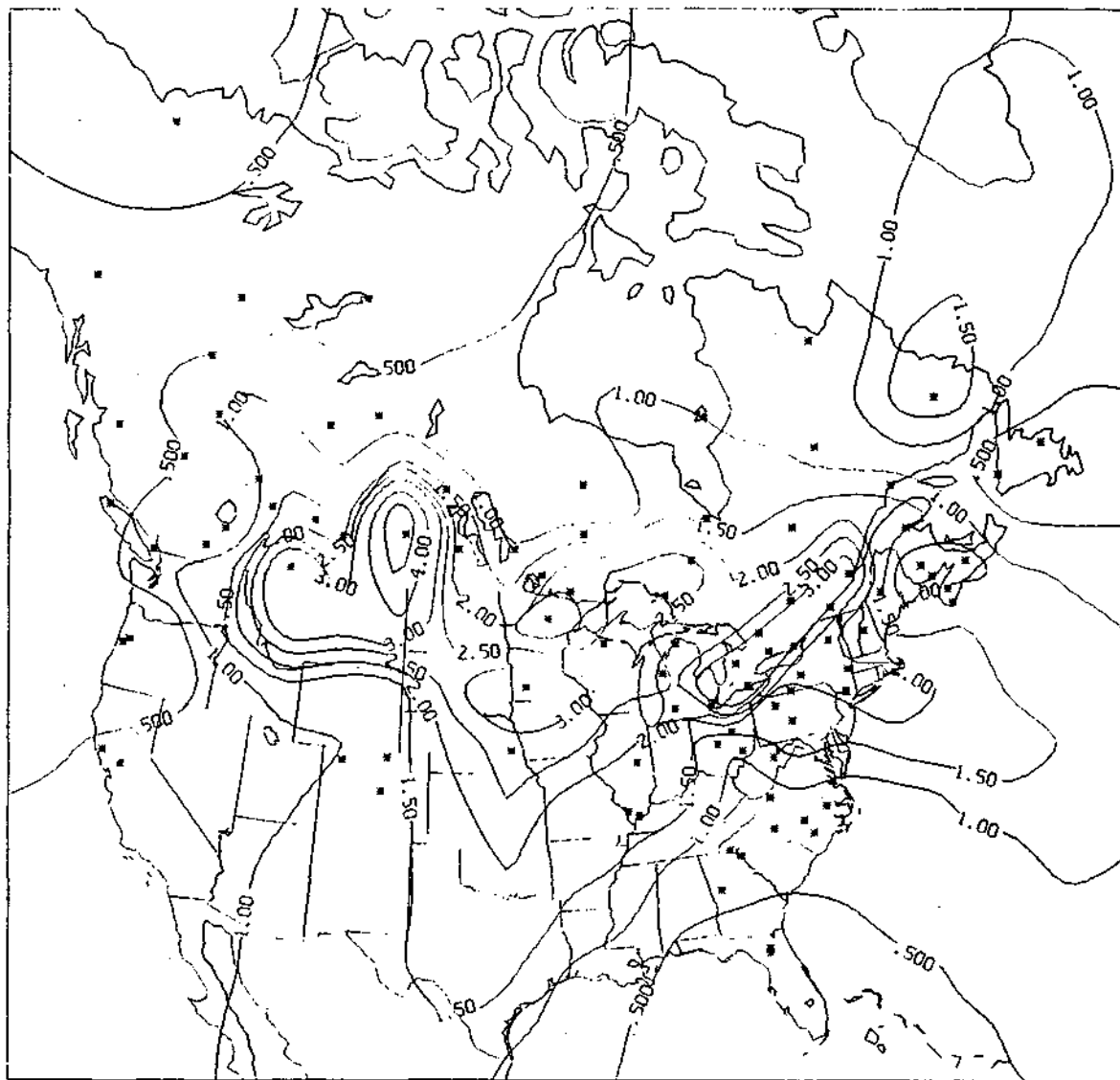


Figure 8. The North American average ammonium concentration (mg/L) distribution for the Summer season obtained from the CANSAP and NADP networks.



NO<sub>3</sub> CONCENTRATION (MG/L)  
NADP-CANSAP FALL

Figure 9. The North American average nitrate concentration (mg/L) distribution for the Fall season obtained from the CANSAP and NADP networks.



NO<sub>3</sub> CONCENTRATION (MG/L)  
NADP-CANSAP WINTER

Figure 10. The North American average nitrate concentration (mg/L) distribution for the Winter season obtained from the CANSAP and NADP networks.

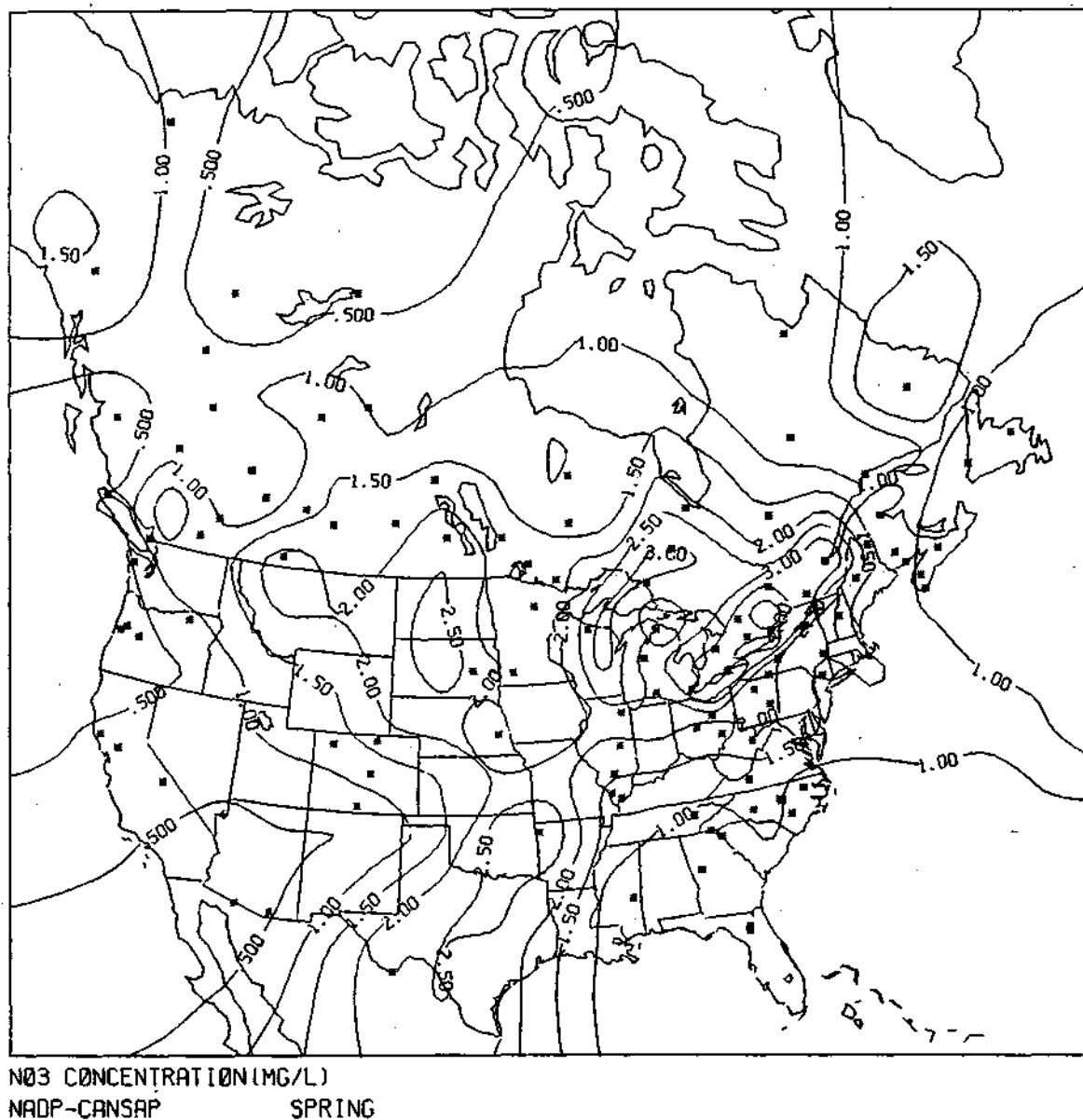


Figure 11. The North American average nitrate concentration (mg/L) distribution for the Spring season obtained from the CANSAP and NADP networks.

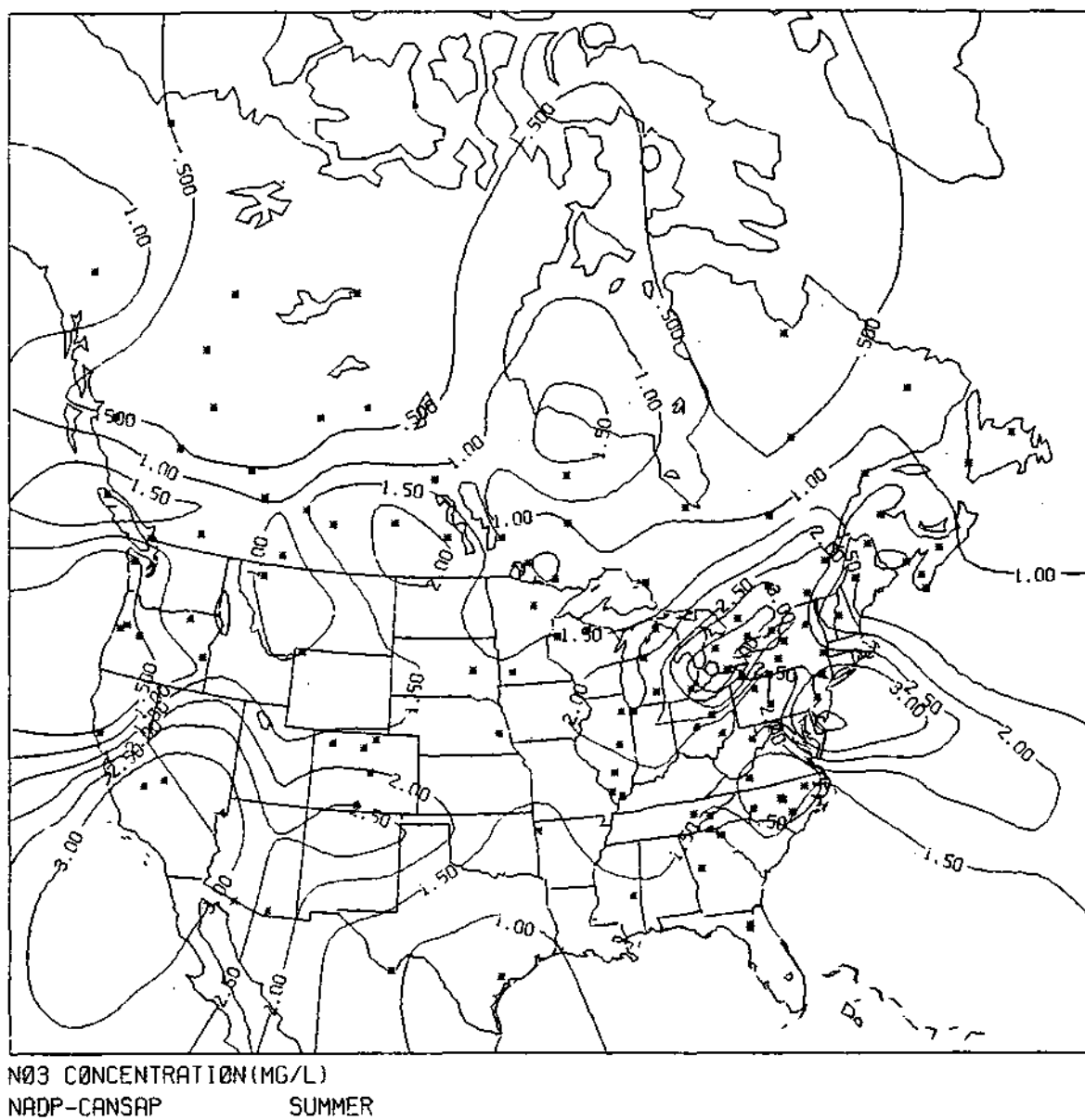


Figure 12. The North American average nitrate concentration (mg/L) distribution for the Summer season obtained from the CANSAP and NADP networks.

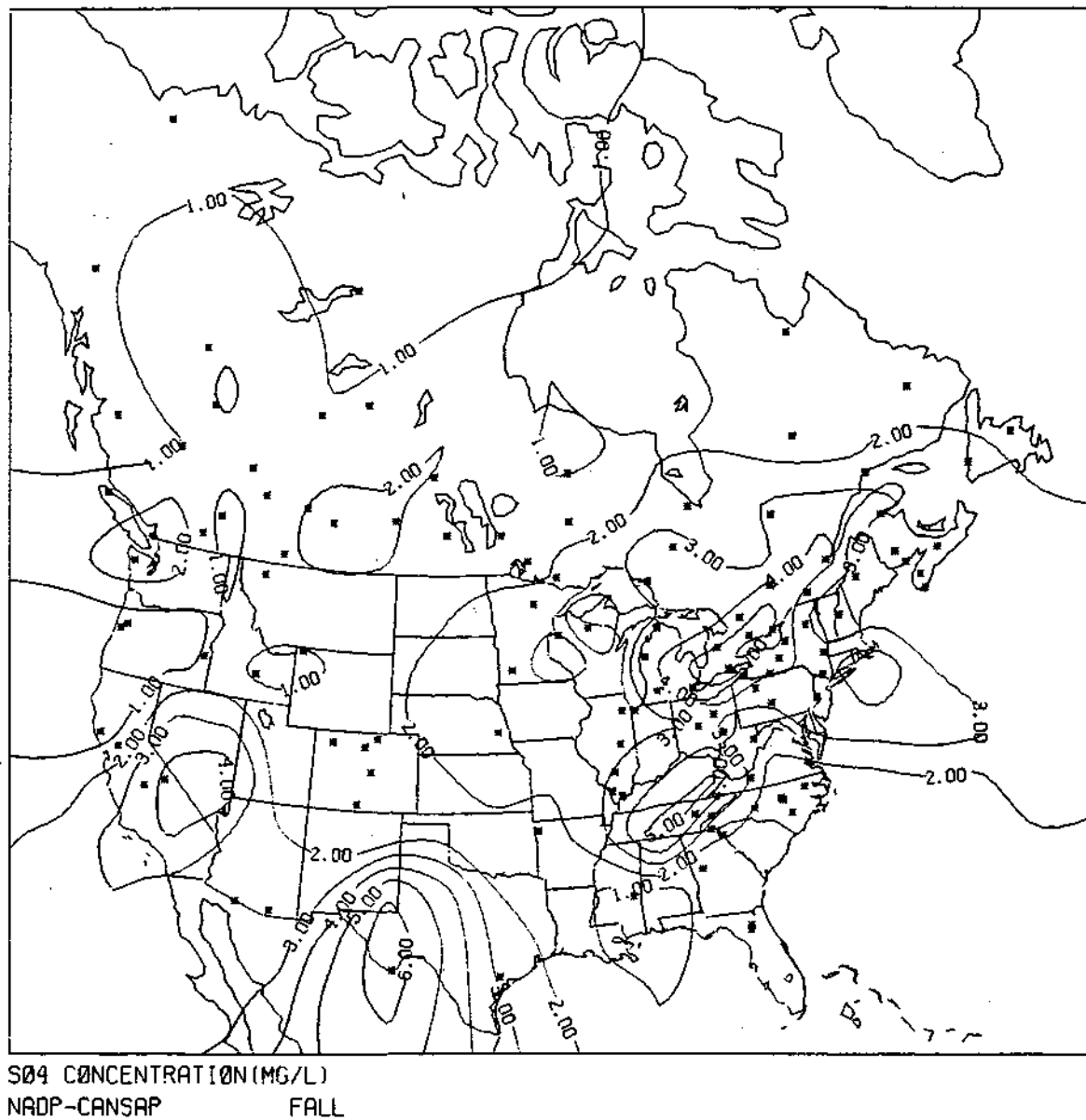
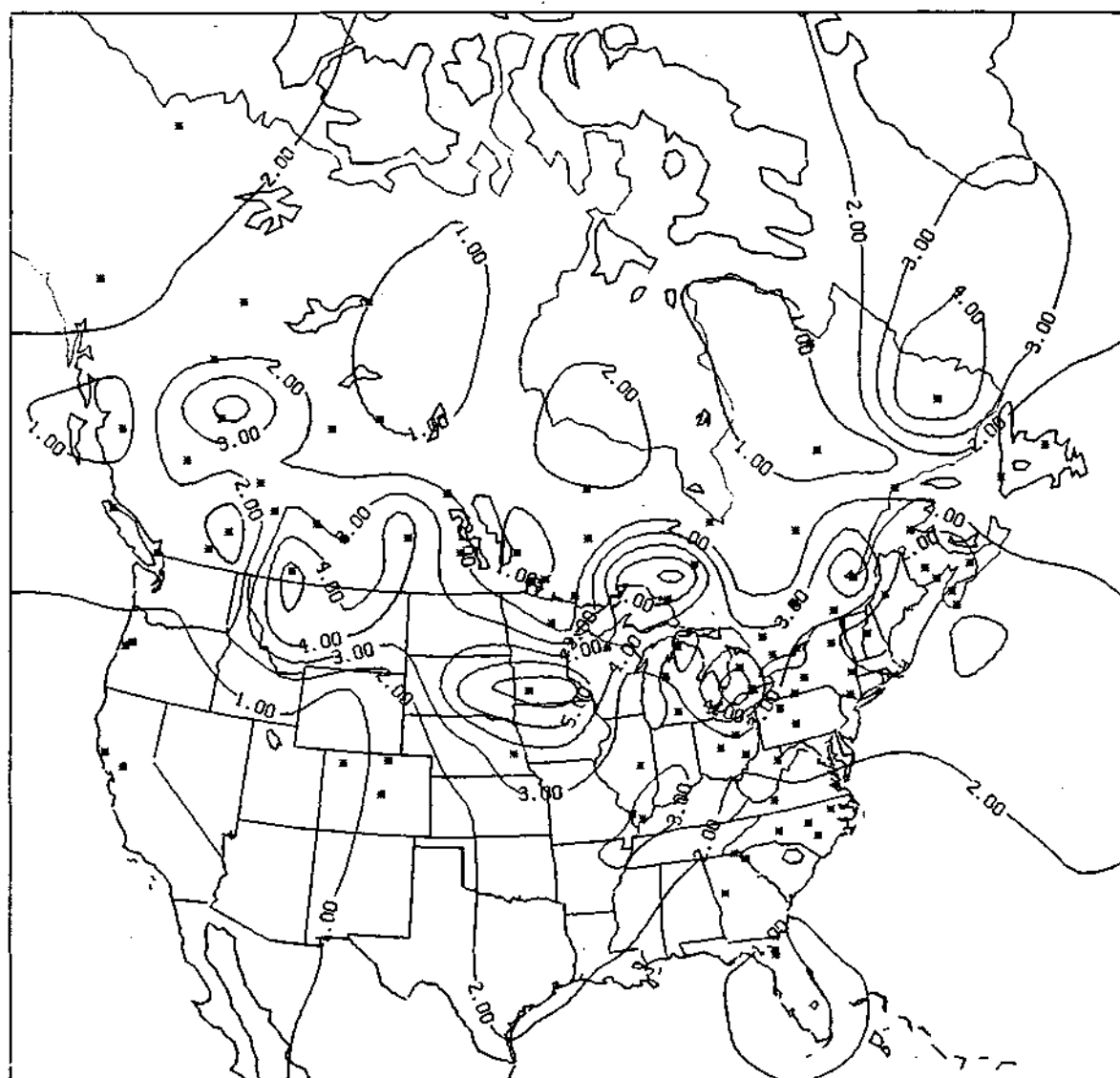


Figure 13. The North American average sulfate concentration (mg/L) distribution for the Fall season obtained from the CANSAP and NADP networks.



SO<sub>4</sub> CONCENTRATION(MG/L)  
NADP-CANSAP WINTER

Figure 14. The North American average sulfate concentration (mg/L) distribution for the Winter season obtained from the CANSAP and NADP networks.

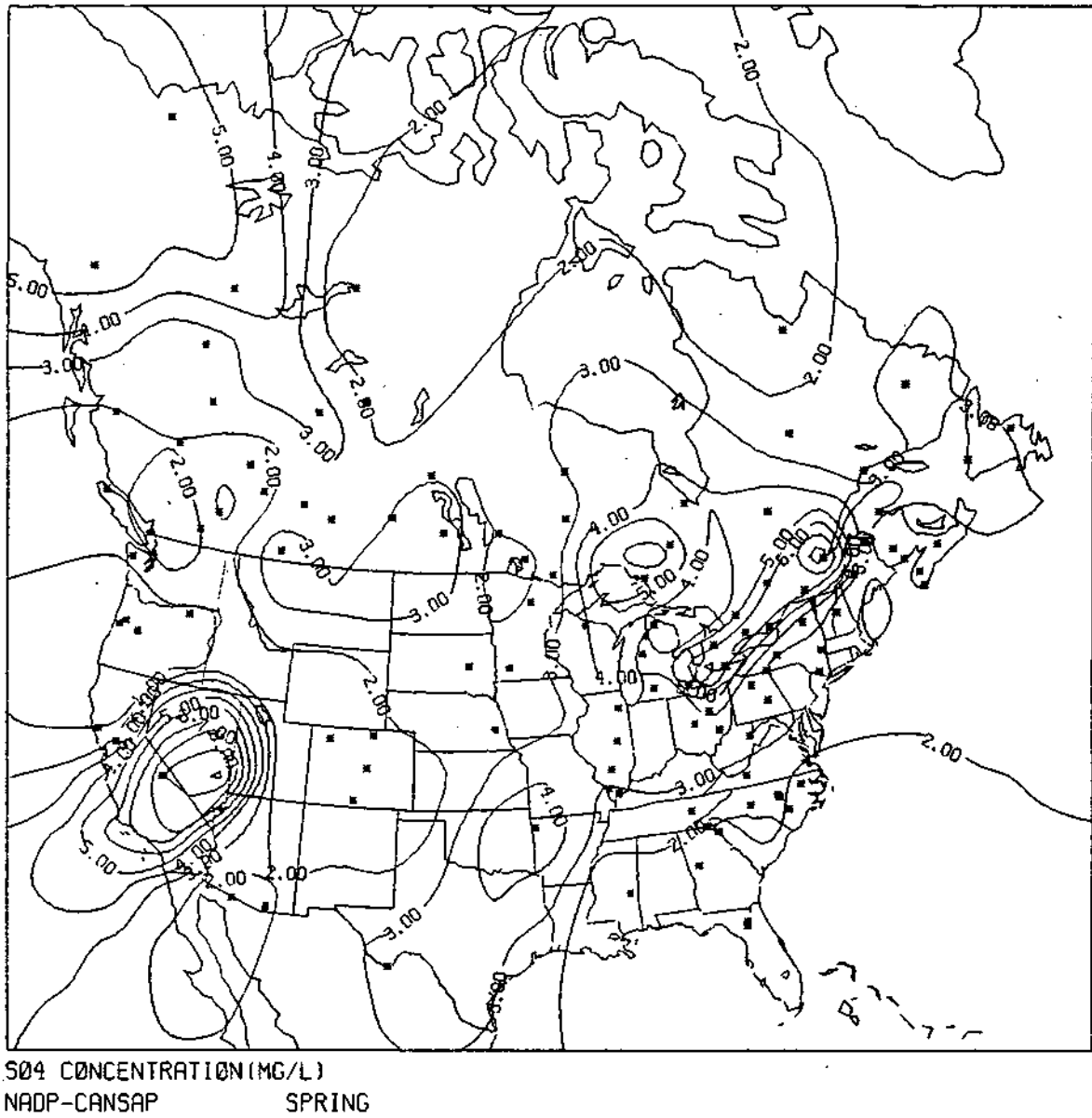


Figure 15. The North American average sulfate concentration (mg/L) distribution for the Spring season obtained from the CANSAP and NADP networks.



maximum appearing parallel to the St. Lawrence valley in much the same area as the other ions described previously. This maximum is further emphasized during the summer season as noted in Fig. 16.

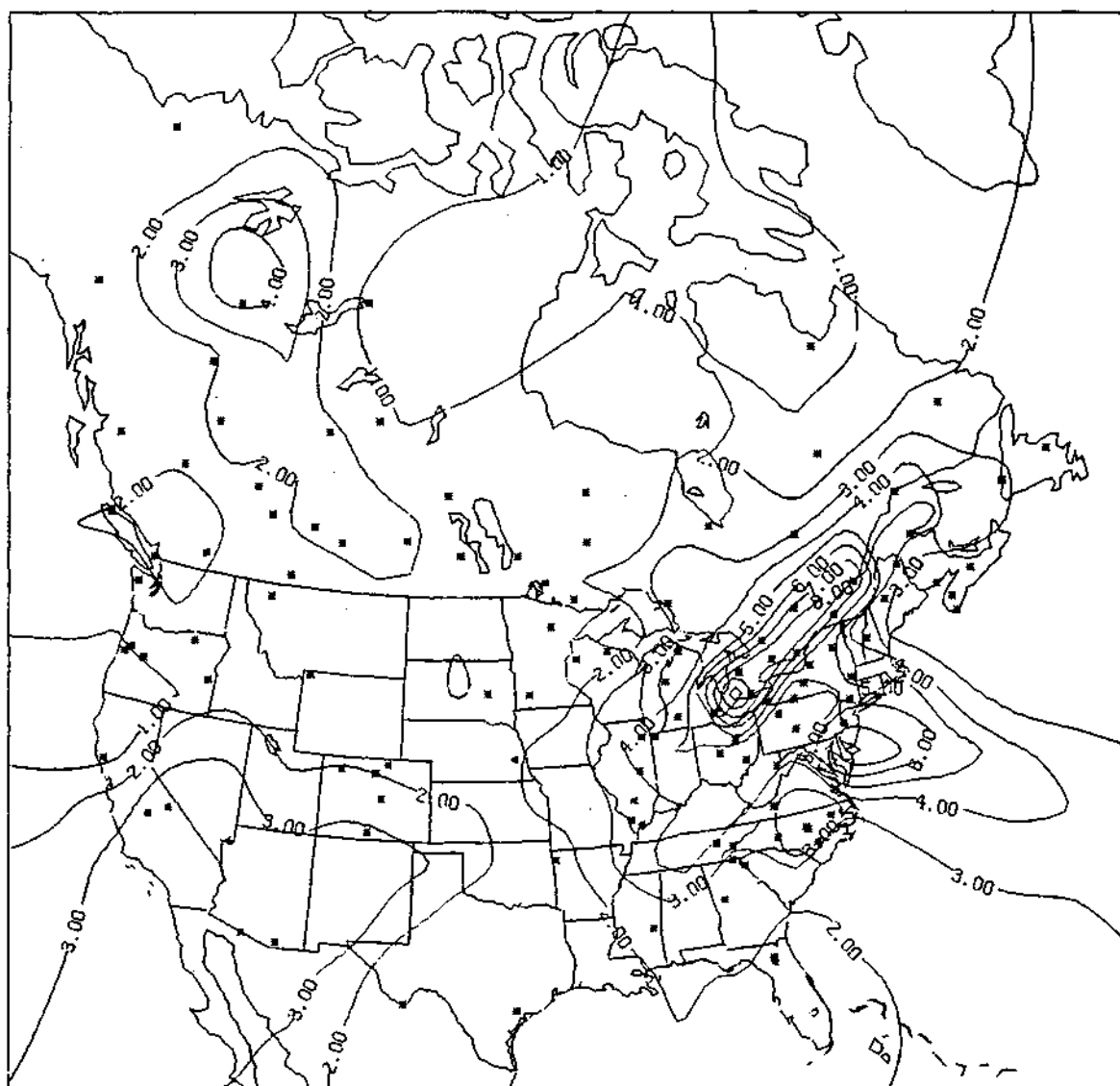
#### Measured pH Distribution

The pH distributions for fall, winter, spring, and summer are shown in Figs. 17-20. During the fall season (Fig. 17), there is a minimum in the pH distribution throughout the northeast states defined by the Mississippi River on the west, Tennessee and North Carolina to the Atlantic coast on the south and into the southeast provinces of Canada on the north. The western region from the Missouri River westward across northern Texas and the Mexican-U.S. border and extending northward toward Hudson Bay in Canada shows relatively high pH values. Contrasting to the minimum pH values of the northeast, the maximum values were observed in the Alberta-Saskatchewan provinces of western Canada. In the winter months (Fig. 18), the minimum pH is still observed in the northeast, as described previously, although extending a little further to the west in the United States with a lowering of the pH values in the Mississippi valley region. The maximum in the western Canadian provinces is still observed in the winter season in spite of the fact that much of the land is typically snow covered.

A very strong gradient in pH, as seen in Fig. 19, is observed in the spring months extending through Iowa, Kansas, Oklahoma, and into eastern Texas. This gradient extends into Canada northward in Manitoba then eastward to south of Hudson Bay. The gradient surrounds the low pH region over the northeast states with a minimum value in the tri-state region of Ohio, Pennsylvania, and northern West Virginia. A maximum in pH occurs again through the Great Plains area reflecting perhaps some of the dry land farming practices extending from the Dakotas to the Texas Panhandle. In summer, surprisingly, the pH distribution is relatively smooth in spite of the convective nature of precipitation in this season (Fig. 20). The strong east-west gradient is still present in approximately the same location as for spring with the lowering of pH over the region including Indiana, Ohio, Pennsylvania, New York, and the southeast provinces of Canada. Values as low as pH 4 were observed in the area of extreme eastern Pennsylvania and New Jersey.

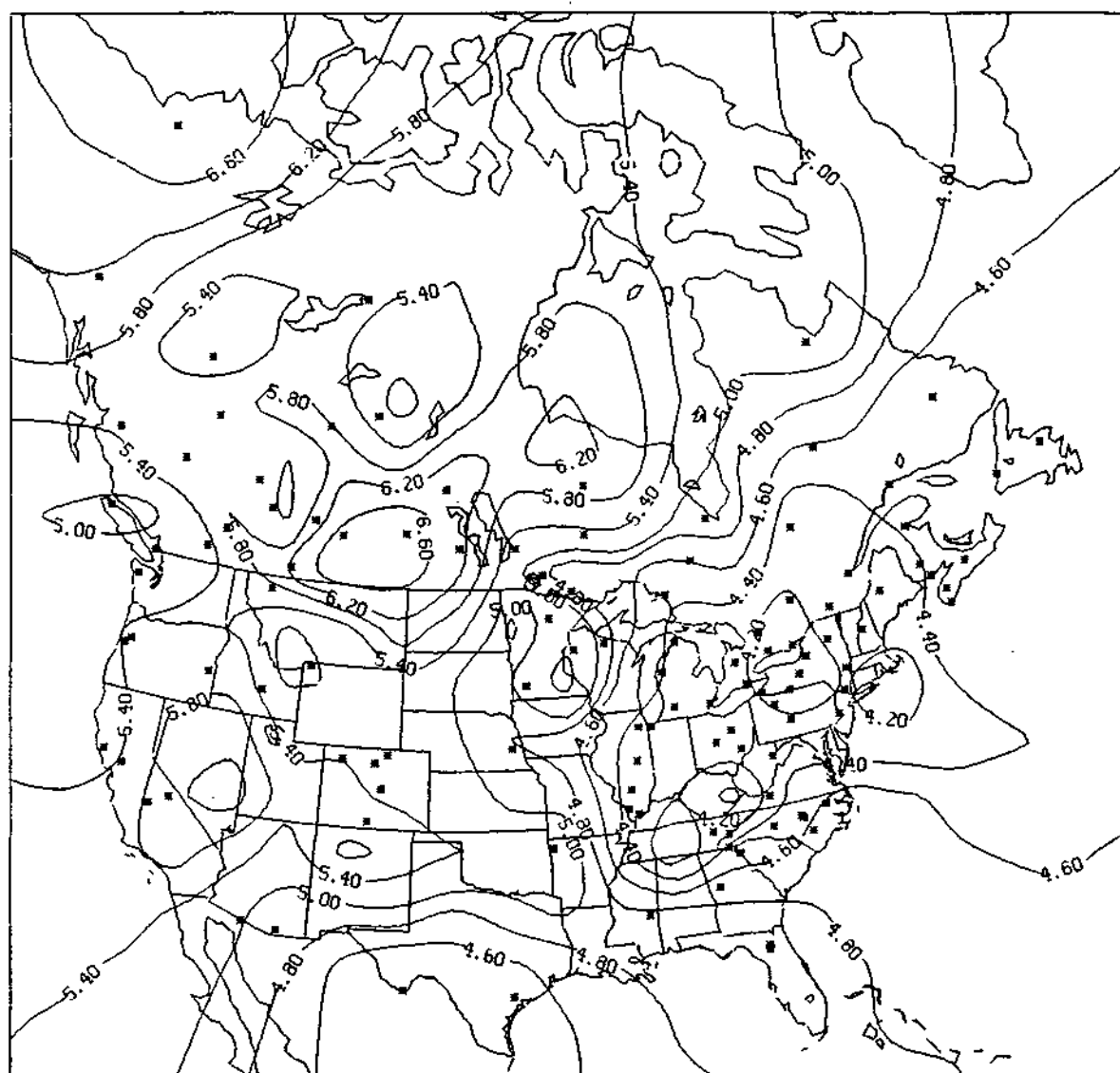
#### Discussion of Concentration Distributions

There are a few points concerning these maps that should be kept in mind when attempting to interpret them in great detail. First, the lines that appear on the map were drawn by objective techniques and, consequently, little credence should be placed on lines extending into areas where no data points are shown on the map. Secondly, a certain amount of smoothing has been introduced through the use of the objective mapping technique used for this work. Thirdly, the maps represent concentrations which are difficult to interpret with regards to local sources, influences of long range transport, and effects since the concentration is influenced not only by all of the meteorological transport and transformation factors, but also by the amount of rainfall. It is generally conceded that the concentration of nearly all



SO<sub>4</sub> CONCENTRATION (MG/L)  
NADP-CANSAP SUMMER

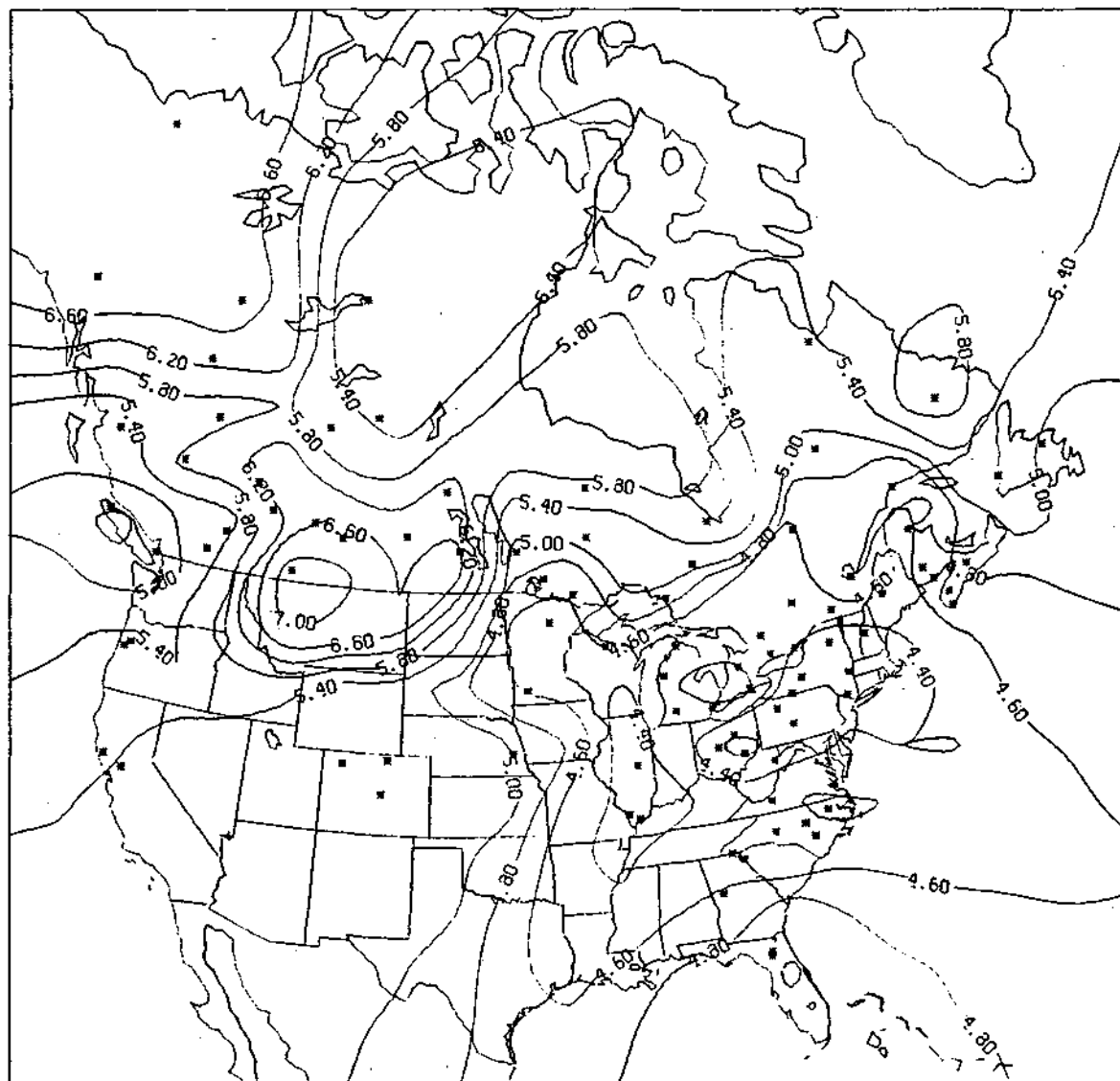
Figure 16. The North American average sulfate concentration (mg/L) distribution for the Summer season obtained from the CANSAP and NADP networks.



MEASURED PH  
NADP-CANSAP

FALL

Figure 17. The North American average pH distribution for the Fall season obtained from the CANSAP and NADP networks.



MEASURED PH  
NADP-CANSAP

WINTER

Figure 18. The North American average pH distribution for the Winter season obtained from the CANSAP and NADP networks.

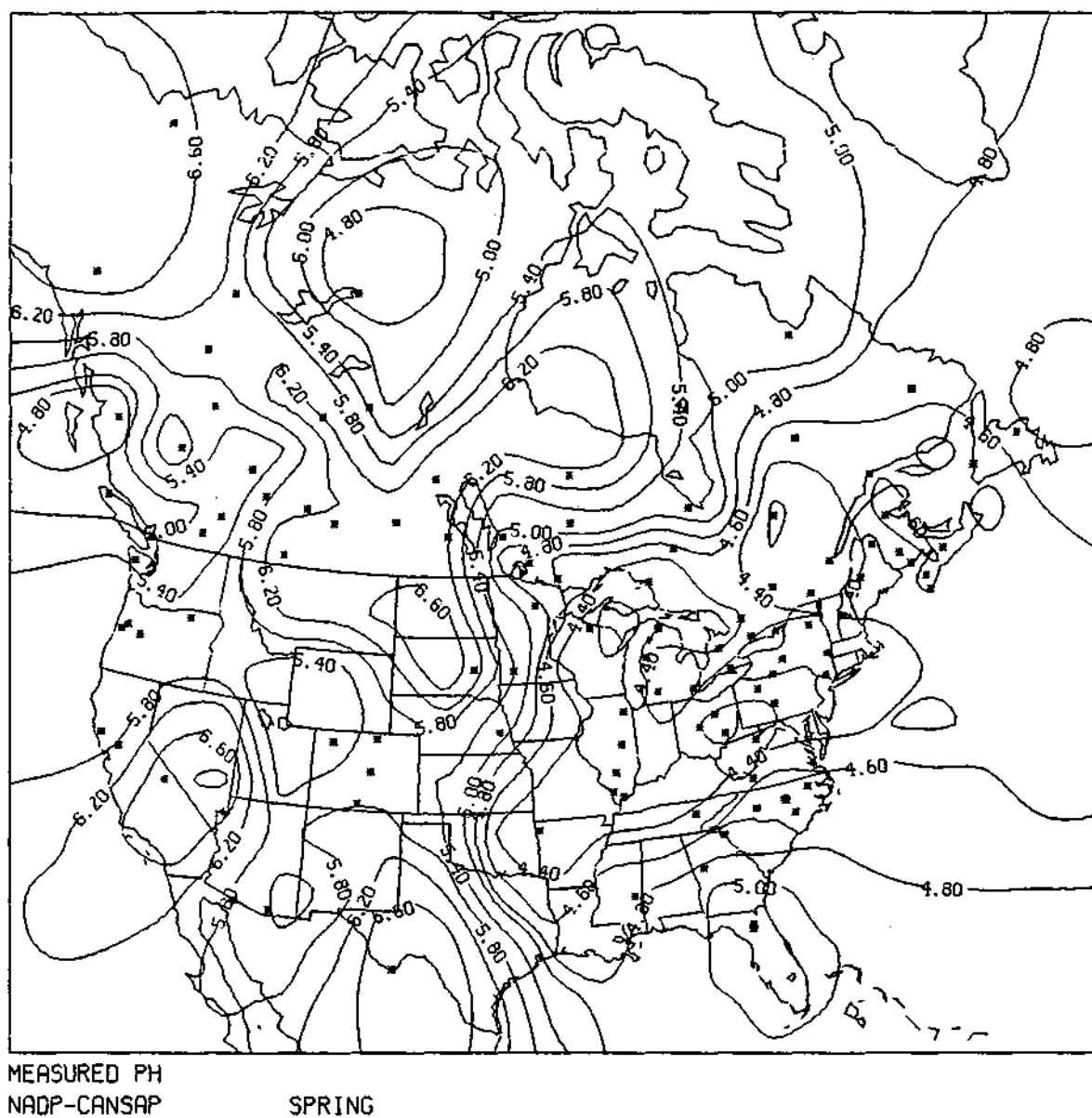


Figure 19. The North American average pH distribution for the Spring season obtained from the CANSAP and NADP networks.

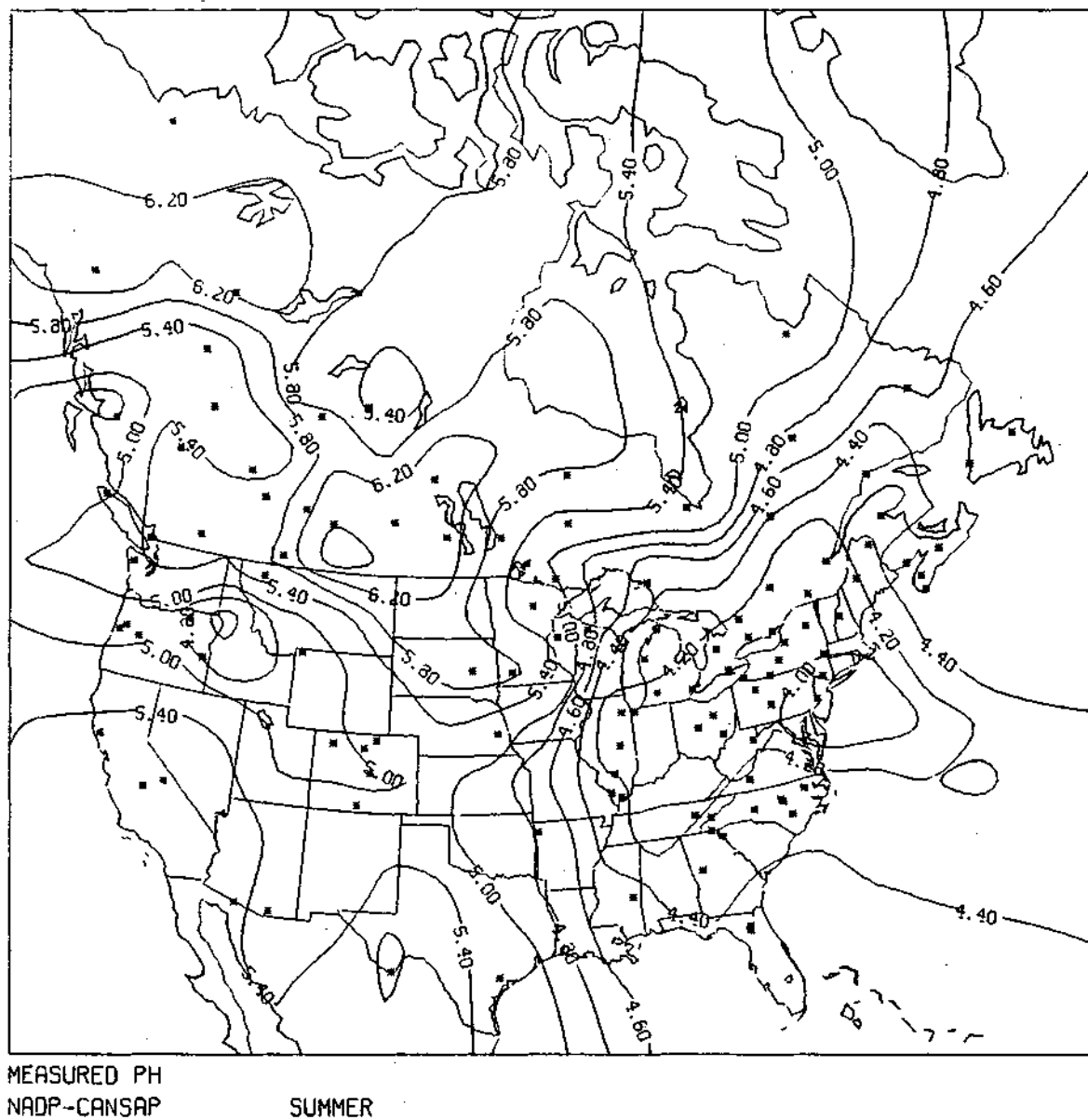


Figure 20. The North American average pH distribution for the Summer season obtained from the CANSAP and NADP networks.

species in precipitation is inversely related to the total rainfall on an event basis, however, attempts to interpret seasonal data with such a relationship may be misleading. Therefore, a better interpretation of the seasonal distribution of precipitation chemistry may be obtained from consideration of both the concentration and the deposition maps. The deposition corresponding to these seasonal concentration distributions will be shown in the next section of this chapter.

Focusing our attention on the fall season, it appears that the maximum values in the cations occurs in the west and northwest while the maximum in the acid-contributing anions occurs in the northeast. The summation of these is reflected in the pH pattern for the fall where the lowest pH values (that is the most acid) are observed in the northeast with more alkaline precipitation observed in the west and northwest.

The winter season shows a relative abundance of calcium along the Canadian-U.S. border with a maximum of ammonium in the central Great Plains and western edge of the middle west. The anions seem to maximize in more northern latitudes along the border states of the U.S. and provinces of Canada. Again, the minimum pH values, however, are observed through the east and northeast states although the pH values are somewhat larger than in other seasons. It is interesting to note that during the winter season the anions are relatively high in the western provinces of Canada possibly in response to increased fossil fuel consumption for heating, but the pH values are also relatively high. The pH, of course, is determined not only by the acid contribution of sulfate and nitrate but also from the other cations in the precipitation such as calcium, ammonium, and magnesium. These cations also maximize in the winter months in that particular region of Canada and apparently are of sufficient concentration to maintain a high level of pH.

In the spring transition season the ammonium and nitrate concentrations show a maximum extending from North Dakota through central Texas while the sulfate concentration shows a maximum along the St. Lawrence River valley and a secondary maximum in the western Canadian provinces. The calcium concentration seems to parallel the sulfate with maxima located in the same areas. (The high value of sulfate in the southwest was determined solely by a single station in California and should be neglected.) The results of the superpositioning of the ammonium and nitrate is to create a maximum gradient in pH in that vicinity, as described previously. This observed relatively strong gradient separates the minimum pH values of the northeastern states from the maximum values observed west of the Missouri River.

During the summer season the acid-forming ions are maximized in the northeast states with particular emphasis on the region extending from western Lake Erie northeast along the St. Lawrence valley. However, this same maximum is observed for the cation species (although there are other maxima in the western states for these particular ions). The result is that in summer the western states have pH values largely greater than 5 with the western Canadian provinces near the U.S. border exceeding 6. At the same time, the northeastern states experienced the lowest pH with values in the extreme eastern Pennsylvania-New Jersey area of  $< 4$ .

In the net, its a curious phenomenon that while many of the greatest concentrations for various ions contributing to the precipitation pH are found in lower Ontario and southeastern Quebec that the lowest precipitation pH values are actually found in the United States over the eastern Midwest, through Pennsylvania, and into New York. A much more detailed analysis of the contributing factors to the pH must be undertaken to fully understand the distribution shown in these seasonal maps. It is also important to determine how the maximum concentration of cations arises in the western Canadian area and the maximum of both anions and cations in the St. Lawrence valley area. It has been claimed that the high concentrations of acid-forming ions may be due to the industrialization along the Ohio River valley. However, that concept and the concentrations shown here are not totally in agreement requiring detailed studies of the meteorological conditions preceeding and following precipitation in that area. For example, for air from the Ohio River to reach the region of maximum concentration a southwesterly component would be required which would intercept eastward moving precipitation systems and perhaps reach the ground with maximum concentrations as observed. However, if the transport wind is moving to the northeast then it is difficult to understand why the maximum concentrations are oriented northeast-southwest. Some of the material will have been scavenged by the southwest portions of an eastward progressing precipitation system resulting in a northwest-southeast oriented maximum concentration. Perhaps we can return to this point during the discussion of the deposition patterns.

#### SEASONAL DEPOSITION DISTRIBUTIONS

##### Calcium Deposition

The fall season calcium deposition is a reflection of the concentration pattern shown in Fig. 1. In Fig. 21 can be seen two major maxima, one located in Saskatchewan corresponding to a maximum in calcium concentration and a secondary maximum deposition in lower Ontario province. This secondary maximum, although nearly of the same magnitude as the western maximum corresponds to a much smaller secondary maximum of concentration but associated with heavier precipitation in that area. The middlewest, west, and eastern parts of the United States are relatively featureless as was the case with the concentration distribution.

The winter deposition pattern in Fig. 22 corresponds almost identically to the concentration pattern of Fig. 2. The greatest deposition is found in the eastern Canadian provinces, again reflecting higher precipitation amounts. Owing to the more uniform distribution of precipitation in the winter season it is not surprising to find such a high correlation between concentration and deposition patterns.

The spring season deposition in Fig. 23 is also a reflection of the concentrations. The secondary maximum of deposition in Ontario arises from a secondary maximum of concentration as seen in Fig. 3.



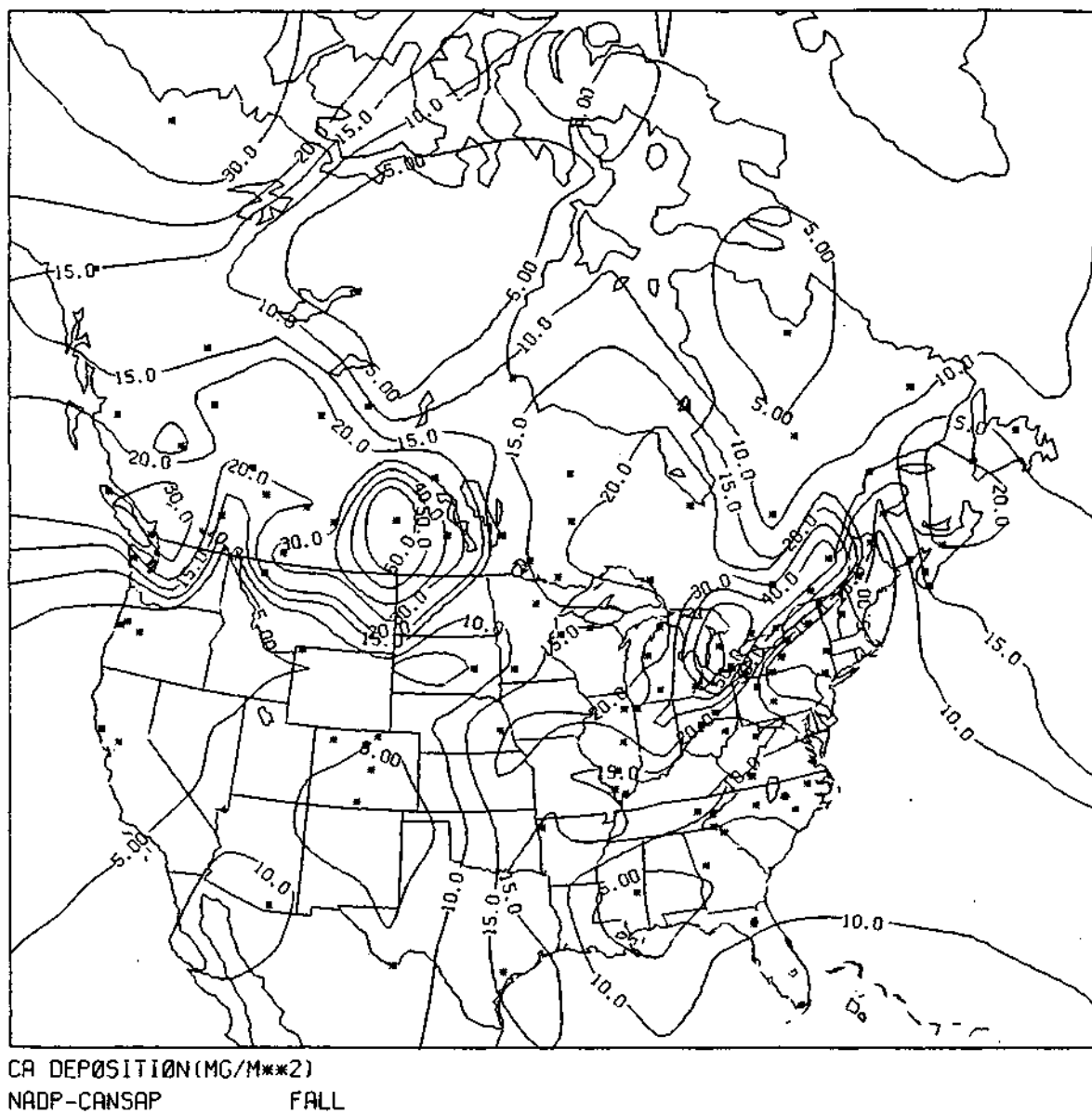
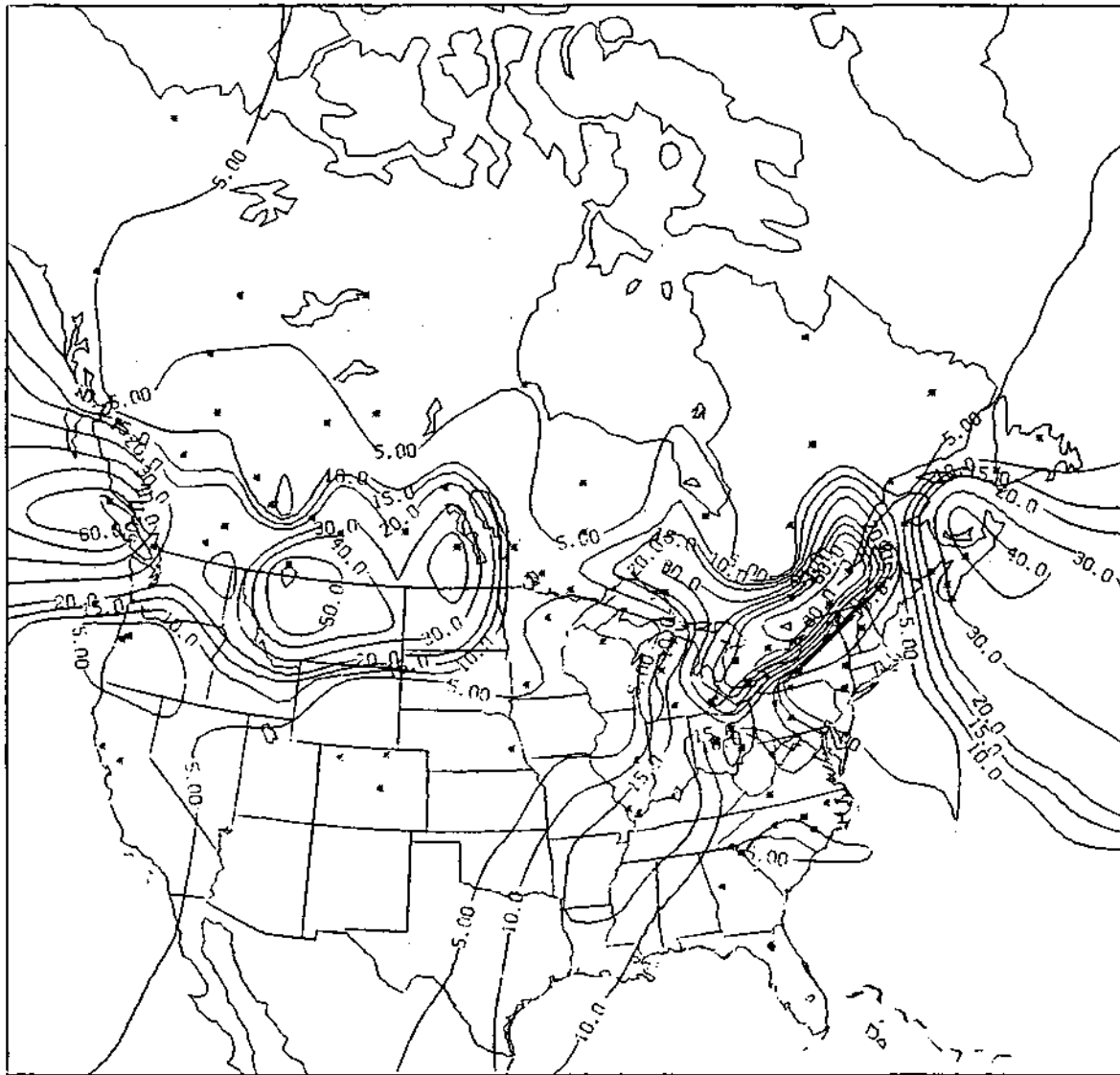
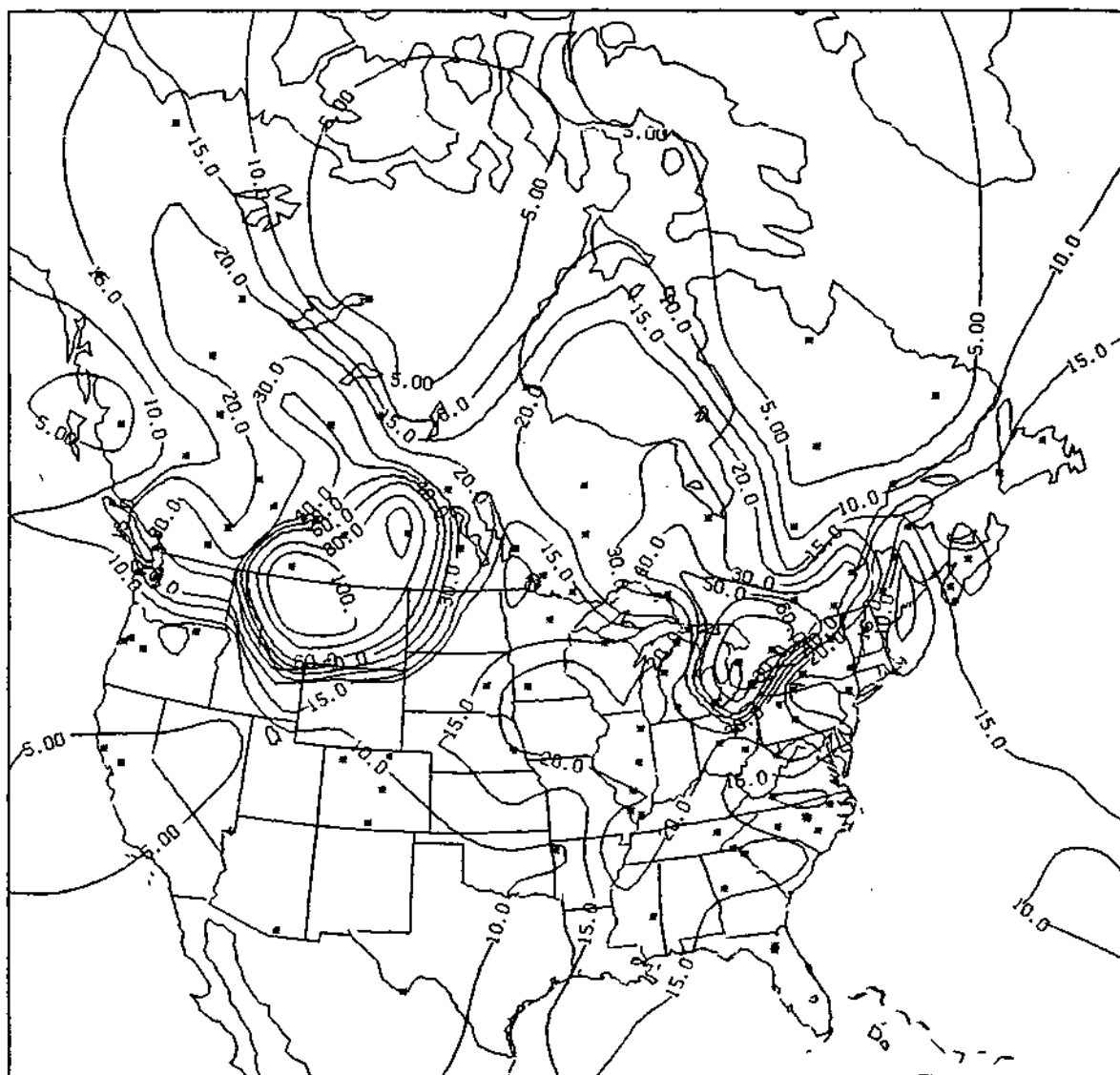


Figure 21. The North American average calcium deposition ( $\text{mg}/\text{m}^2$ ) distribution for the Fall season obtained from the CANSAP and NADP networks.



CA DEPOSITION(MG/M\*\*2)  
NADP-CANSAP WINTER

Figure 22. The North American average calcium deposition ( $\text{mg/m}^2$ ) distribution for the Winter season obtained from the CANSAP and NADP networks.



CA DEPOSITION(MG/M\*\*2)  
NADP-CANSAP      SPRING

Figure 23. The North American average calcium deposition ( $\text{mg}/\text{m}^2$ ) distribution for the Spring season obtained from the CANSAP and NADP networks.

The summer distribution of calcium deposition shown in Fig. 24 illustrates a gradual increase of calcium deposition from west to east across North America. Again the maxima are located in the western provinces of Canada and along the U.S.-Canadian border in the east with generally high values extending across the Midwest. In general, this distribution conforms to the features of the concentration distribution shown in Fig. 4.

#### Ammonium Deposition

The fall season deposition pattern in Fig. 25 is very similar to the concentration pattern of Fig. 5. The maximum over southern Ontario and secondary maximum in Minnesota are reflections of similar concentration maxima shown in Fig. 5. However, the winter deposition shown in Fig. 26 is not as easily correlated to the concentration pattern of Fig. 6. The concentration, as mentioned previously, shows a distinct maximum in the central Great Plains whereas the deposition pattern shows a relatively minor area of maximum values extending to the northeast from central Arkansas to eastern Quebec. This shows that the deposition is highly dependent upon precipitation. For example, while the concentrations were very high in eastern Nebraska, the precipitation in the winter season is comparatively light resulting in light ammonium deposition.

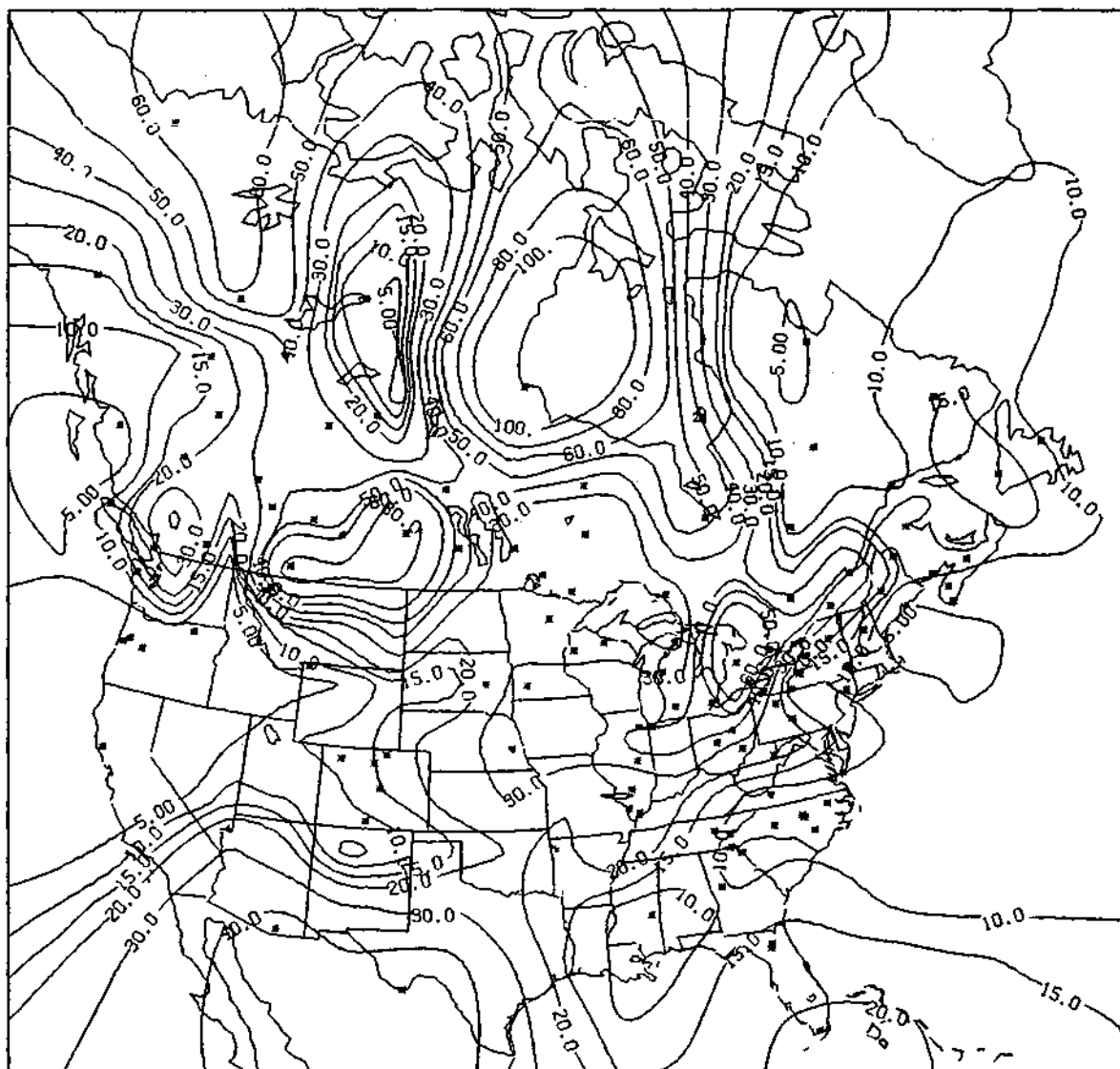
The spring season deposition, shown in Fig. 27, bears little resemblance to the concentration pattern of Fig. 7. The dominating feature of Fig. 7 was a maximum extending throughout the Great Plains from north to south whereas the maximum ammonium deposition shows a pattern maximizing east-west extending from Nebraska through the Midwest and Lake states to lower Ontario. A secondary maximum of deposition is noted over the southeast states from South Carolina to Mississippi.

Similarly, the summer pattern retains an east-west maximum deposition area from South Dakota through northern Illinois into the eastern Great Lake states and lower Ontario (Fig. 28). This area does correspond to a relative maximum of concentration shown in Fig. 8 but there appears to be greater variability of deposition in Fig. 28. The increased deposition variability is an indication of the complexity of interpreting the data since the deposition depends not only on the concentration of Fig. 8 but also on the precipitation which is more variable in summer than in other seasons of the year.

#### Nitrate Deposition

The fall season deposition, shown in Fig. 29, parallels the concentration distribution shown in Fig. 9. Each significant concentration maximum shown in Fig. 9 is also reflected in a maximum in deposition in the fall season.

In the winter season however, the concentration pattern shows a relative maximum area along the international border dipping into the U.S. over the western Midwest whereas the deposition pattern shows a strong maximum deposition over the western sections of Pennsylvania, northeast Ohio and lower Ontario (Fig. 30). There is a minor low deposition area shown for both fall and winter in north-central Pennsylvania reflecting lower precipitation in that particular area.



CA DEPOSITION(MG/M\*\*2)  
NADP-CANSAP SUMMER

Figure 24. The North American average calcium deposition ( $\text{mg}/\text{m}^2$ ) distribution for the Summer season obtained from the CANSAP and NADP networks.

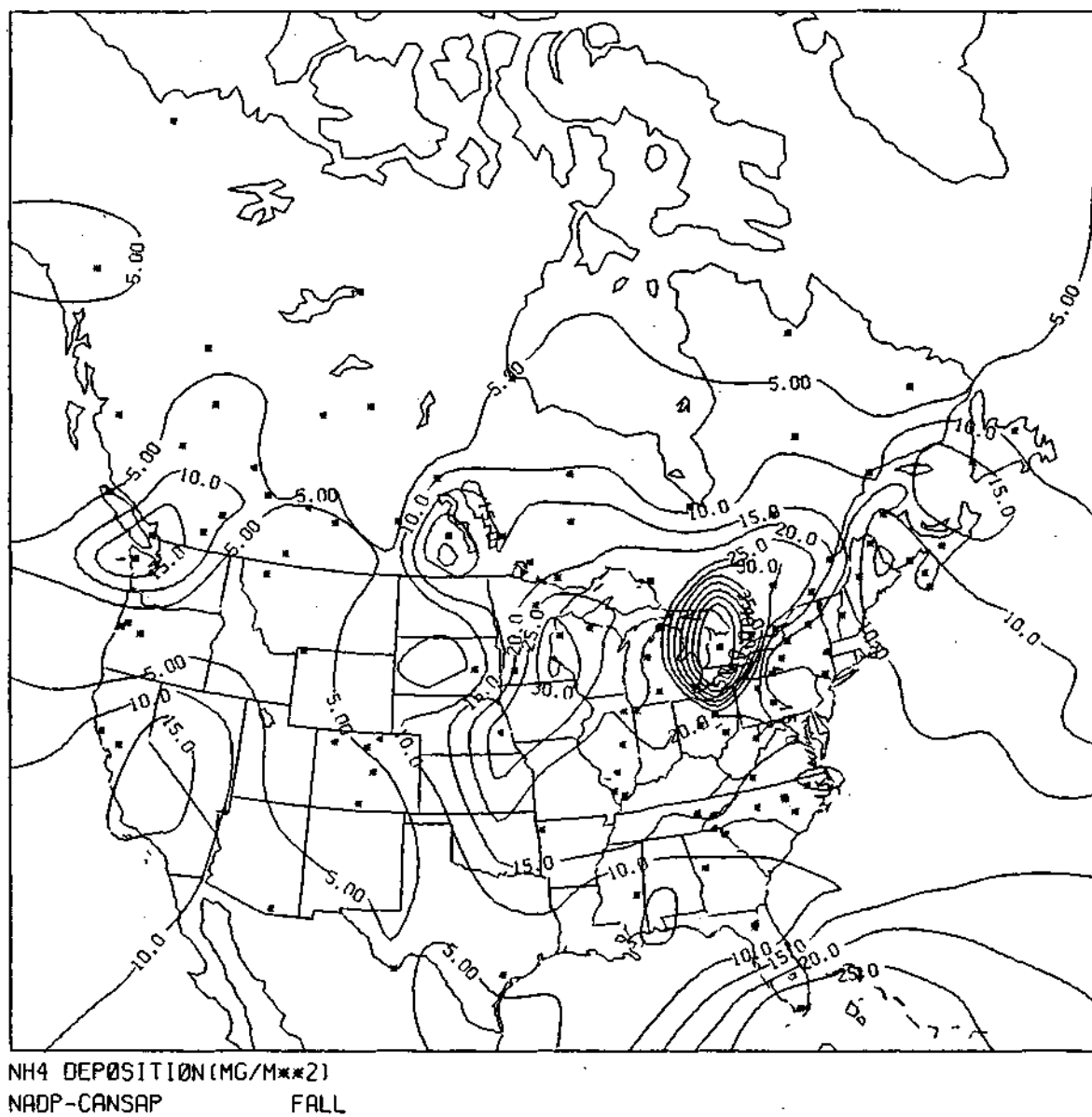


Figure 25. The North American average ammonium deposition ( $\text{mg/m}^2$ ) distribution for the Fall season obtained from the CANSAP and NADP networks.

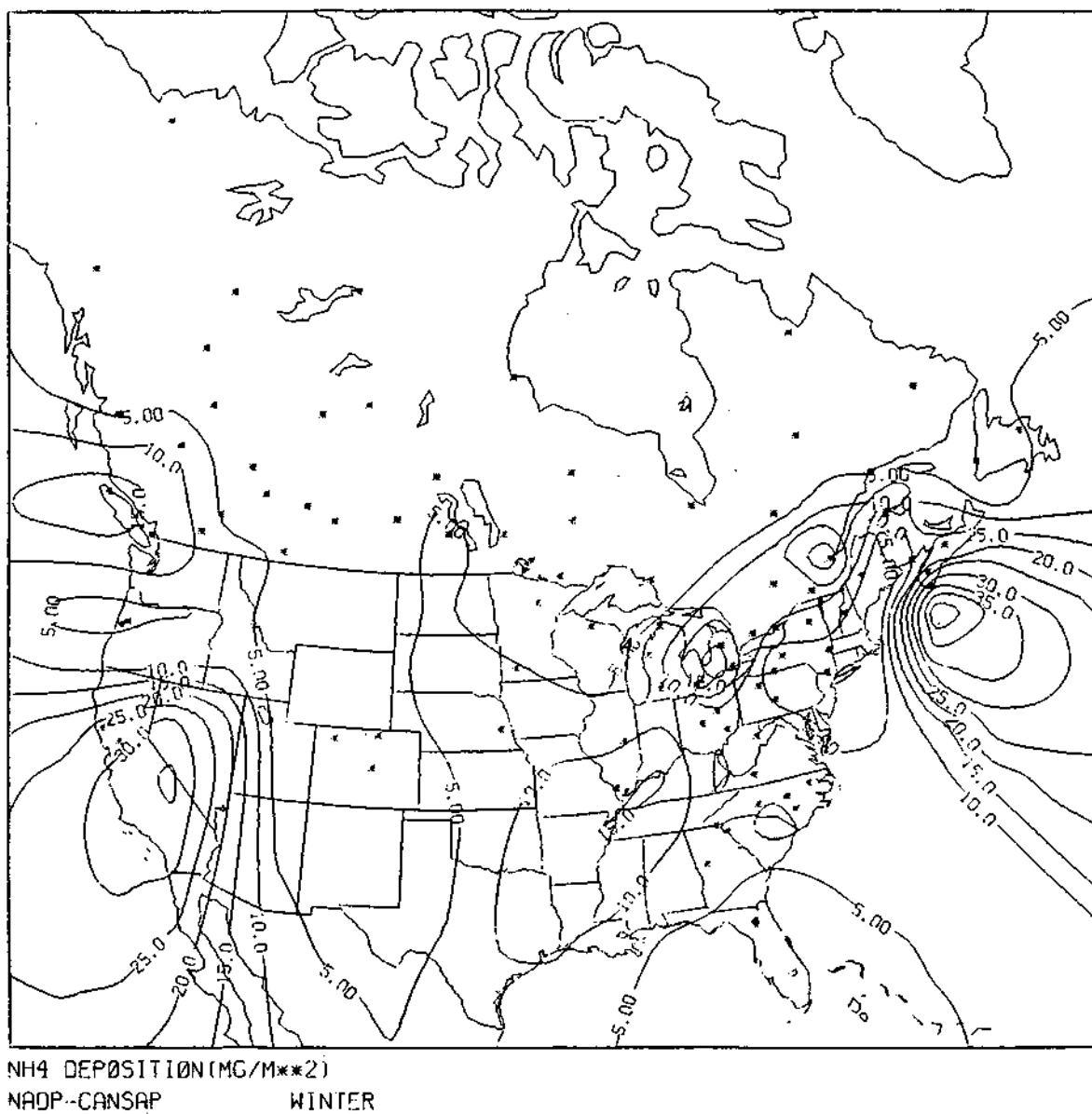


Figure 26. The North American average ammonium deposition ( $\text{mg}/\text{m}^2$ ) distribution for the Winter season obtained from the CANSAP and NADP networks.

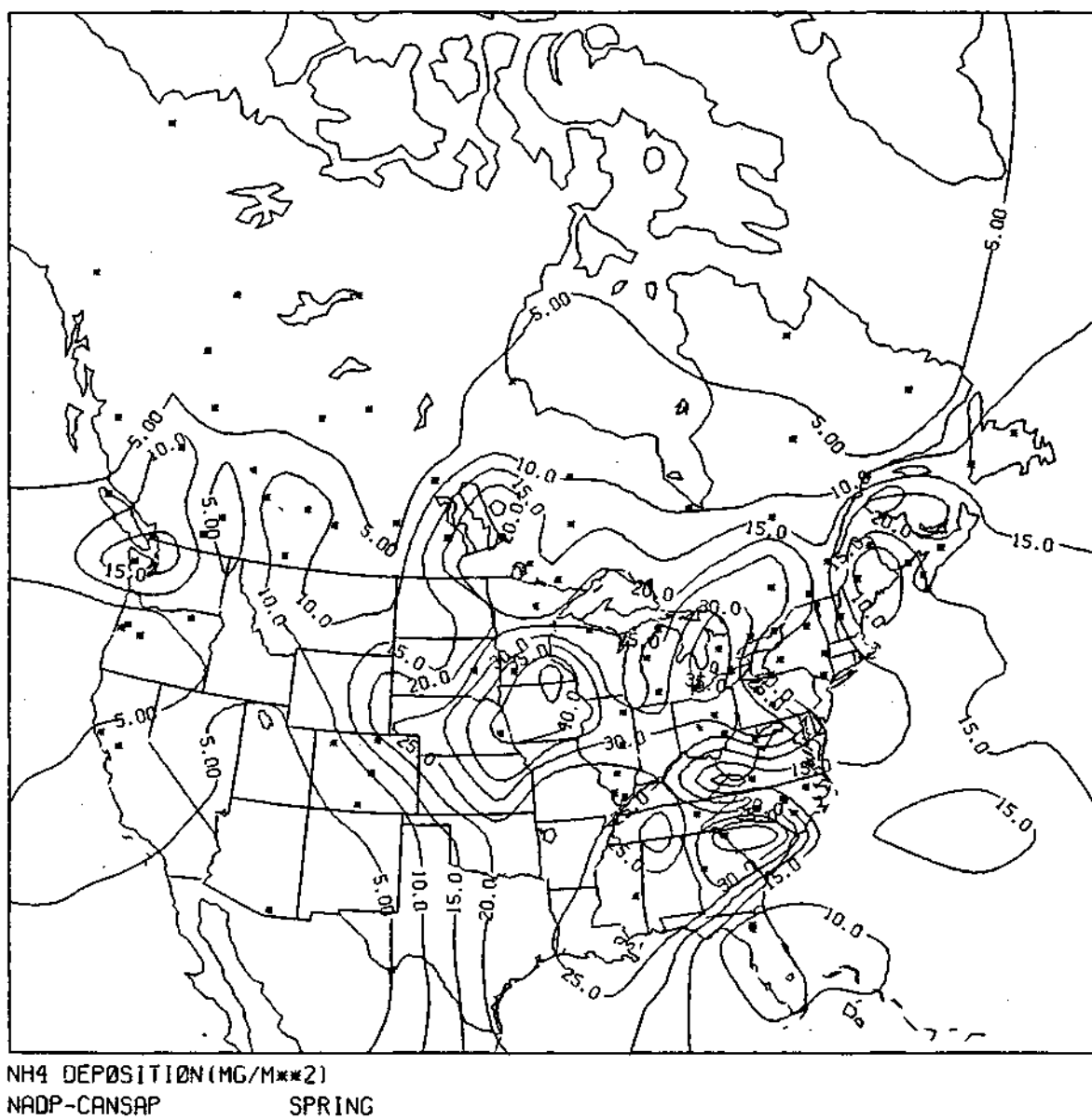
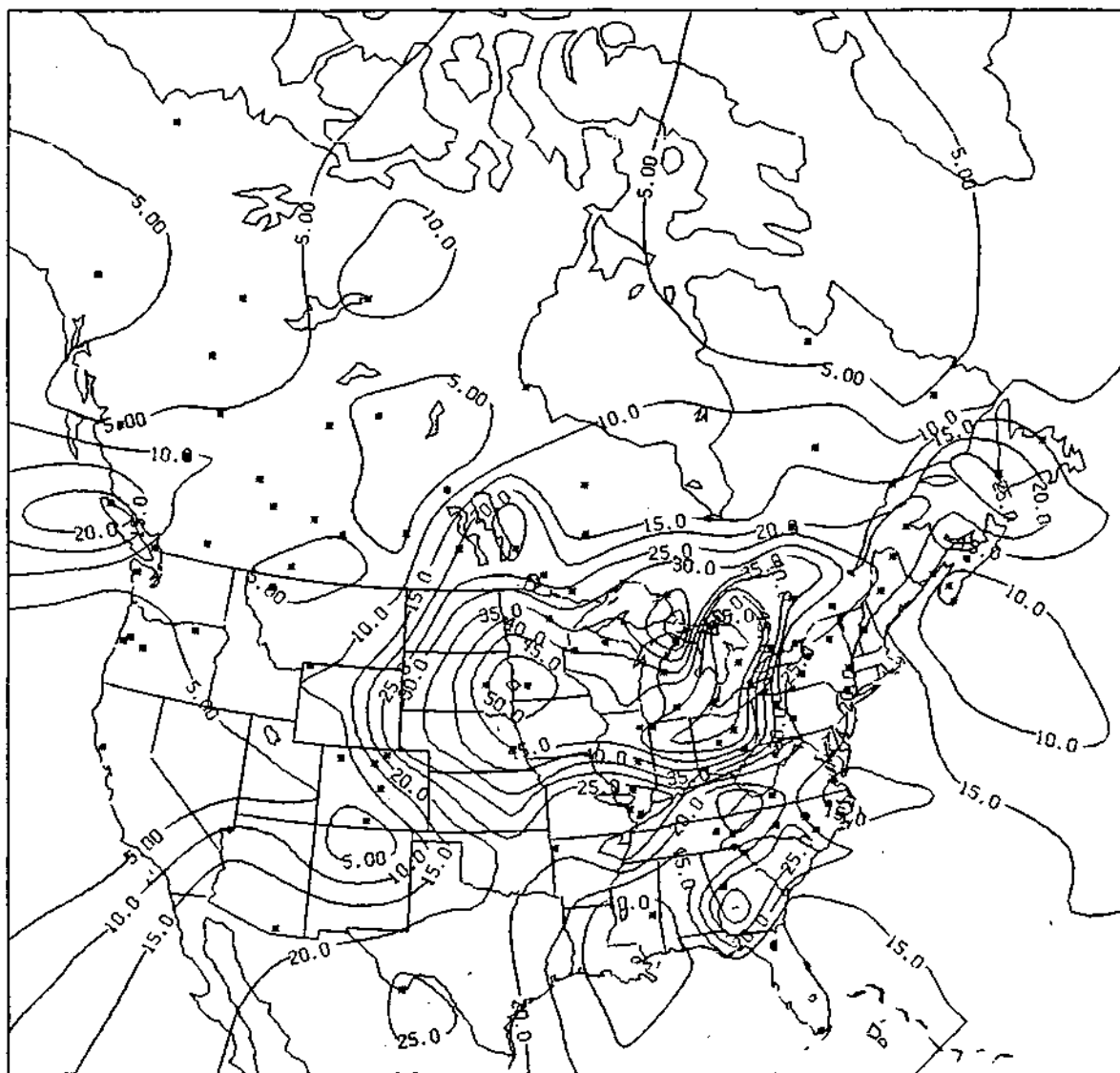


Figure 27. The North American average ammonium deposition ( $\text{mg/m}^2$ ) distribution for the Spring season obtained from the CANSAP and NADP networks.





NH<sub>4</sub> DEPOSITION(MG/M\*\*2)  
NADP-CANSAP SUMMER

Figure 28. The North American average ammonium deposition ( $\text{mg}/\text{m}^2$ ) distribution for the Summer season obtained from the CANSAP and NADP networks.

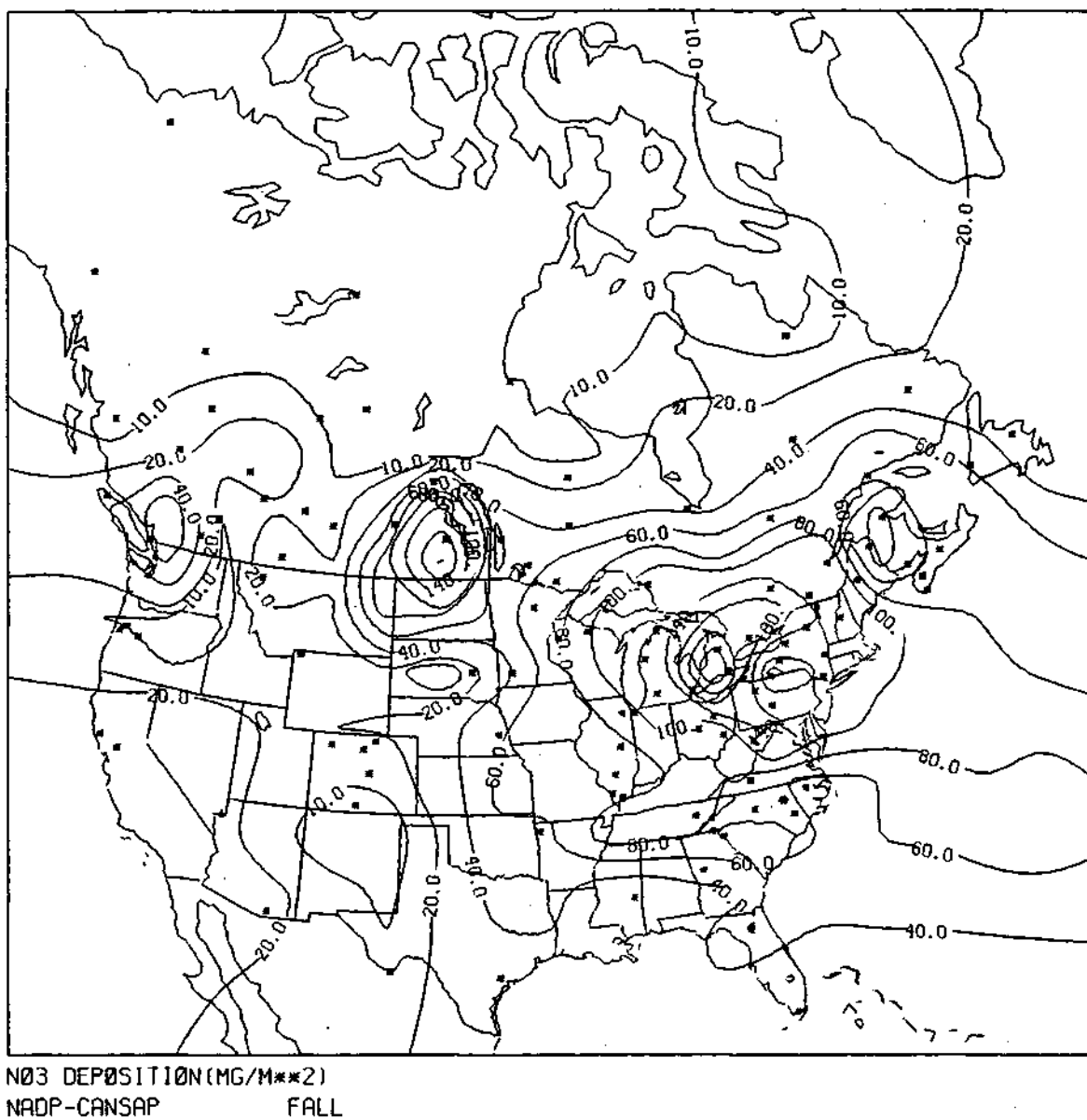
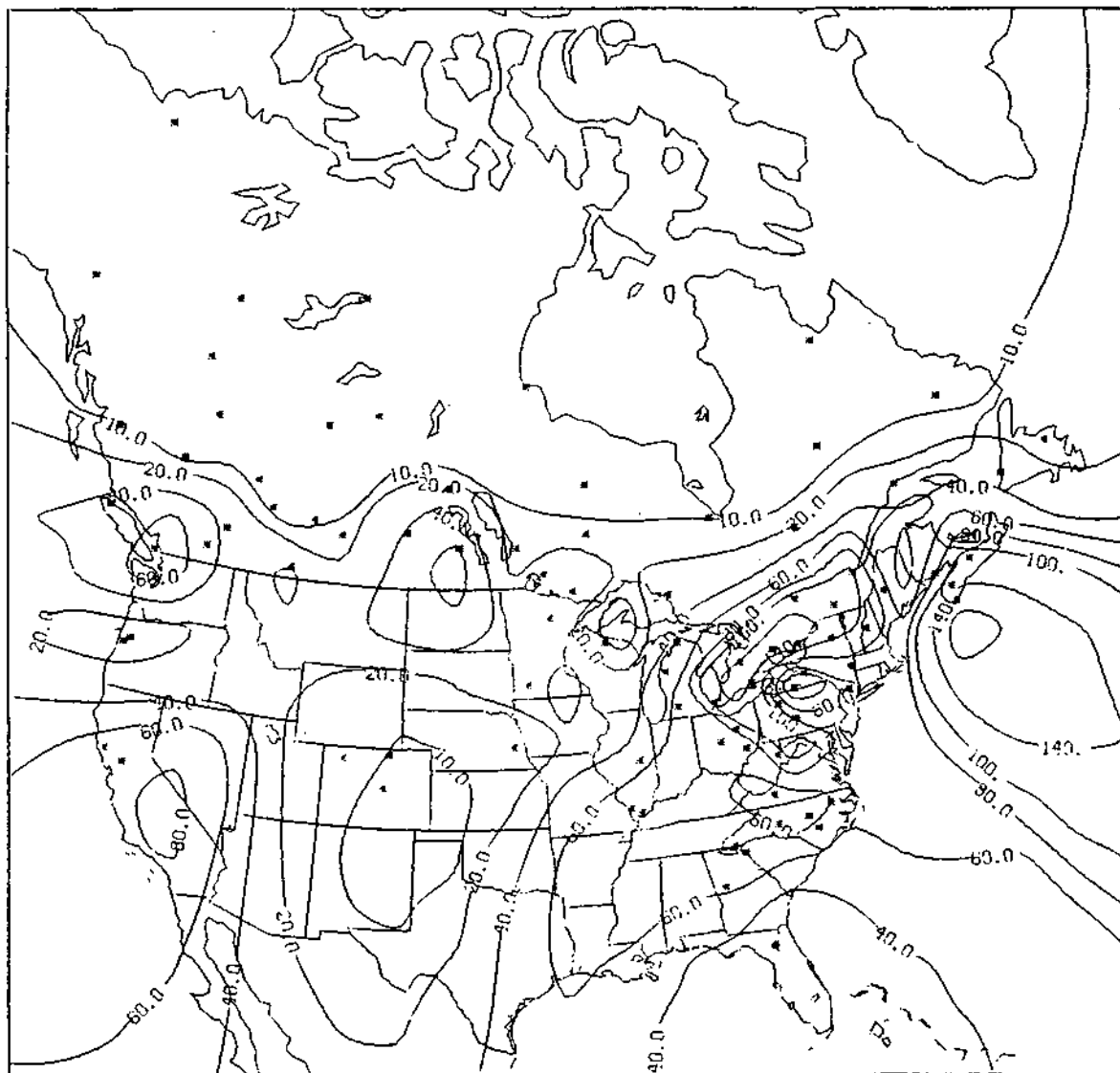


Figure 29. The North American average nitrate deposition ( $\text{mg}/\text{m}^2$ ) distribution for the Fall season obtained from the CANSAP and NADP networks.



N03 DEPOSITION(MG/M\*\*2)  
NADP-CANSAP WINTER

Figure 30. The North American average nitrate deposition ( $\text{mg}/\text{m}^2$ ) distribution for the Winter season obtained from the CANSAP and NADP networks.

The spring nitrate deposition in Fig. 31 bears little resemblance to the concentration pattern of Fig. 11. There is a clear maximum nitrate deposition over eastern Ohio, lower Ontario and western New York and Pennsylvania whereas the maximum in concentration (shown in Fig. 11) is centered on the area north of Lakes Erie and Ontario. Similarly, there is an increasing gradient oriented north-south through the Great Plains extending toward the northeast maximum whereas the concentration pattern shows a relative maximum through the Great Plains from the Dakotas to central Texas.

The summer season shows the maximum deposition of nitrate (Fig. 32) centered on central Ohio with an orientation into New York state in the east and Illinois in the west. In fact, this maximum dominates the North American distribution with values decreasing southwest and north from the Ohio maximum. Comparison of Fig. 32 with Fig. 12 shows that there is little resemblance of the deposition of nitrate and its observed concentration. The maximum in concentration as with other ions is centered in lower Ontario whereas the deposition is displaced to the southeast. This nearly north-south distribution of maximum deposition does not reflect the nearly east-west maximum concentration distribution.

#### Sulfate Deposition

The fall sulfate deposition shown in Fig. 33 shows a relative maximum over southern Ontario with a secondary maximum in Manitoba. There is a relative minimum in sulfate deposition over north-central Pennsylvania on the New York state line. These features are not readily identifiable in the sulfate concentration distribution shown in Fig. 13.

The winter deposition pattern of sulfate shown in Fig. 34 shows a maximum extending from southeast Canada toward the southern states with isolated centers in Alabama and over southern Ontario. Again a minimum is noted over north-central Pennsylvania. This relatively north-south distribution of maximum deposition does not reflect the nearly east-west maximum concentration distribution shown in Fig. 14.

In contrast to the spring season concentration pattern of sulfate in Fig. 15, the deposition maximum appears over Ohio, Pennsylvania and southward into northern Georgia and Alabama (Fig. 35). Again, similar to the winter season there seems to be an overall maximum over the eastern states with a north-south orientation while the maximum in concentration extends along the St. Lawrence valley in Canada with a minor maximum extending southwestward over northwest Arkansas.

In the summer season shown in Fig. 36, the deposition pattern is rather simple with a major maximum over the area from Illinois to the East coast and from West Virginia northward into lower Ontario and Quebec provinces with decreasing values outward in all directions. This is a fairly faithful replication of the concentration pattern shown in Fig. 16. The major differences are that the highest concentrations of sulfate are observed in southern Ontario and Quebec whereas the deposition maximum occurs in a broader band and further south into the Midwest and Atlantic coast states.

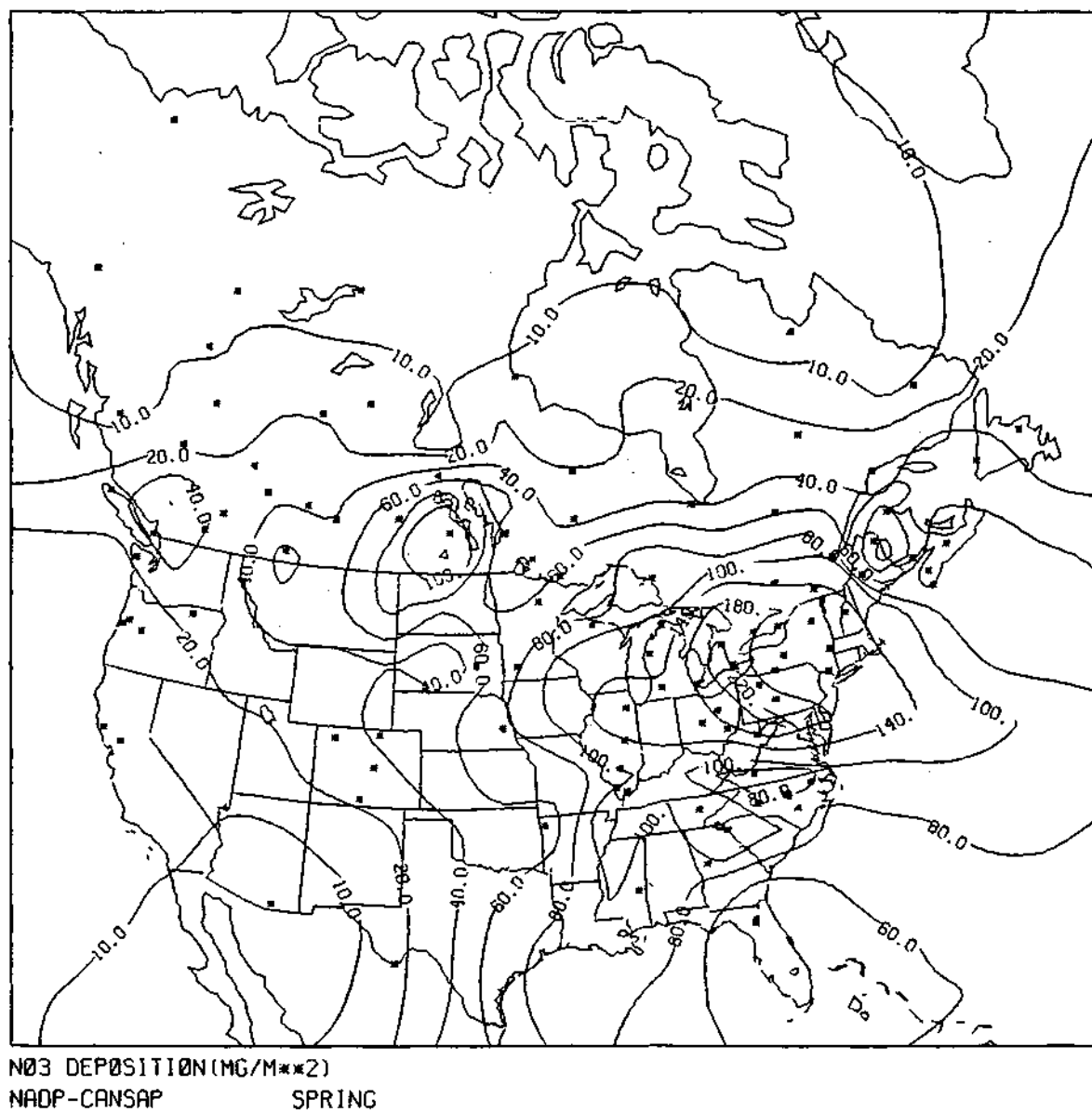
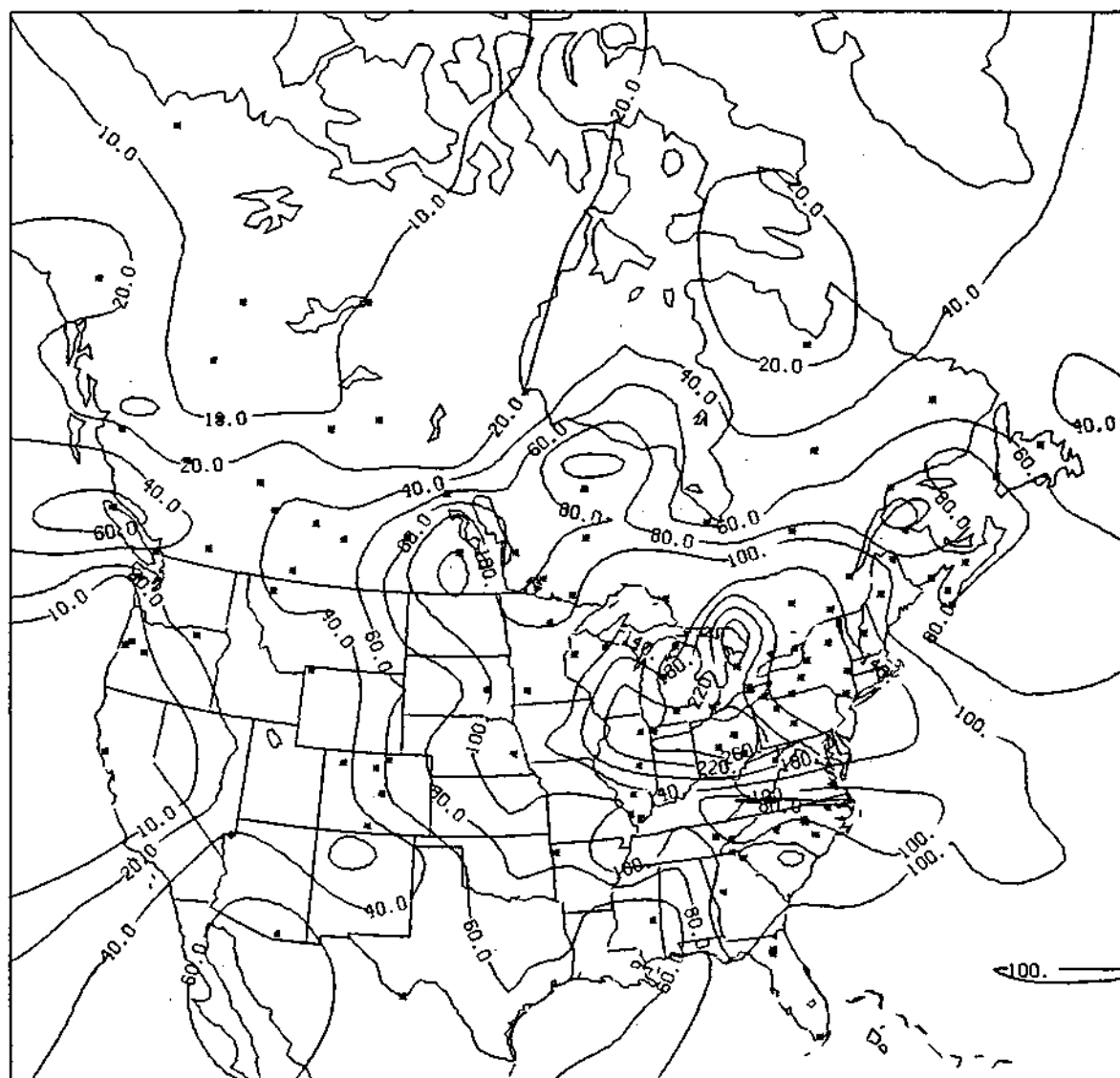


Figure 31. The North American average nitrate deposition ( $\text{mg/m}^2$ ) distribution for the Spring season obtained from the CANSAP and NADP networks.



N03 DEPOSITION(MG/M\*\*2)  
NADP-CANSAP SUMMER

Figure 32. The North American average nitrate deposition ( $\text{mg}/\text{m}^2$ ) distribution for the Summer season obtained from the CANSAP and NADP networks.

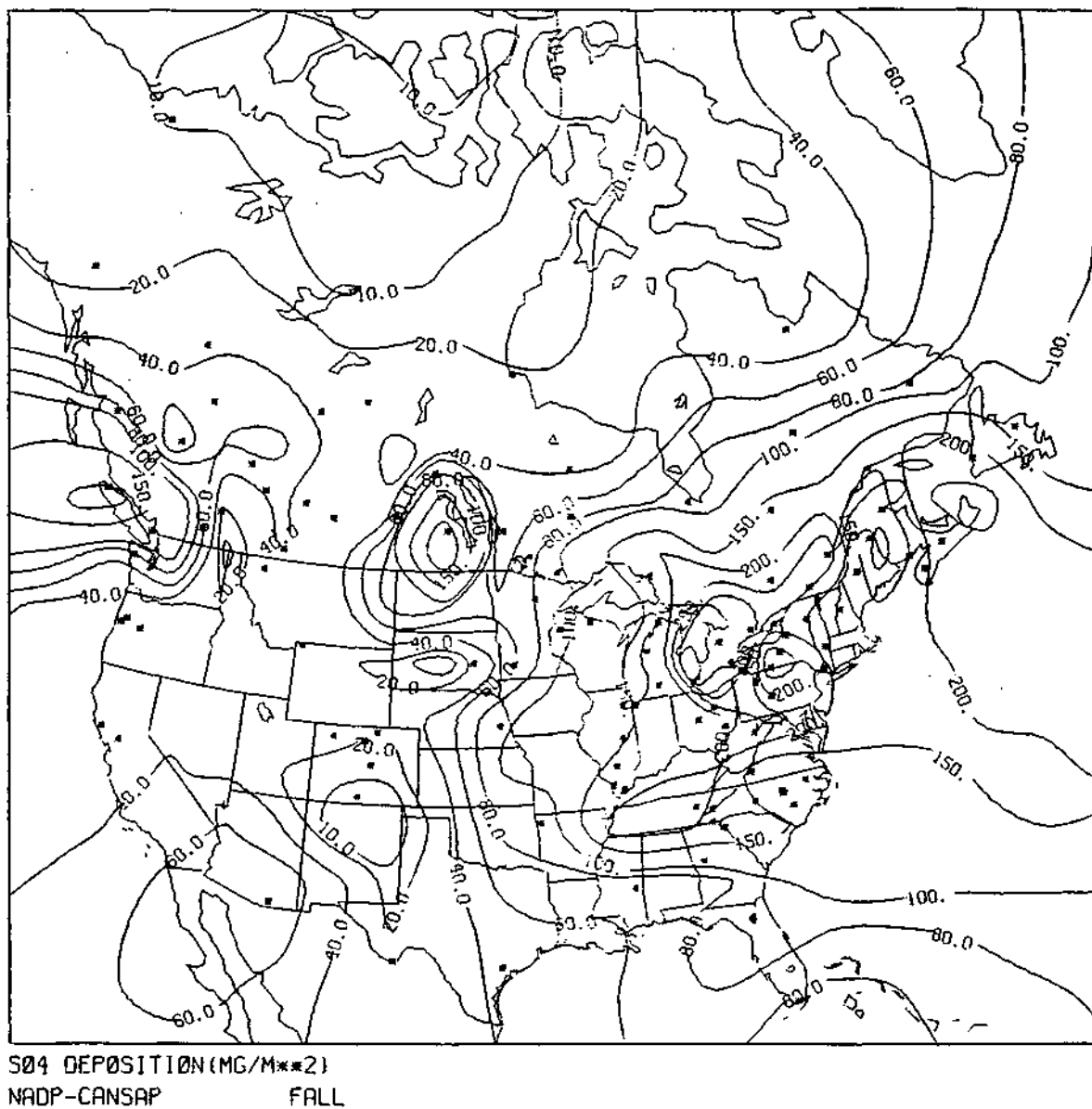
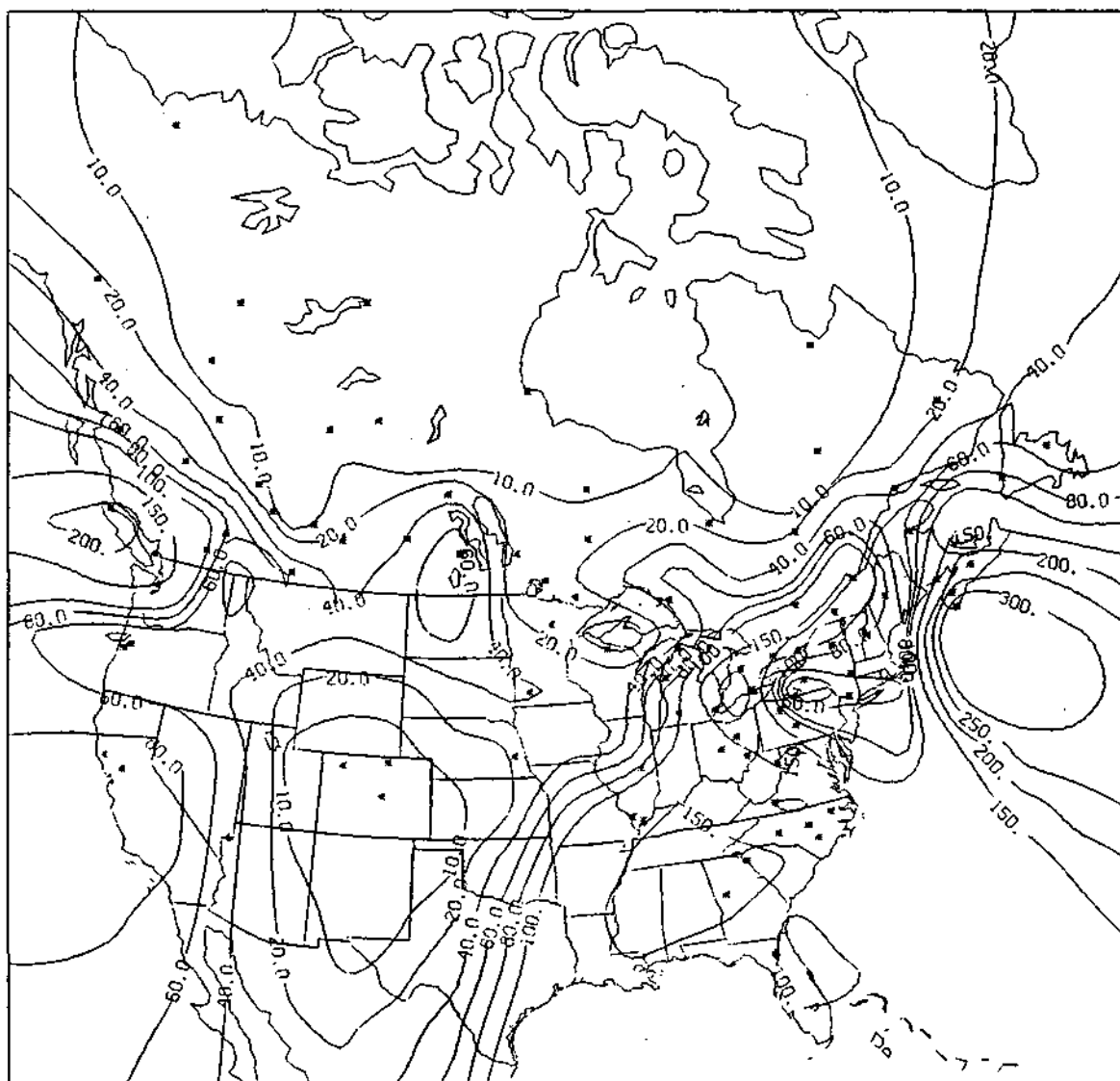


Figure 33. The North American average sulfate deposition ( $\text{mg/m}^2$ ) distribution for the Fall season obtained from the CANSAP and NADP networks.



SO<sub>4</sub> DEPOSITION(MG/M<sup>2</sup>)  
NADP-CANSAP WINTER

Figure 34. The North American average sulfate deposition ( $\text{mg}/\text{m}^2$ ) distribution for the Winter season obtained from the CANSAP and NADP networks.



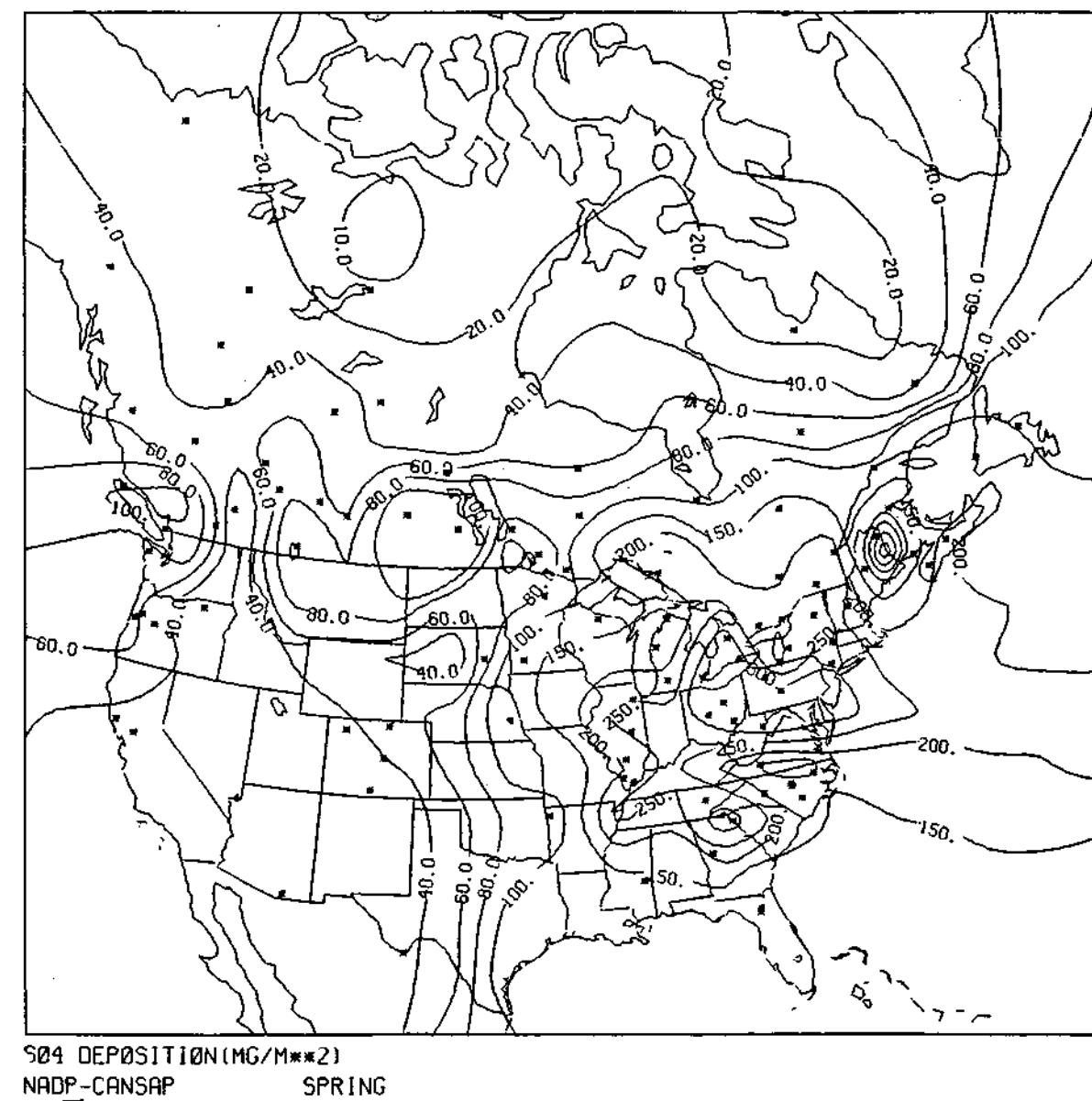
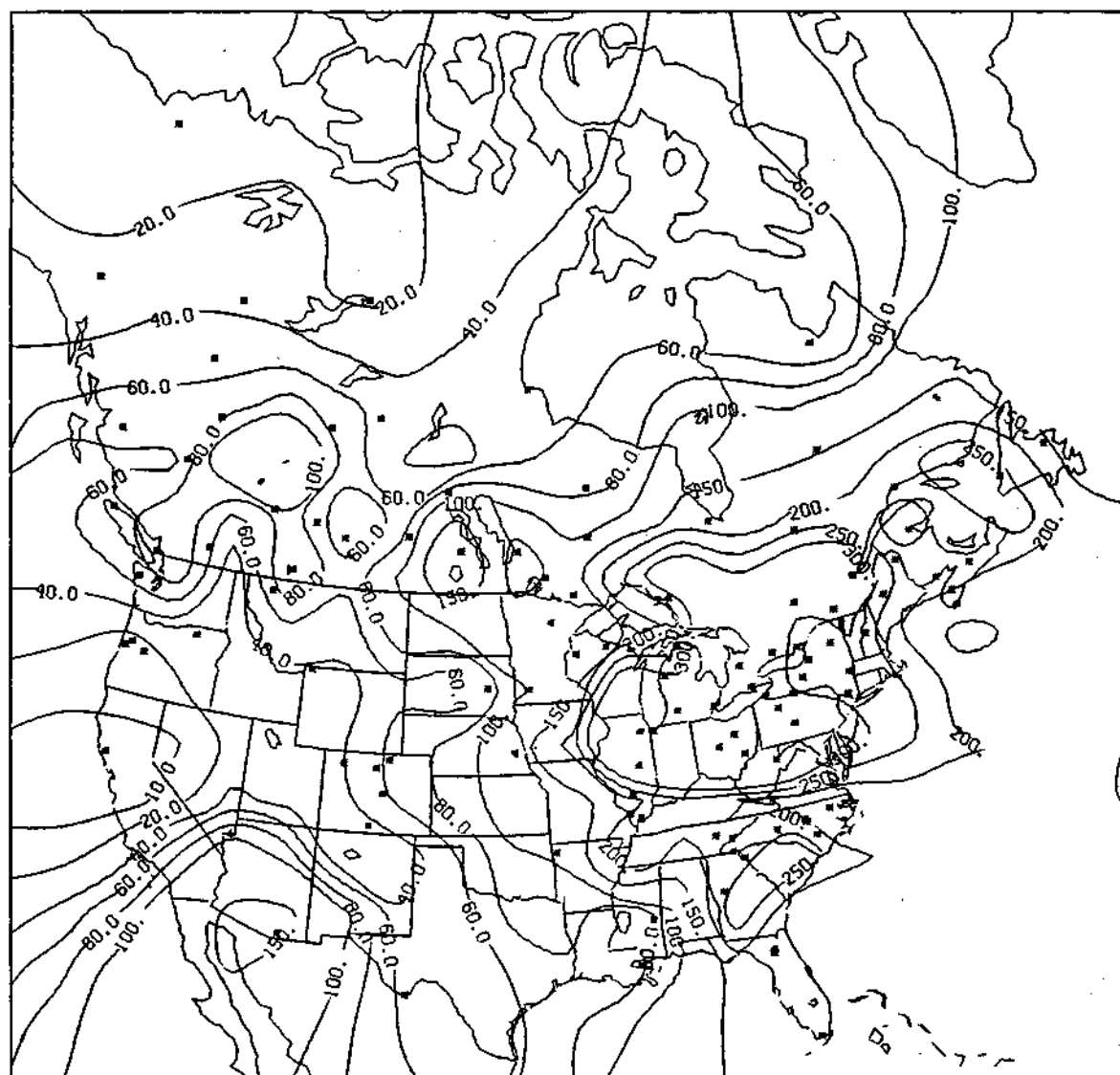


Figure 35. The North American average sulfate deposition ( $\text{mg}/\text{m}^2$ ) distribution for the Spring season obtained from the CANSAP and NADP networks.



S04 DEPOSITION(MG/M\*\*2)  
NADP-CANSAP SUMMER

Figure 36. The North American average sulfate deposition ( $\text{mg}/\text{m}^2$ ) distribution for the Summer season obtained from the CANSAP and NADP networks.

### Hydrogen Ion Deposition Distribution

The seasonal deposition of hydrogen ion is shown in Figs. 37-40. The greatest deposition in the fall season (Fig. 37) occurs over the northeast United States with a maximum over lower Ontario extending southward into Ohio and Pennsylvania. A small minimum occurs again in north-central Pennsylvania. A relatively large maximum appears in Manitoba which corresponds to a relative maximum of pH shown in Fig. 17. This maximum hydrogen ion deposition likely occurs from the relatively high concentrations of the nitrate and sulfate observed in that area.

The winter deposition shown in Fig. 38 shows a fairly strong gradient of hydrogen ion deposition oriented northeast-southwest through the western Midwest into the lower eastern Canadian provinces. The deposition maximizes in southeastern Ohio and the central Atlantic coast states. An isolated maximum is also seen in the Manitoba area corresponding to that observed during the fall season.

The spring and summer patterns shown in Figs. 39 and 40 are similar, but with the greatest deposition occurring in the summer months corresponding to the heavier rainfall observed in that season. Generally there is a strong east-west gradient through the Great Plains in spring (Fig. 39) with the Manitoba high still present. The gradient extends east toward Lower Hudson's Bay. To the east and south of this maximum gradient, the hydrogen ion deposition maximizes through central Ohio and along the southern Pennsylvania-Maryland state line. During the summer season (Fig. 40), the very strong gradient through the high plains is still present in almost the same location as during spring, but the maximum deposition area is greater in magnitude and covers an area with an east-west orientation from Illinois to New Jersey encompassing parts of New York, West Virginia, and northern Kentucky.

### Discussion of Deposition Distributions

The first major observation to be made is that while the precipitation concentrations for the cations and anions discussed previously occur largely in Canada, the maximum ion deposition occurs over the United States. Most importantly, the maximum deposition of the hydrogen ion occurs (in this relatively small sample of a little more than two years) not in the New York state - lower Ontario region but further south and somewhat west of that area. Of course, it must be borne in mind that these data are preliminary in the sense that they represent a relatively short sampling time. Perhaps as additional data are acquired from both of these networks in future years a more stable and clarified picture will emerge.

## ANNUAL CONCENTRATION AND DEPOSITION DISTRIBUTIONS

The entire data sets from both networks were integrated to provide annual average concentration, deposition, and total rainfall distributions. These are

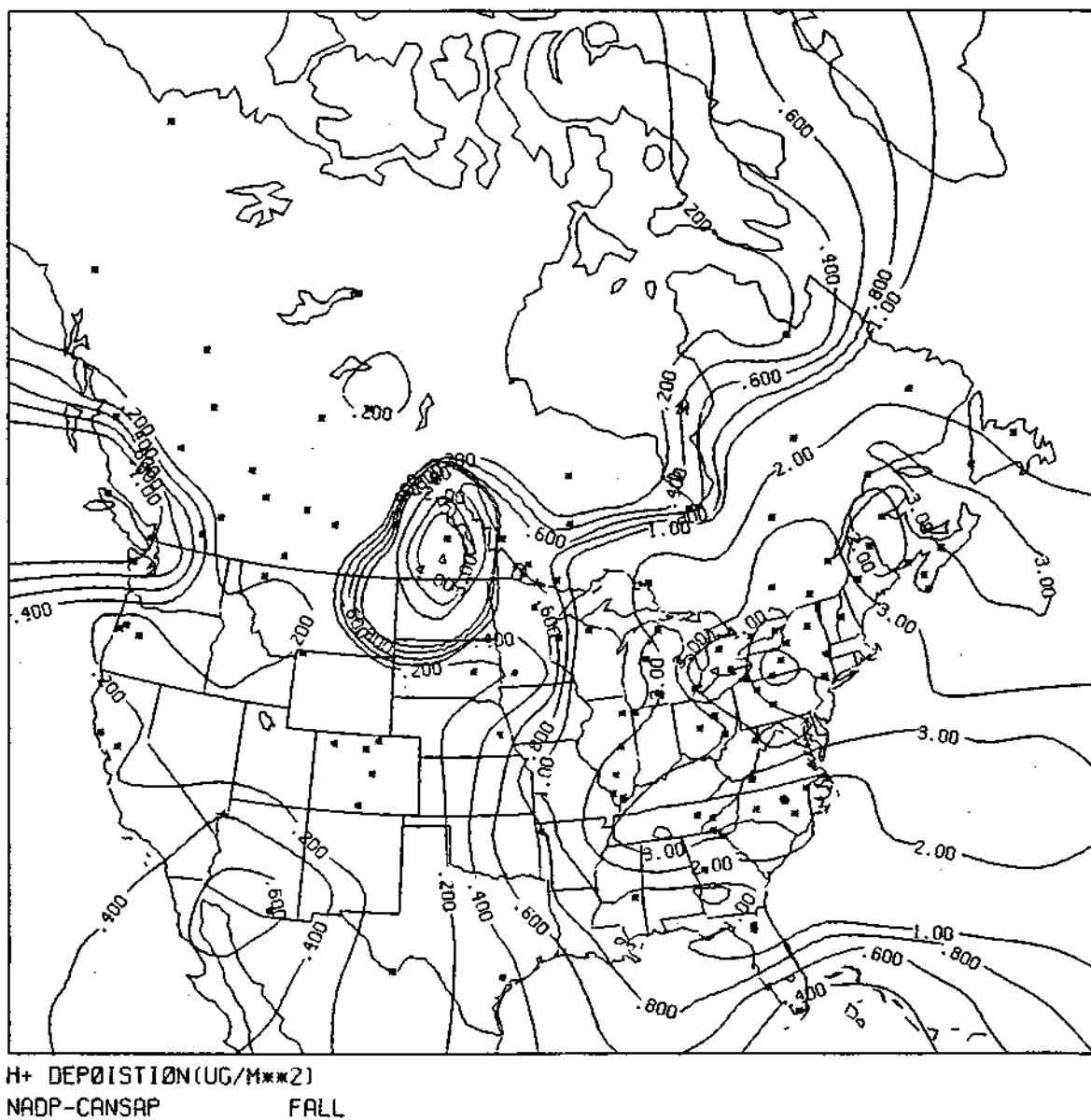


Figure 37. The North American average hydrogen ion deposition ( $\mu g/m^2$ ) distribution for the Fall season obtained from the CANSAP and NADP networks.

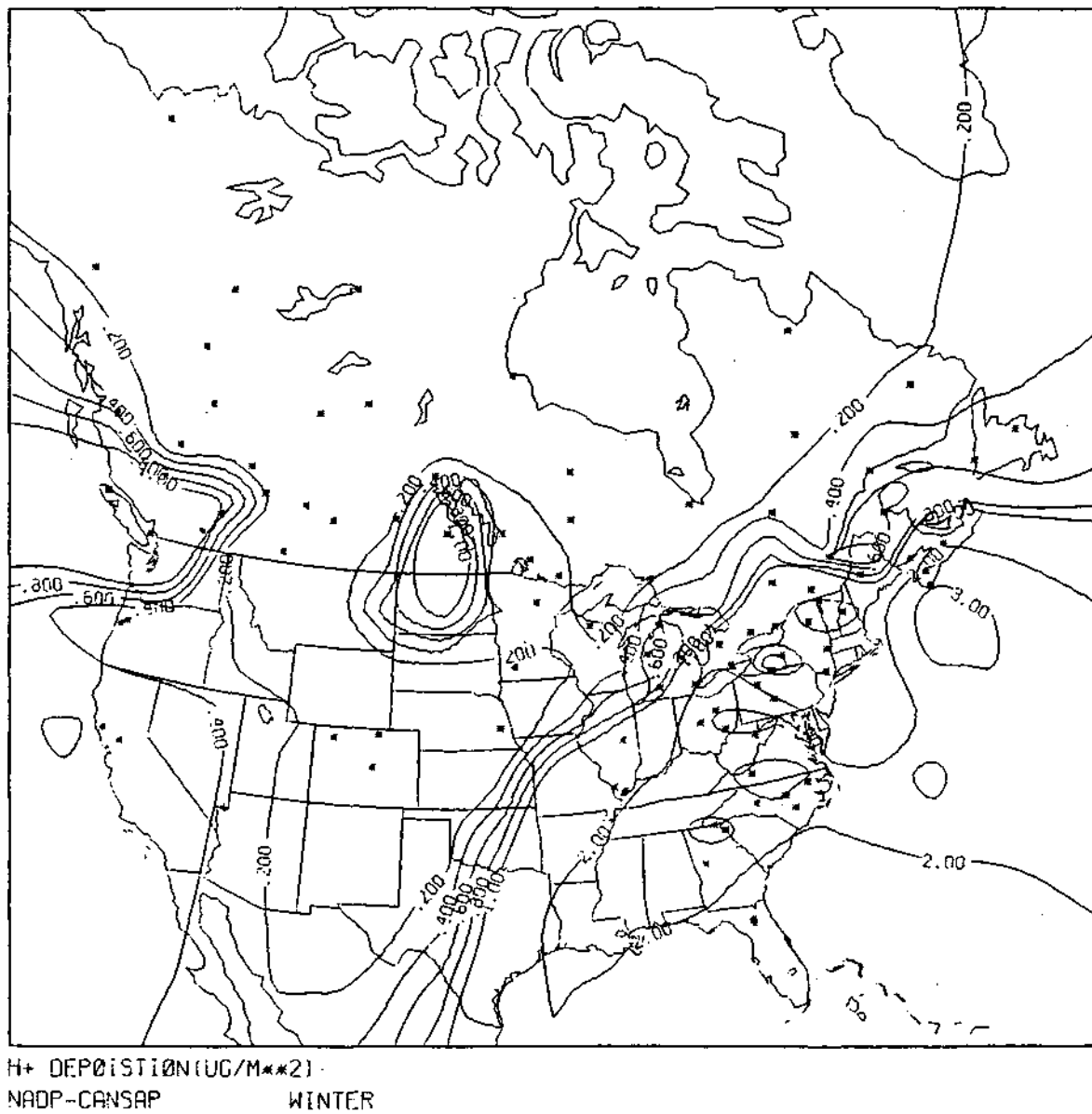
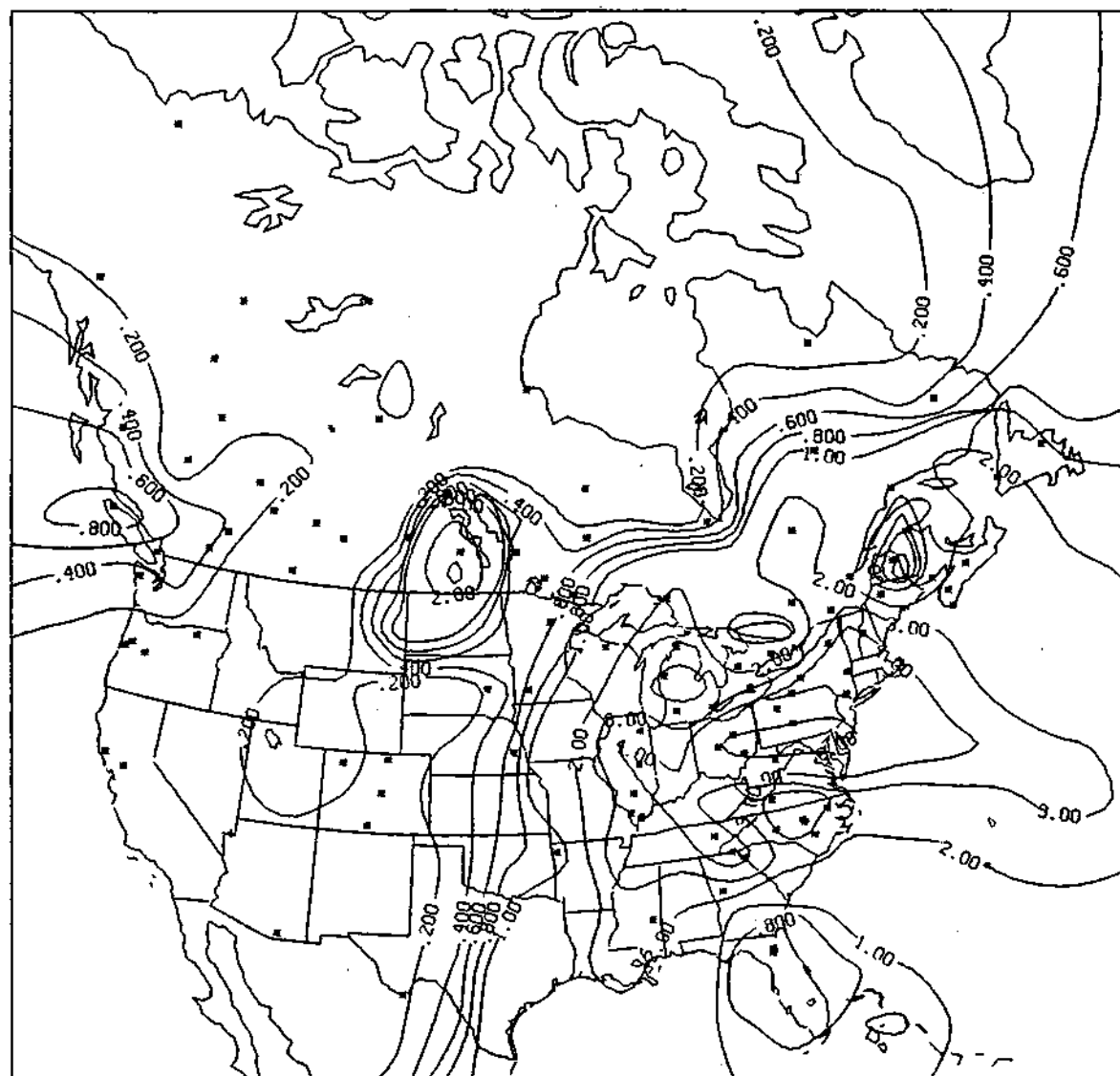


Figure 38. The North American average hydrogen ion deposition ( $\mu\text{g}/\text{m}^2$ ) distribution for the Winter season obtained from the CANSAP and NADP networks.



H+ DEPOSITION(UG/M\*\*2)  
NADP-CANSAP SPRING

Figure 39. The North American average hydrogen ion deposition ( $\mu\text{g}/\text{m}^2$ ) distribution for the Spring season obtained from the CANSAP and NADP networks.

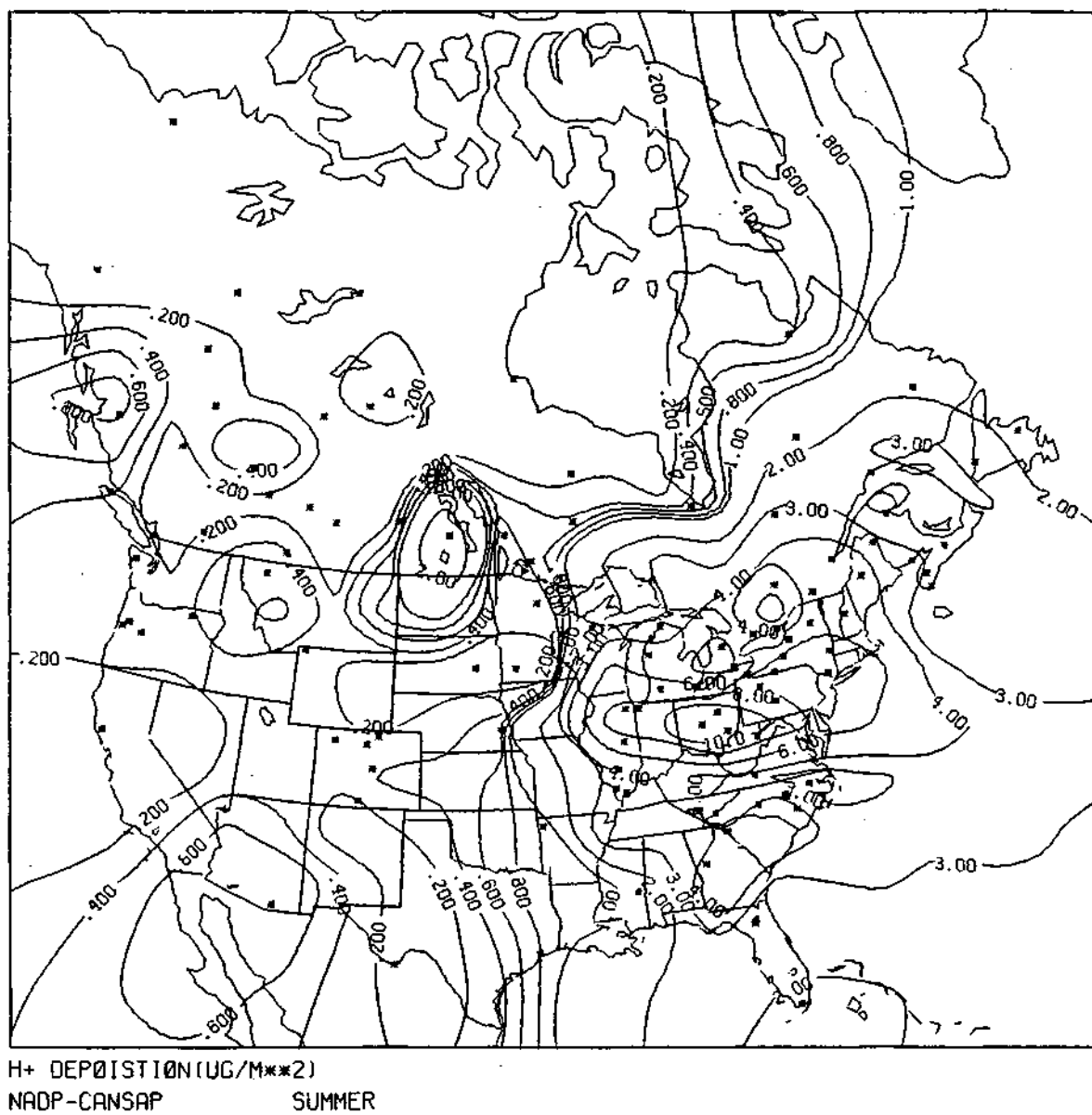


Figure 40. The North American average hydrogen ion deposition ( $\mu g/m^2$ ) distribution for the Summer season obtained from the CANSAP and NADP networks.

shown in Figs. 41 through 51 and, of course, are subject to change as the chemical climatology is developed in future years.

#### Precipitation Distribution

As can be seen in Fig. 41, the precipitation for the period of data collection included in this analysis was less than 50 cm over much of the western U.S. while the states east of the Mississippi River experienced precipitation ranging from 100 to 300 cm. Vancouver Island in extreme southwestern Canada received the most precipitation exceeding 400 cm. The extreme northeast U.S. from Maine along the northeast coast to lower New York and eastern Pennsylvania with values less than 100 cm reflect the prolonged drought of that locale. The maximum rainfall in the northeast occurred in a narrow belt from upper Quebec through lower Ontario, eastern Ohio, and southwestern Pennsylvania to the East coast. This area should be remembered as we discuss the deposition patterns of various ion species.

#### Calcium Concentration and Deposition

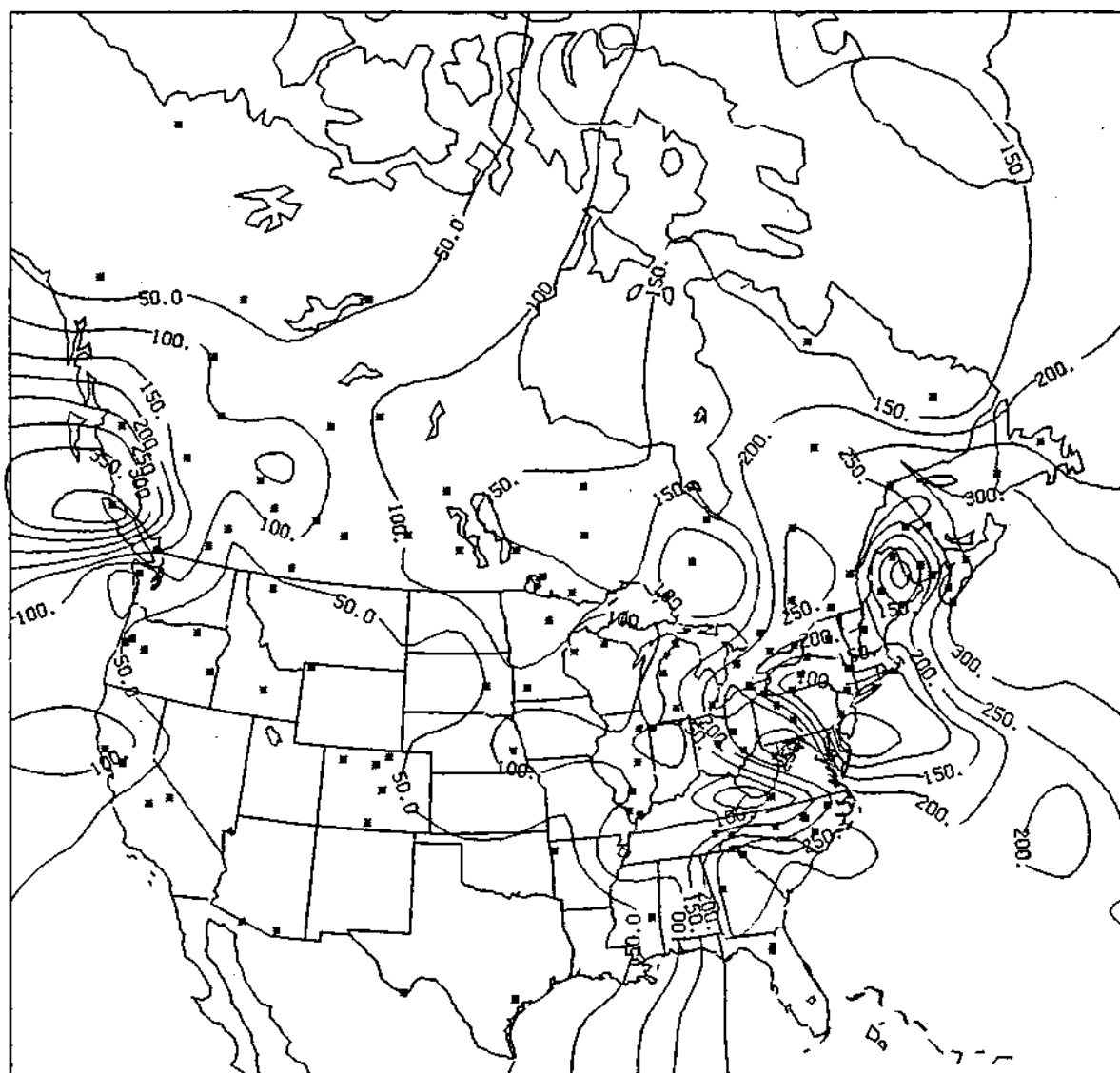
The annual average calcium concentration (Fig. 42) is similar to the individual seasonal values presented earlier with maxima in Alberta and lower Saskatchewan and the secondary maximum over lower Ontario paralleling the St. Lawrence valley. These concentrations maximize with values of 2.8 and 1.2 mg/L respectively, are 5 to 10 times greater than values over the lower Midwest and Southeast United States. The deposition pattern shown in Fig. 43 also shows the same maxima as the concentration distributions. Relatively low average deposition is observed over the southeast and the far west with maximum values along the Canadian border and in the Midwest extending from Illinois northeastward to lower Ontario and Quebec.

#### Ammonium Concentration and Deposition

The average annual ammonium concentration is shown in Fig. 44. Three maxima appear in this distribution with all of them confined to the United States. A western maximum is centered in Nevada and across central California, a central maximum is centered in Nebraska, and a somewhat smaller but significant northeastern maximum is located over extreme southeast Ontario in the vicinity of Detroit, Michigan.

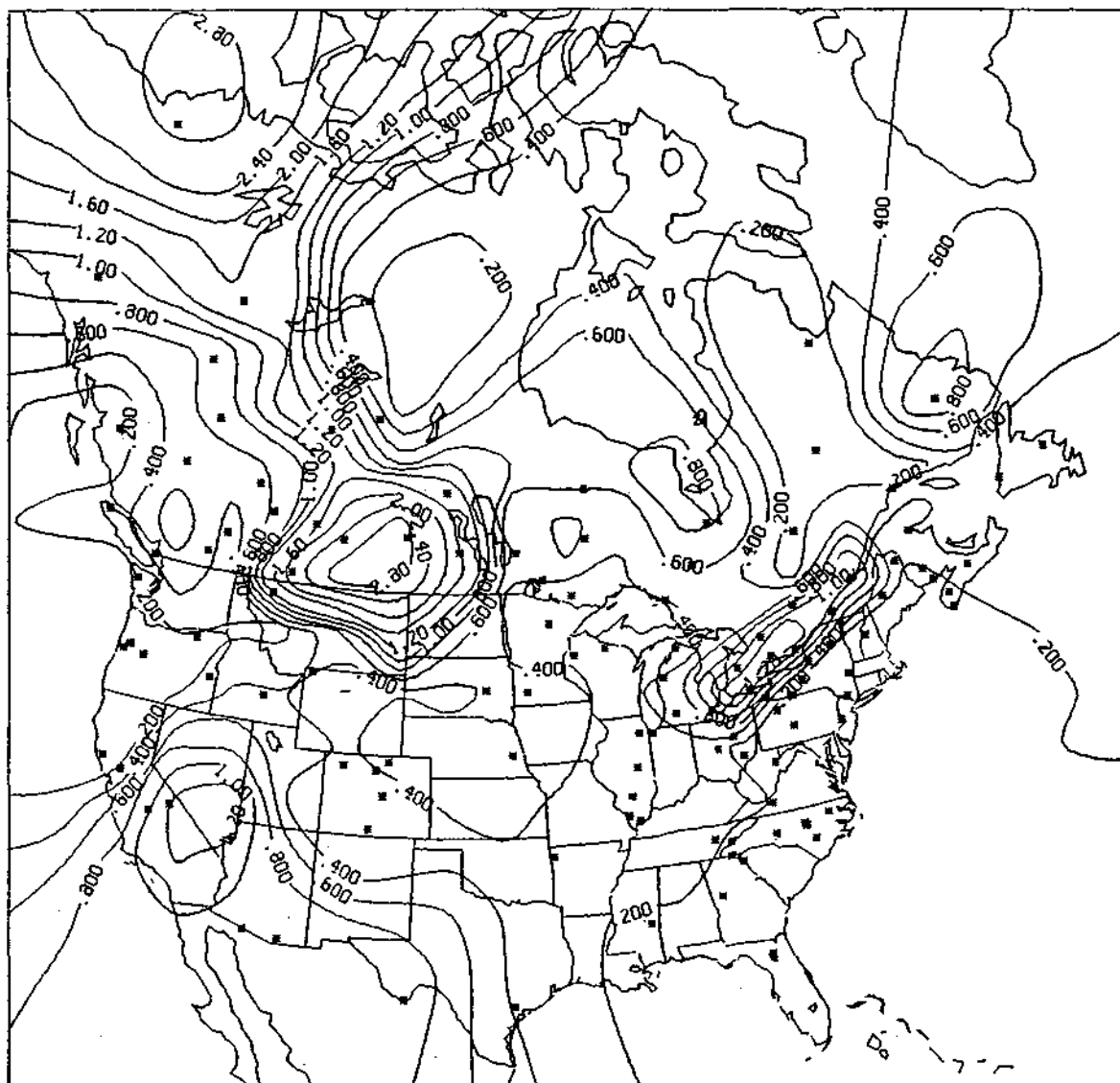
All of these maxima can also be seen in the deposition pattern shown in Fig. 45. However, because of the precipitation distribution the maximum deposition of ammonium is located over southwest Ontario with a value in excess of 50 mg/m<sup>2</sup> as compared with 35 over lower Minnesota. It should be noticed that the deposition maximum in the Great Plains is somewhat displaced to the east of the concentration maximum. This displacement is largely due to the increase of precipitation to the east as can be seen in Fig. 41.





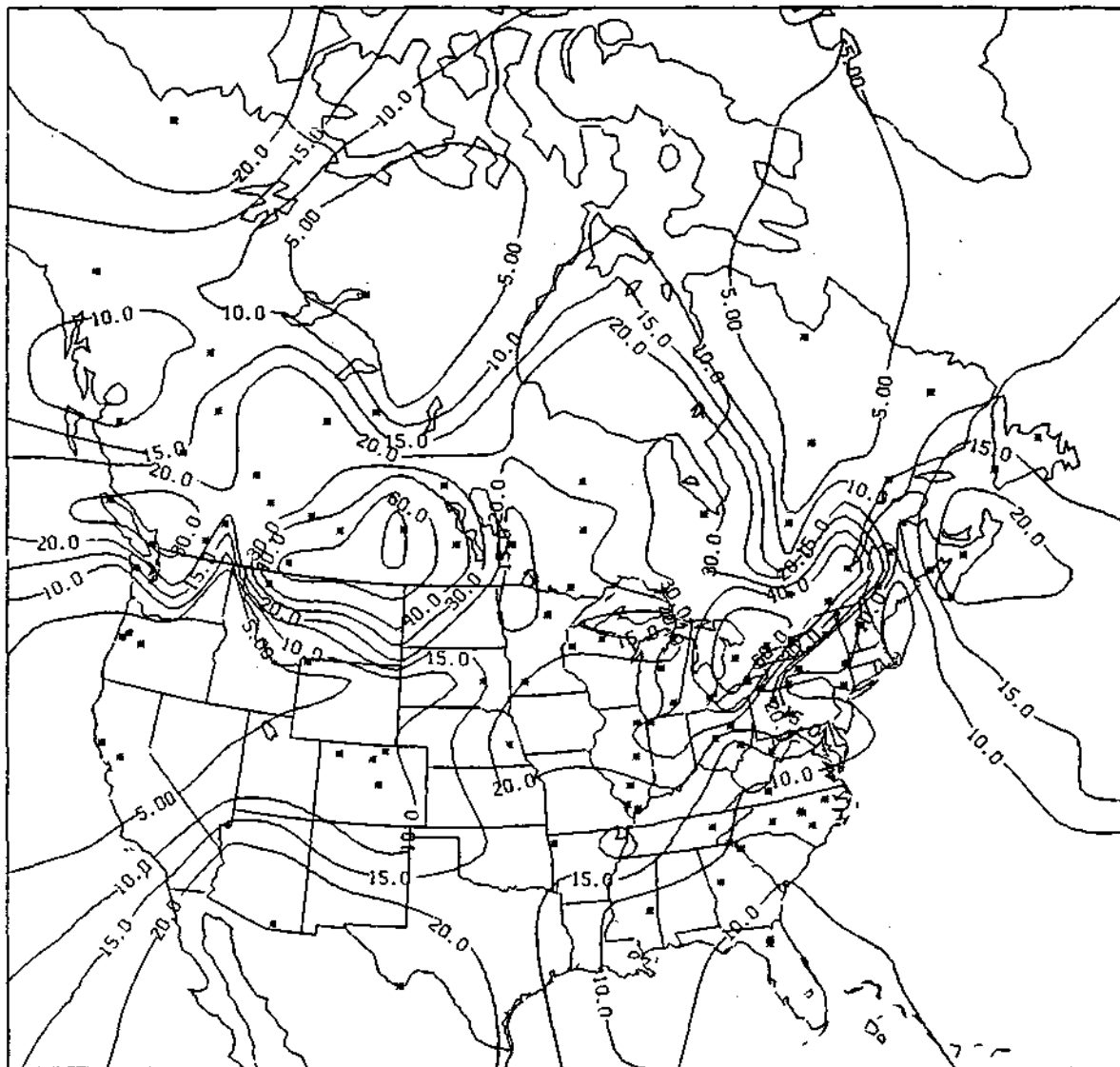
RAINGAGE SAMPLE VOLUME (CM)  
NADP-CANSAP                  ANNUAL

Figure 41. The distribution of accumulated precipitation over North America obtained from the CANSAP and NADP networks. The numbers represent the equivalent depth in cm of the volume of precipitation obtained at each site accumulated over its period of operation.



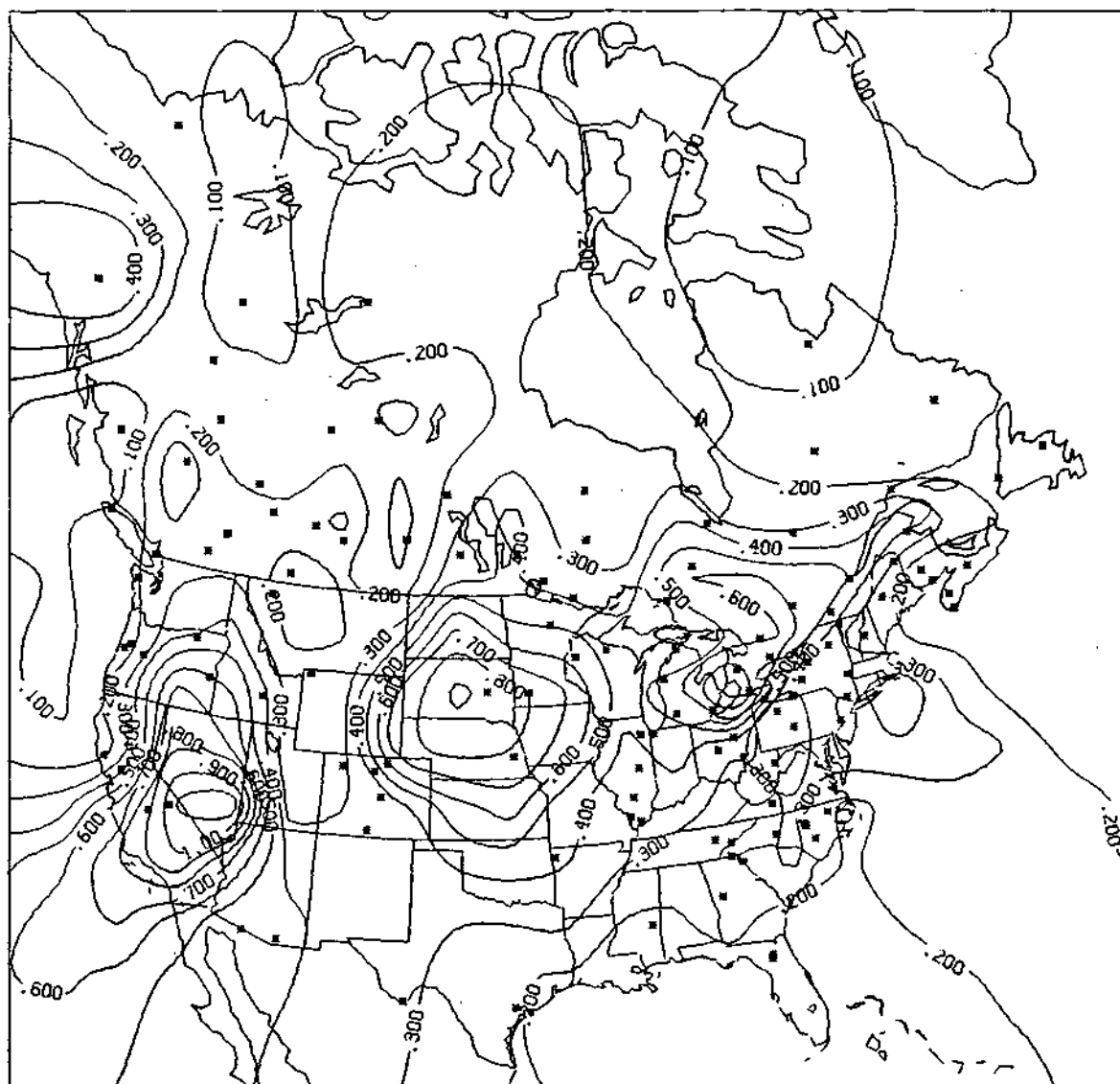
CA CONCENTRATION(MG/L)  
NADP-CANSAP          ANNUAL

Figure 42. The average annual calcium concentration (mg/L) over North America from the combined CANSAP and NADP networks.



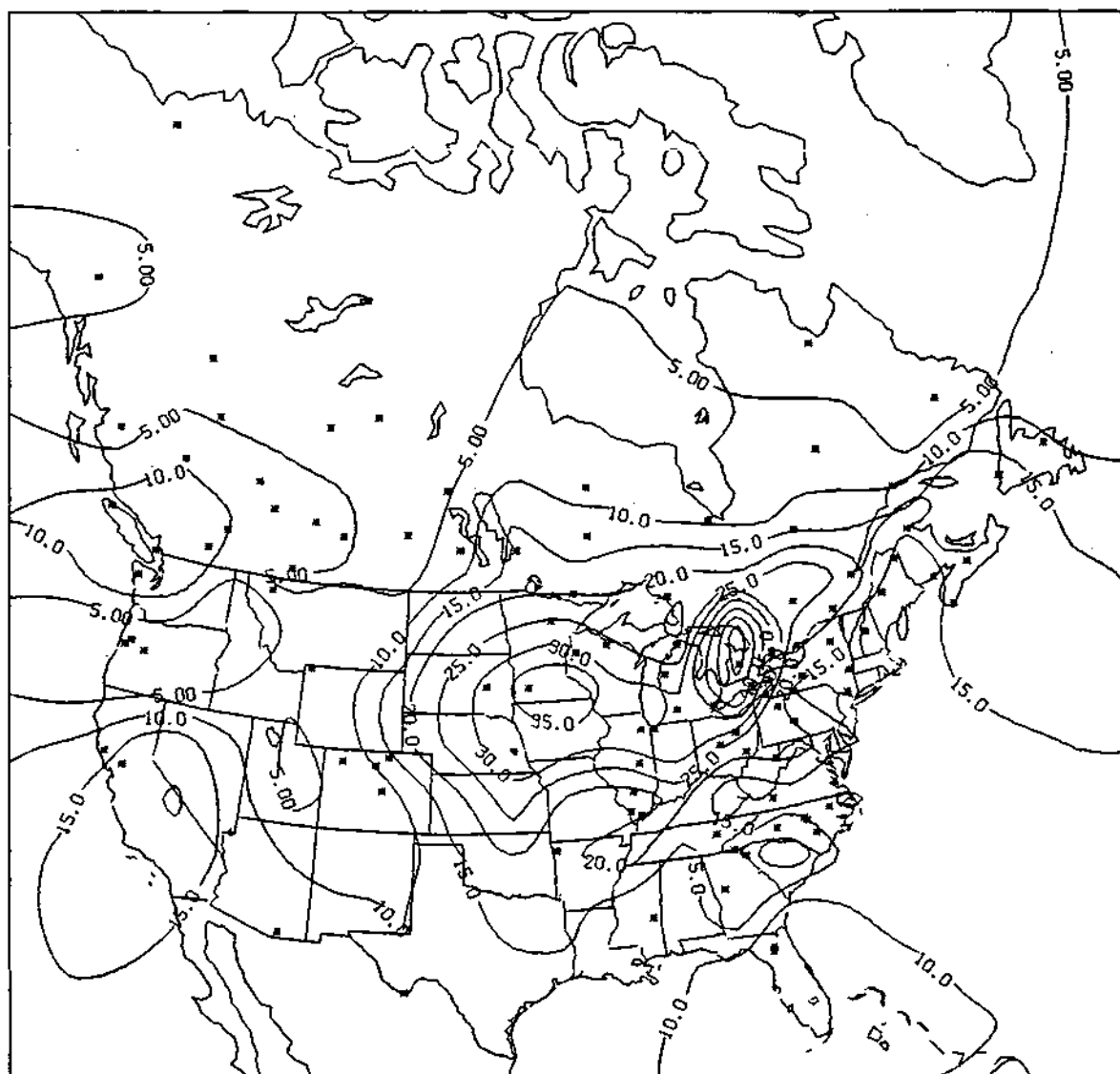
CA DEPOSITION(MG/M\*\*2)  
NADP-CANSAP                  ANNUAL

Figure 43. The average annual calcium deposition ( $\text{mg}/\text{m}^2$ ) over North America from the combined CANSAP and NADP networks.



NH<sub>4</sub> CONCENTRATION(MG/L)  
NADP-CANSAP                  ANNUAL

Figure 44. The average annual ammonium concentration (mg/L) over North America from the combined CANSAP and NADP networks.



NH<sub>4</sub> DEPOSITION(MG/M\*\*2)  
NADP-CANSAP                  ANNUAL

Figure 45. The average annual ammonium deposition ( $\text{mg}/\text{m}^2$ ) over North America from the combined CANSAP and NADP networks.

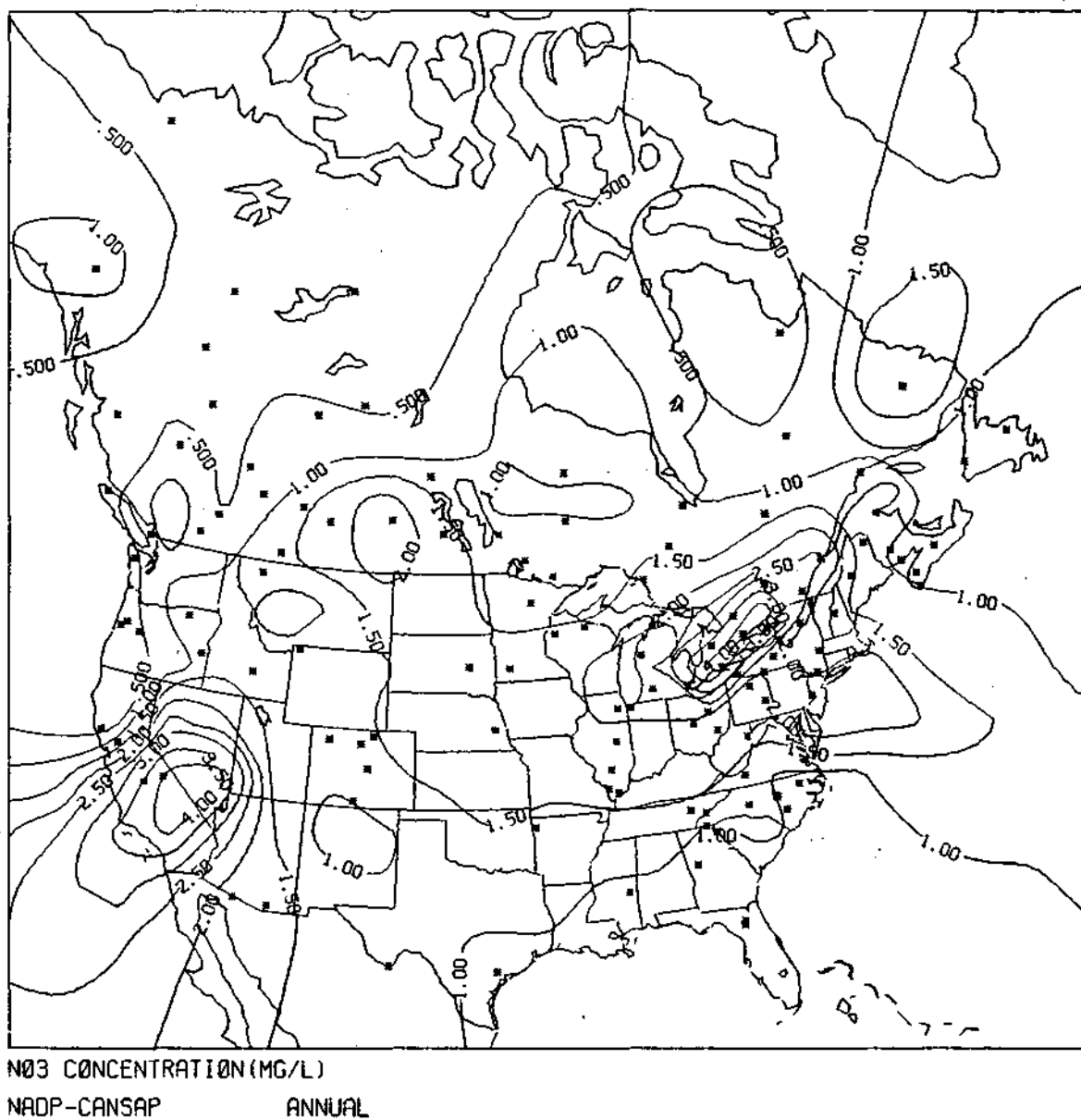


Figure 46. The average annual nitrate concentration (mg/L) over North America from the combined CANSAP and NADP networks.

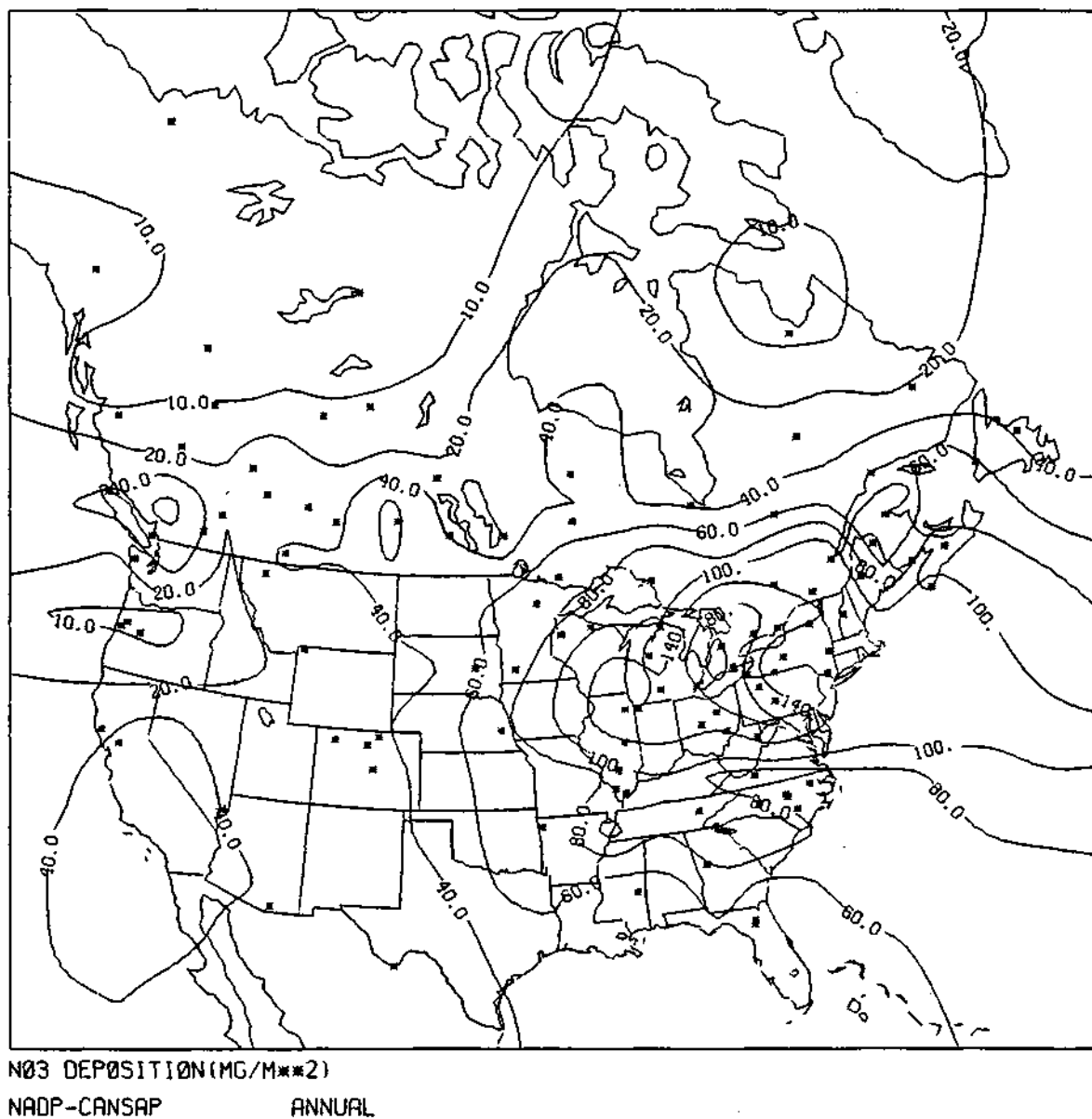


Figure 47. The average annual nitrate deposition ( $\text{mg}/\text{m}^2$ ) over North America from the combined CANSAP and NADP networks.

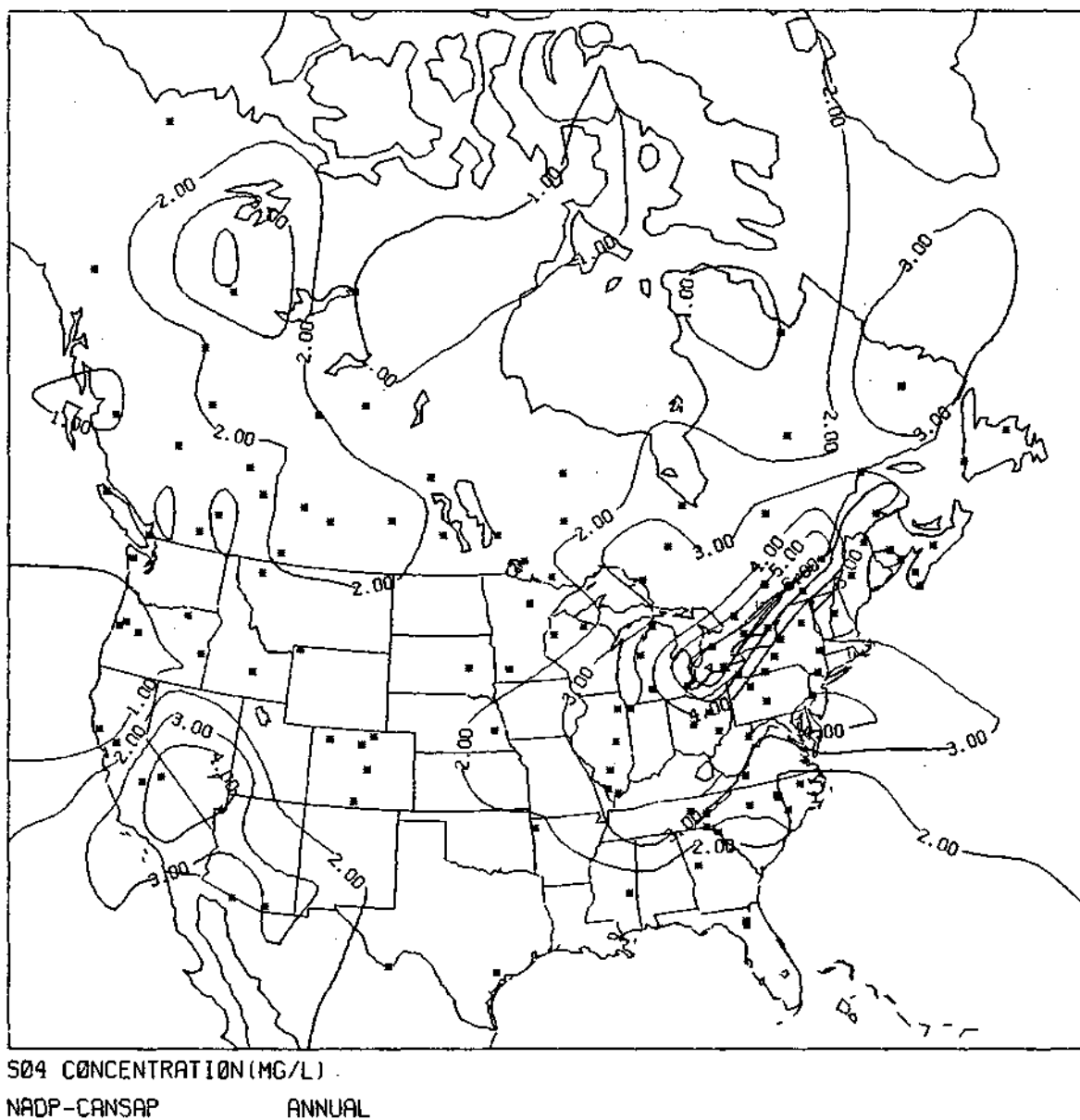


Figure 48. The average annual sulfate concentration (mg/L) over North America from the combined CANSAP and NADP networks.



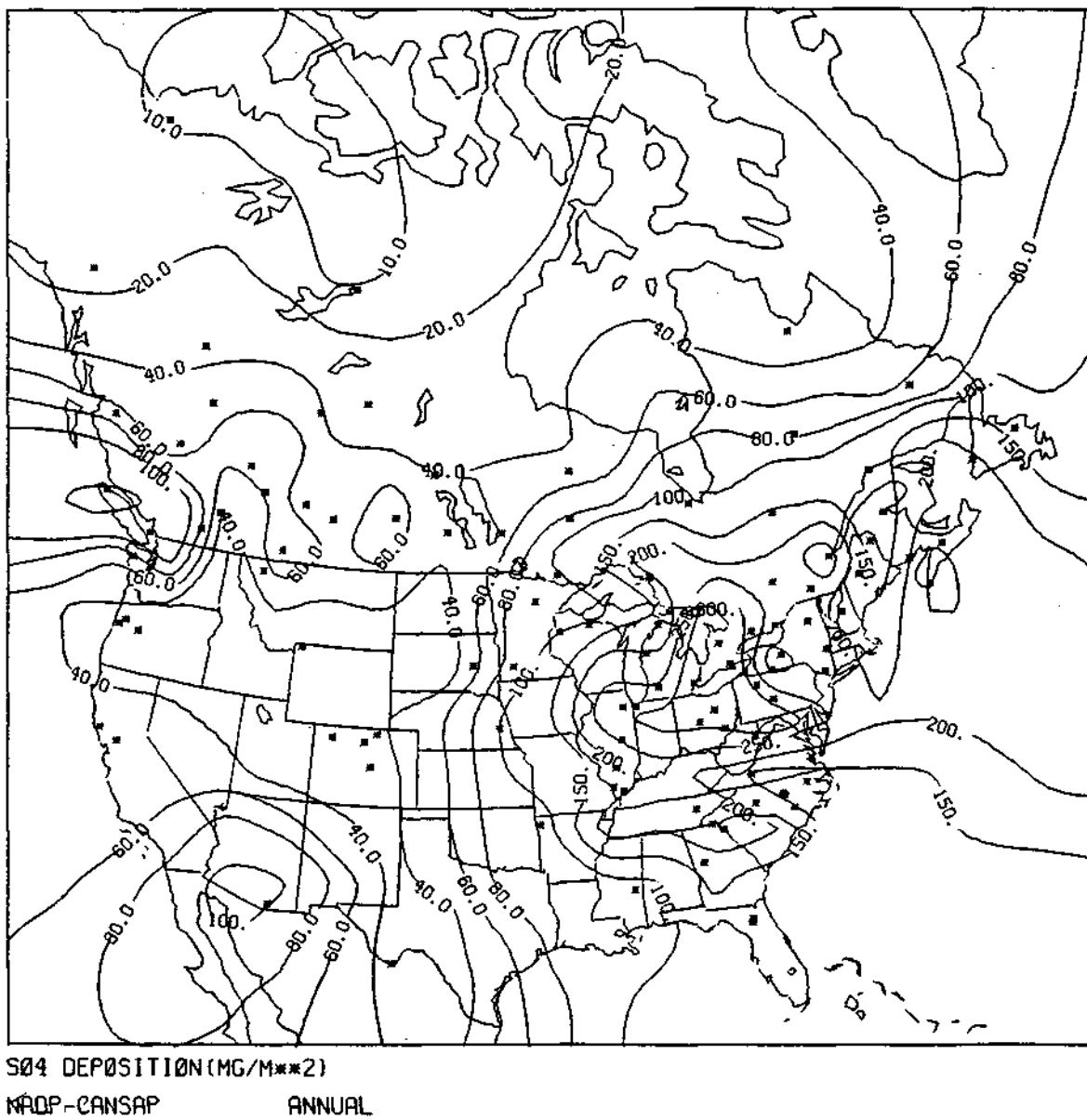
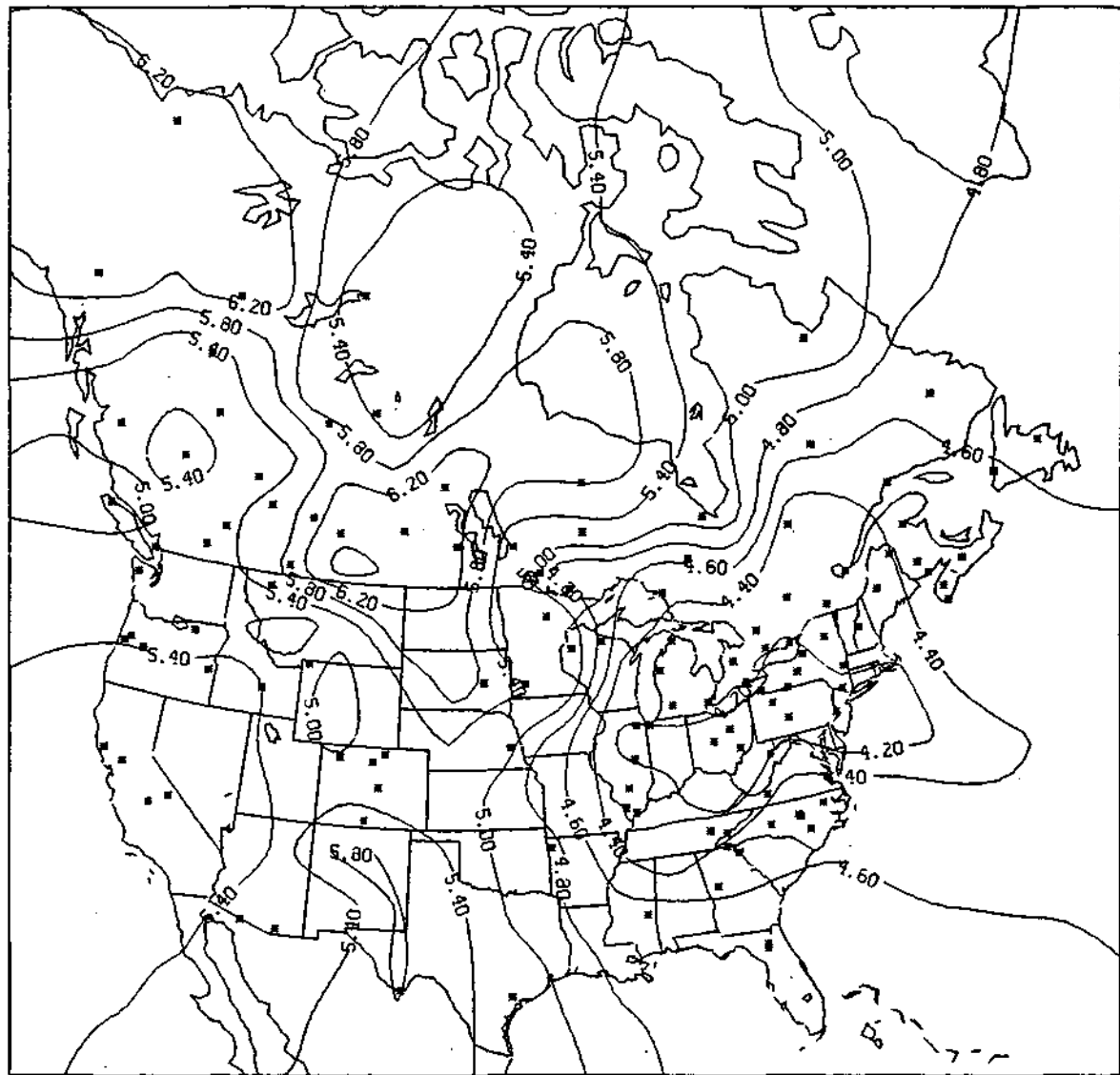


Figure 49. The average annual sulfate deposition ( $\text{mg/m}^2$ ) over North America from the combined CANSAP and NADP networks.

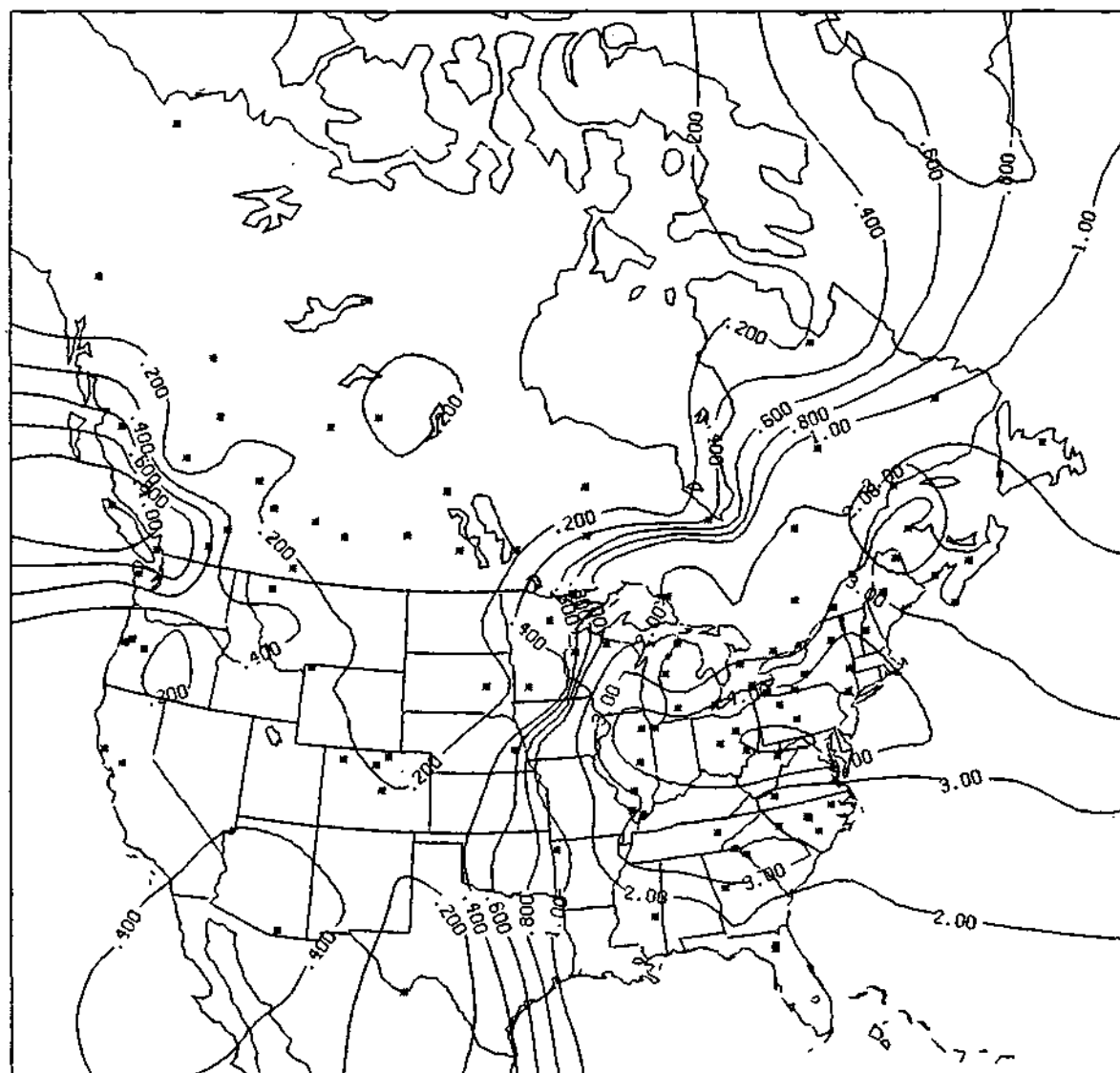


MEASURED PH

NADP-CANSAP

ANNUAL

Figure 50. The precipitation-weighted annual mean pH distribution over North America from the CANSAP and NADP networks.



H+ DEPOSITION(UG/M\*\*2)  
NADP-CANSAP . ANNUAL

Figure 51. The hydrogen ion deposition distribution over North America derived from the CANSAP and NADP networks.

### Nitrate Concentration and Deposition

The annual average nitrate concentration shows relatively high values extending from south-central Canada southward to the central Great Plains and into the Midwest and increasing to a maximum in the northeast (Fig. 46). The central core of greater than 4 mg/L is located over southeast Ontario just north of Lakes Erie and Ontario. There is a secondary maximum of equal magnitude located over southern Nevada largely arising from the single station measurement in Blythe, California. This secondary maximum is likely a sampling artifact.

The deposition of nitrate (Fig. 47) is observed to maximize in a rather . symmetric manner over the Midwest from Illinois to Ohio with a central value of greater than 220 mg/m<sup>2</sup> just east of Detroit, Michigan.

The heaviest nitrate deposition extends in a nearly north-south direction with values in excess of 180 mg/m<sup>2</sup> from Lake Ontario to northern West Virginia. The major deposition pattern lies east-west from Iowa to the East coast with somewhat lower values in the drought-stricken areas of southeast New York and eastern Pennsylvania.

### Sulfate Concentration and Deposition

The average annual sulfate concentration shown in Fig. 48 shows a maximum of > 2 mg/L covering the area from eastern Nebraska northeastward into Canada north of Lake Superior and southeastward into northern Georgia and North Carolina. The maximum within this area extends from just east of Detroit and parallel to the St. Lawrence valley with values exceeding 7 mg/L in extreme southeast Ontario. Again, similar to the nitrate concentration, a maximum is also observed in southern Nevada derived from the single station in California and is an artifact of the objective analysis used.

The deposition of sulfates shown in Fig. 49 shows a very systematic distribution. A major north-south gradient extends through the Great Plains with values beginning at 40 mg/m<sup>2</sup> and increasing to a maximum of > 300 mg/m<sup>2</sup> located over northern Ohio, western Pennsylvania and southern Ontario. The deposition amounts in eastern New York state and New England decrease to values comparable to those estimated for Iowa and northern Wisconsin. This deposition pattern largely arises from the heavier precipitation in the eastern Midwest associated with the sample collection.

### pH and Hydrogen Ion Deposition

The annual precipitation-weighted mean pH distribution is shown in Fig. 50. The major features to be noted is the maximum pH area of Alberta, Saskatchewan and western Manitoba in Canada with an extension into the northern Great Plains, balanced by an extensive area of relatively low pH values from the western Midwest to the East coast. An area of pH < 4.2 extends from eastern Illinois in an east-west direction through Indiana, Ohio, Pennsylvania and the

lower half of New York state. The values in New England are approximately equivalent to those of the lower peninsula of Michigan.

The hydrogen ion deposition shown in Fig. 51 reflects the pH and precipitation patterns to produce a very strong gradient in a north-south orientation extending from northeastern Minnesota southward to the Gulf Coast of Texas. As this gradient traverses eastern Canada it follows an east-west path just south of Hudson Bay. Again, the relatively symmetric pattern maximizes in southeastern Ohio, southwestern Pennsylvania and northern West Virginia decreasing outward in all directions from that central core of lower hydrogen ion deposition.

#### Discussion of the Annual Concentration and Deposition Distribution

These annual patterns seem to show that with the exception of pH, the maximum concentrations (both the cations and anions) appear in Canada and seem not to be related to the presumed Ohio River valley source that has been widely acclaimed. The deposition patterns, however, maximize in the United States, largely because of more precipitation in the U.S. as opposed to the eastern regions of Canada. It remains to observe over the coming years the changes of these patterns and to determine their stability with time so as to begin to determine trends.

All of these data beg for interpretation as to the causes for the distributions shown. For example, what is the explanation for the relatively large values of cations in Alberta and Saskatchewan producing such high pH values in that area. Likewise while, we suspect fossil fuel burning is responsible for the acidic components in the eastern states, one should also be alert to the possibility of natural sources contributing in a major way to the observed patterns.

Future work will address some of the more interesting case studies which contribute to the overall annual and seasonal patterns that have been discussed here. In any event, a considerable modeling effort would be required to attempt to simulate the distribution shown and then to further simulate their changes with respect to energy production strategies that may be employed for the future.

#### REFERENCE

- Achtemeier, G. L., P. H. Hildebrand, P. T. Schickedanz, B. Ackerman, S. A. Changnon, Jr., and R. G. Semonin, 1977: Illinois Precipitation Enhancement Program and Evaluation Techniques for the High Plains Cooperative Program, Illinois State Water Survey Final Report, Contract 14-06-D-7197, Illinois State Water Survey, Champaign, 6-12, Appendix B.

## CHAPTER 9

### A NEW SEQUENTIAL RAINWATER SAMPLER

Gary J. Stensland

#### INTRODUCTION

In order to study the chemical deposition pattern from convective raincells it is necessary to obtain several consecutive samples from the individual rain showers that comprise a convective storm system. The required sequence of samples can be collected manually, at great expense in manpower. This chapter will describe a rather simple automatic sampler designed to collect such a sequence of samples. The sampler was field tested in summer 1980 at Hilo, Hawaii as part of a NOAA project. Some of the preliminary sequential data, relating hydrogen ion to various anions, will be discussed.

#### Description and Evaluation of the Instrument

The sequential sampler was designed with the following considerations in mind:

1. The sampler should be able to collect one sample for each 0.01 inch of rainfall, with enough volume per sample to allow for measurement of pH and the major ions.
2. The sample advance times should be known precisely enough to allow for the calculation of accurate rain rates, even in heavy showers.
3. The collection funnel should be automatically uncovered only during rain events to prevent dry deposition onto the funnel of the chemicals that are to be measured in the rainwater.
4. The sampler should have the capacity to collect samples continuously during twenty-four hours of unattended operation, and for total rainfalls of about 2 inches.
5. The surfaces coming in contact with the rainwater should all be plastic.
6. The sampler should be easy to construct, reliable, rugged and inexpensive, to the greatest extent possible.

The sequential sampler which was built to meet these constraints is shown in Fig. 1. The top panel shows the three major components: the wet/dry sampler to protect the collecting funnel, the tipping bucket raingage to provide an electrical signal for each 0.01 inch of rainfall, and the aluminum shelter housing the remaining equipment. The bottom panel of Fig. 1 shows the

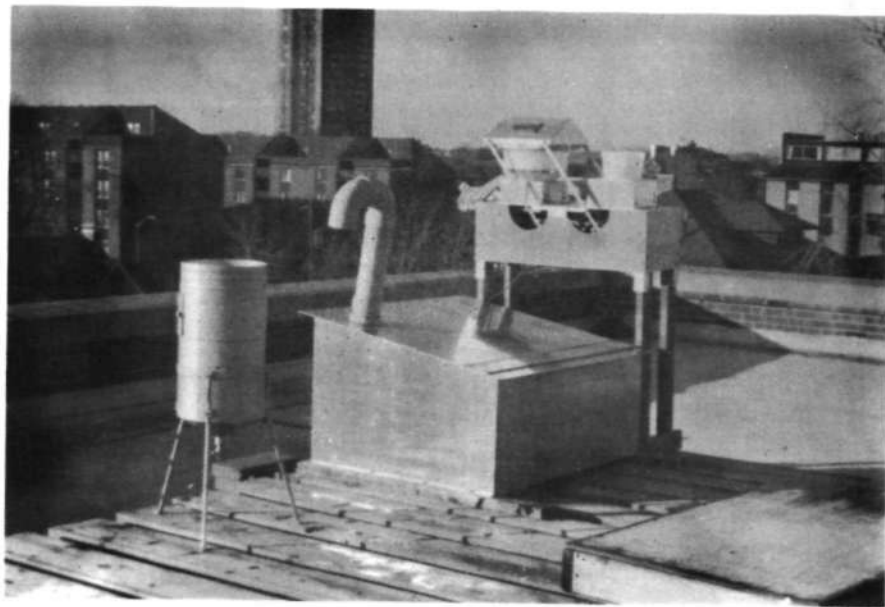
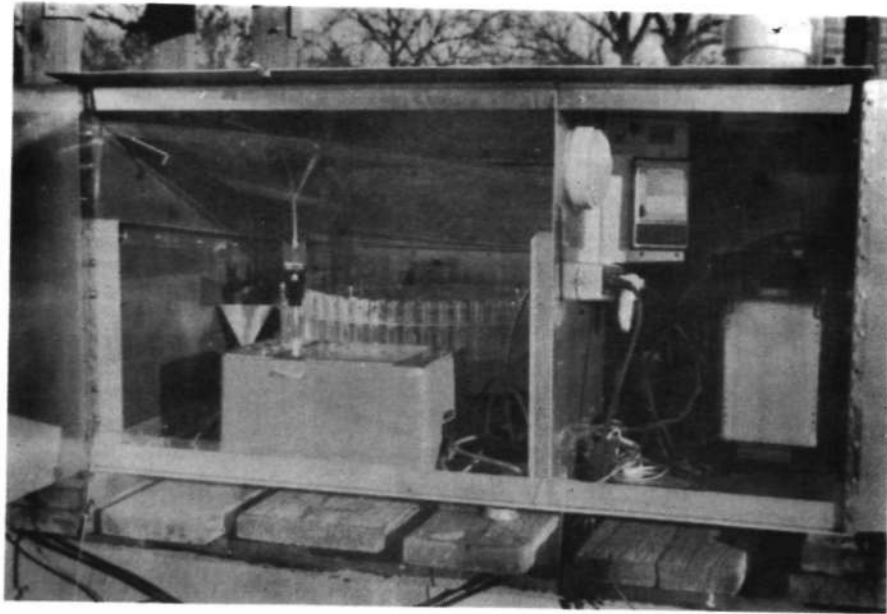


Figure 1. Sequential Rainwater Sampling System

equipment inside the shelter. On the left is a commercially available laboratory fractionator. The fractionator is one of the cheapest models available, but has the advantages of a) a large sample rack which holds up to 240 test tubes to collect the sequential rain samples, b) enough spacing between test tubes to allow for overflow without contaminating nearby tubes, and c) a simple system to align the dispensing tube over the test tubes, namely a mechanical deflector which mounts in two of the test tube holes. The 12 inch funnel and the flexible tubing were polyethelene. To readily direct the rain-water into the test tubes, it was found advantageous to insert a flat strip of plastic, 0.5 inches long, into the end of the dispensing tube. The end of the strip was cut to a point and left extending about 0.1 inch out of the tube. The test tubes used were disposable (i.e., inexpensive) polyethelene tubes with a capacity at overflowing of about 19 mL of water and an outside diameter of about 16 mm. The tubes came with water-tight screw caps which provided added convenience. Somewhat limited leaching tests with deionized water and pH 3 mineral acid solutions on the polystyrene tubes indicate that the tubes are satisfactory for acid rain studies where pH, conductivity, and the major ions are being measured. For a 12 inch funnel, calculations predict that 0.01 inch of rainfall should produce a 18.5 mL sample when the collection funnel has an inside diameter for 12 inches. However, flow surges through the plumbing, a finite time of less than 1 second to advance a test tube, and the characteristics of the tipping bucket raingage interacted to provide typical water volumes in the test tubes which ranged from about 16 to 19 mL for each tip of the raingage. During advances from one test tube to the next, some sample water was lost; the added complexity to design a system to collect this lost rainwater does not seem necessary.

For cleanliness, the fractionator and test tubes are normally shielded with plexiglas panels. In this way the aluminum shelter box can be opened to service the X-Y recorders and visually inspect the fractionator and yet minimize dust from settling into the sample test tubes.

The tipping bucket X-Y recorder was geared to run at 6 inches per hour, with a roll of chart paper lasting 5.5 days. This device was the backup system for determining rain rates. In heavy rain showers, rates of 6 inches/hour are possible, producing 0.01 inch in about six seconds. Therefore, a dual speed X-Y recorder was used to record a) if the recorder was on fast or slow speed, b) if the wet/dry was open or closed, and c) the time of a tip of the raingage and the concurrent advance of the fractionator to the next test tube. On fast speed the chart advanced at 1.5 inches/minute and a roll of paper lasted 5.5 hours. Considering only the precision in measuring distances between peaks on the chart, we estimate that the calculated rain rates had a precision of  $\pm 13\%$  at 6 inches/hour and  $\pm 1\%$  at 0.5 inches/hour. The chart speed decreased by a factor of 60 when the recorder was in the slow speed mode.

Fairly simple electronic circuitry was built to link the X-Y recorders, raingage, fractionator, and wet/dry sampler. The circuits were designed such that the X-Y recorder changed from slow speed to fast speed when the wet/dry opened to expose the funnel for sample collection. If more than 10 minutes elapsed between the opening of the wet/dry or the occurrence of the last tip of the raingage, the X-Y recorder automatically switched back to slow speed.



During the field tests when up to 90 samples were obtained in 24 hours of rather steady rain conditions, the roll of chart paper was almost totally used up.

During the 12 day field test at Hilo, Hawaii about 350 sequential samples were collected with no data gaps. Two problems did arise. The wet/dry malfunctioned but the sequential sampler had been designed to operate in an alternate mode without a wet/dry protecting the funnel and thus no data were lost. The fractionator also malfunctioned by advancing somewhat erratically. This problem has since been traced to a faulty felt spacer and has been corrected. The most important modification of the sequential sampling system in the future will be to design a cassette tape data logging system as the primary system with the X-Y strip charts serving as a back-up system.

#### PRELIMINARY SEQUENTIAL DATA RESULTS

The field testing of the sampler was accomplished at Hilo, Hawaii through the support of NOAA. Approximately 350 rainwater samples were collected at Hilo and these are being analyzed and interpreted as part of the DOE contract since the samples are relevant to the acid rain problem.

In Table 1 are presented data for 2 samples collected on June 12. The first line of the Table lists the chemistry data for a rather acid sample, with a measured pH of 4.09. The second line lists the data for the same sample after the contribution due to sea salt had been subtracted off, with sodium being used as the sea salt tracer. The important point is that the remaining ions are dominated by sulfate and hydrogen, and thus there is the strong suggestion that the low pH is due to sulfuric acid.

The second sample listed in Table 1 had a measured pH of 5.21. The point of this sample is that for such high pH samples, the subtraction of the sea salt components does not lead to a situation where the hydrogen ion can be clearly associated with a single anion.

The data in Table 2 address the same issue except that more samples are considered. The linear correlation coefficient values relating hydrogen ion to various combinations of anions indicate that the free acidity is related best to excess sulfate. Nitrate and excess chloride are generally present in the Hilo samples at rather low levels. The addition of these two anions, which could be associated with acid compounds, did not increase the correlation coefficient values.

#### Conclusion

A sequential rain sampler has been built and field tested. It performed well and has the important advantage that it is quite easy to build in quantity since the major components are commercially available.

Table 1. Chemistry data for two rain samples from Hilo, Hawaii.

Hilo, June 12, 0.02" Sequential Samples, $\mu\text{eq/L}$												
<u>Sample</u>	<u>Off Time</u>	<u>Ca<sup>++</sup></u>	<u>Mg<sup>++</sup></u>	<u>K<sup>+</sup></u>	<u>Na<sup>+</sup></u>	<u>NH<sub>4</sub><sup>+</sup></u>	<u>H<sup>+</sup></u>	<u>NO<sub>3</sub><sup>-</sup></u>	<u>Cl<sup>-</sup></u>	<u>SO<sub>4</sub><sup>=</sup></u>	<u>Meas. pH</u>	<u>Cal. pH</u>
2308	1545	9	43	4	191	6	81	8	223	96	4.09	4.13
2308*	1545	1	0	0	0	6	81	8	1	74		
2300	1405	3	14	2	56	1	6	2	70	19	5.21	4.79
2300*	1405	1	10		0	16		2	5	12		

---

\*Corrected for sea salt.

Table 2. Correlation of  $H^+$  to various anions for 49 Hilo, Hawaii rain samples.

Hilo, June 12-13, 49 Sequential Samples, yeq/L

Na versus H  $r = .54$

$$SO_4^* = .80 H^+ + 4.0 \quad r = .93$$

$$NO_3 + SO_4^* = .88 H^+ + 6.85 \quad r = .93$$

$$Cl^* + NO_3 + SO_4^* = .87 H^+ + 15.83 \quad r = .84$$

$$SO_4 = 1.01 H^+ + 14.5 \quad r = .86$$

-----

$$\text{at pH} = 4, H^+ = 100; \frac{SO_4^*}{H^+} = \frac{.80 H^+ + 4.0}{H^+} = \frac{80 + 4}{100} = .84$$

$$\text{at pH} = 5, H^+ = 10; \frac{SO_4^*}{H^+} = \frac{.80 H^+ + 4.0}{H^+} = \frac{8 + 4}{10} = 1.24$$

The ratio depends on  $H^+$  unless intercept = 0.0

---

\*Corrected for sea salt.

Data collected with the sampler at Hilo, Hawaii suggest that the acid rain at Hilo is probably due mostly to sulfuric acid.

#### Acknowledgements

Bruce Komadina designed and built the electronic components for the sequential sampling system and provided ideas for the mechanical components which were fabricated with the assistance of James Harry.

## APPENDIX

### Reports, Reprints, and Preprints

- C00-1199-1 Huff, F. A., 1963: Study of rainout of radioactivity in Illinois. First Progress Report to U. S. Atomic Energy Commission. Contract AT(11-1)-1199, 58 p.
- C00-1199-2 Huff, F. A., 1964: Study of rainout of radioactivity in Illinois. Second Progress Report to U. S. Atomic Energy Commission. Contract AT(11-1)-1199, 61 p.
- C00-1199-3 Huff, F. A., 1965: Radioactive rainout relations on densely gaged sampling networks. Water Resources Res., 1(1), 97-108.
- C00-1199-4 Huff, F. A. and G. E. Stout, 1965: Distribution of radioactive rainout in convective rainfall. J. Appl. Meteor., 3(6), 707-717.
- C00-1199-5 Huff, F. A., 1965: Study of rainout of radioactivity in Illinois. Third Progress Report to U. S. Atomic Energy Commission. Contract AT(11-1)-1199, 66 p.
- C00-1199-6 Huff, F. A., 1965: Radioactive rainout relations in convective rainstorms. Res. Report No. 1 to U. S. Atomic Energy Commission. Contract AT(11-1)-1199, 131 p.
- C00-1199-7 Feteris, P. J., 1965: 1964 Project Springfield studies. Res. Report No. 2 to U. S. Atomic Energy Commission. Contract AT(11-1)-1199, 20 p.
- C00-1199-8 Huff, F. A. and W. E. Bradley, 1965: Study of rainout of radioactivity in Illinois. Fourth Progress Report to U. S. Atomic Energy Commission. Contract AT(11-1)-1199, 20 p.
- C00-1199-9 Stout, G. E. and F. A. Huff, 1967: Rainout characteristics for hydrological studies. Symposium on Isotopes in Hydrology. Vienna, 61-72.
- C00-1199-10 Bradley, W. E. and P. J. Feteris, 1966: Study of rainout of radioactivity in Illinois. Fifth Progress Report to U. S. Atomic Energy Commission. Contract AT(11-1)-1199, 26 p.
- C00-1199-11 Bradley, W. E. and G. E. Martin, 1967: An airborne precipitation collector. J. Appl. Meteor., 6, (4), 717-723.
- C00-1199-12 Huff, F. A. and G. E. Stout, 1968: Relation between Ce144 and Sr90 rainout in convective rainstorms. Tellus, 20(1), 82-87
- C00-1199-13 Huff, F. A. and G. E. Stout, 1967: Time distributions of radioactivity and chemical constituents in rainfall. Proc. USAEC Meteor. Info. Meeting, Chalk River, Canada, 503-513.

- C00-1199-14 Huff, F. A., W. E. Bradley, and P. J. Feteris, 1967: Study of rainout of radioactivity in Illinois. Sixth Progress Report to U. S. Atomic Energy Commission. Contract AT(11-1)-1199, 19 p.
- C00-1199-15 Wilson, J. W. and P. T. Jones III, 1968: Tracing tropospheric radioactive debris by isentropic trajectories. Res. Report No. 3 to U. S. Atomic Energy Commission. Contract AT(11-1)-1199, 33 p.
- C00-1199-16 Lyons, W. A. and J. W. Wilson, 1968: The control of summertime cumuli and thunderstorms by Lake Michigan during non-lake breeze conditions. Satellite and Mesometeor. Res. Paper No. 74 to U. S. Atomic Energy Commission. Contract AT(11-1)-1199, 32 p.
- C00-1199-17 Wilson, J. W. and W. E. Bradley, 1968: Study of rainout of radioactivity in Illinois. Seventh Progress Report to U. S. Atomic Energy Commission. Contract AT(11-1)-1199, 64 p.
- C00-1199-18 Stout, G. E., 1969: Study of rainout of radioactivity in Illinois. Eighth Progress Report to U. S. Atomic Energy Commission. Contract AT(11-1)-1199, 49 p.
- C00-1199-19 Semonin, R. G., 1970: Study of rainout of radioactivity in Illinois. Ninth Progress Report to U. S. Atomic Energy Commission. Contract AT(11-1)-1199, 55 p.
- C00-1199-20 Semonin, R. G., 1971: Study of rainout of radioactivity in Illinois. Tenth Progress Report to U. S. Atomic Energy commission. Contract AT(11-1)-1199, 56 p.
- C00-1199-21 Adam, J. R. and R. G. Semonin, 1970: Collection efficiencies of raindrops for submicron particulates. Proc. Symposium on Precip. Scavenging, Richland, Wash., 151-159.
- C00-1199-22 Adam, J. R. and R. G. Semonin, 1970: A technique for the experimental measurement of collection efficiency. Proc. Conf. Cld. Phys., Ft. Collins, Colo., 139-140.
- C00-1199-23 Semonin, R. G. and J. R. Adam, 1971: The washout of atmospheric particulates by rain. Proc. Conf. Air Pollution Meteor., Raleigh, N. Car., 65-68.
- C00-1199-24 Changnon, S. A., Jr., F. A. Huff, and R. G. Semonin, 1971: METROMEX: An Investigation of Inadvertent Weather Modification. Bull. Amer. Meteor. Soc., 52(10), 958-967
- C00-1199-25 Cataneo, R., J. R. Adam, and R. G. Semonin, 1971: Interaction between equal-sized droplets due to the wake effect. J. Atmos. Sci., 28(3), 416-418.
- C00-1199-26 Cataneo, R. and D. L. Vercellion, 1972: Estimating rainfall rate-radar reflectivity relationships for individual storms. J. Appl. Meteor., 11(1), 211-213.

- C00-1199-27 Semonin, R. G., 1972: Tracer chemical experiments in Midwest convective clouds. Proc. Third Conf. Weather Mod., Rapid City, S. Dak., 83-87.
- C00-1199-28 Semonin, R. G., 1972: The use of chemical and biological tracers in cloud physics. Intern. Conf. Cld. Phys., London.
- C00-1199-29 Semonin, R. G., 1972: Study of rainout of radioactivity in Illinois. Interim Eleventh Progress Report to U. S. Atomic Energy Commission. Contract AT(11-1)-1199, 12 p.
- C00-1199-30 Adam, J. R., R. Cataneo, D. F. Gatz, and R. G. Semonin, 1973: Study of rainout of radioactivity in Illinois. Eleventh Progress Report to U. S. Atomic Energy Commission. Contract AT(11-1)-1199, 157 p.
- C00-1199-31 Henderson, T. J. and D. W. Duckering, 1973: Final Report METROMEX 1973: A summary of operations conducted by Atmospherics Incorporated during the period 7 July through 19 August 1973, 51 p.
- C00-1199-32 Changnon, S. A., Jr., R. G. Semonin, and W. P. Lowry, 1972: Results from METROMEX. Preprint Vol. Conf. on Urban Environ. and Second Conf. on Biometeor., Philadelphia, Amer. Meteor. Soc, 191-197.
- C00-1199-33 Grosh, R. C. and R. G. Semonin, 1973: Moisture budgets and wind fields of thunderstorms passing over an urban area in the Midwest. Preprint Vol. Eighth Conf. on Severe Local Storms, Denver, Amer. Meteor. Soc, 130-137.
- C00-1199-34 Huff, F. A., Editor, 1973: Summary Report of METROMEX Studies, 1971-1972. Illinois State Water Survey Rept. of Invest. No. 74, Urbana, 169 p.
- C00-1199-35 Gatz, D. F. 1972: Washout ratios in urban and non-urban areas. Preprint Vol. Conf. on Urban Environ. and Second Conf. on Biometeor., Philadelphia, Amer. Meteor. Soc, 124-128.
- C00-1199-36 Lowry, W. P., 1973: 1973 Operational Report for METROMEX. Illinois State Water Survey, Urbana, 63 p.
- C00-1199-37 A collection of papers, 1974:  
Staff: METROMEX: An overview of Illinois State Water Survey Projects.  
Huff, F. A. and P. T. Schickedanz: METROMEX: Rainfall analysis.  
Gatz, D. F.: METROMEX: Air and rain chemistry analysis.  
Ackerman, B.: METROMEX: Wind fields over St. Louis in undisturbed weather.  
Semonin, R. G. and S. A. Changnon, Jr.: METROMEX: Summary of 1971-1972 results.  
Bull. Amer. Meteor. Soc, 55(2), 89-100.
- C00-1199-38 Semonin, R. G. and D. F. Gatz, 1974: Study of rainout of radioactivity in Illinois. Twelfth Progress Report to U. S. Atomic Energy Commission. Contract AT(11-1)-1199, 21 p.

- C00-1199-39 Henderson, T. J. and D. W. Duckering, 1972: Final Report METROMEX 1973: A summary of operations conducted by Atmospheric Inc. during the period 5 July through 15 August 1972, 34 p.
- C00-1199-40 Ackerman, B., 1974: Wind fields over the St. Louis metropolitan area. J. Air Poll. Cont. Assoc., 24, 232-236.
- C00-1199-41 Rattonetti, A., 1974: Determination of soluble Cadmium, Lead, Silver, and Indium in rainwater and stream water with the use of flameless atomic absorption. Anal. Chem., 46, 739-742.
- C00-1199-42 Ackerman, B., 1974: Wind profiles and their variability in the planetary boundary layer. Prep. Vol. Symp. on Atmos. Diffusion and Air Poll., Santa Barbara, Amer. Meteor. Soc, 19-22.
- C00-1199-43 Gatz, D. F., 1974: St. Louis air pollution: Estimates of aerosol source coefficients and elemental emission rates. Prep. Vol. Symp. on Atmos. Diffusion and Air Poll., Santa Barbara, Amer. Meteor. Soc, 109-114.
- C00-1199-44 Ackerman, B., 1974: Spatial variability of the wind velocity in the lowest 500 meters. Prep. Vol. Sixth Conf. on Aerospace and Aeronautical Meteor., El Paso, Amer. Meteor. Soc, 325-328.
- C00-1199-45 Cataneo, R., 1974: Operational aspects of Project METROMEX - An inadvertent weather modification study. Prep. Vol. Fourth Conf. on Wea. Mod., Ft. Lauderdale, Amer. Meteor. Soc, 379-381.
- C00-1199-46 Semonin, R. G. and S. A. Changnon, Jr., 1974: METROMEX: Lessons for precipitation enhancement in the Midwest. Prep. Vol. Fourth Conf. on Wea. Mod., Ft. Lauderdale, Amer. Meteor. Soc, 353-357.
- C00-1199-47 Braham, R. R., Jr., 1974: 1974 Operational Report for METROMEX. Univ. of Chicago, 39 p.
- C00-1199-48 Gatz, D. F., 1975: Relative contributions of different sources of urban aerosols: Application of a new estimation method to multiple sites in Chicago. Atmos. Environ., 9, 1-18.
- C00-1199-49 Henderson, T. J. and D. W. Duckering, 1975: Final Report METROMEX 1974: A summary of operations conducted by Atmospheric Inc. during the period 7 July through 17 August 1974, 48 p.
- C00-1199-50 Semonin, R. G., 1975: Study of rainout of radioactivity in Illinois. Thirteenth Progress Report to U. S. Atomic Energy Commission. Contract AT(11-1)-1199, 24 p.
- C00-1199-51 Semonin, R. G., 1976: Study of air pollution scavenging. Fourteenth Progress Report to the Energy Research and Development Admin. Contract AE(11-1)-1199, 23 p.



- C00-1199-52 Semonin, R. G., B. Ackerman, D. F. Gatz, S. D. Hilberg, M. E. Peden, R. K. Stahlhut, and G. J. Stensland, 1977: Study of air pollution scavenging. Fifteenth Progress Report to the Energy Research and Development Administration. Contract AE(11-1)-1199, 120 p.
- C00-1199-53 Semonin, R. G., D. F. Gatz, M. E. Peden, G. J. Stensland, 1978: Study of Atmospheric Pollution Scavenging. Sixteenth Progress Report to the Department of Energy, Division of Biomedical and Environmental Research, Contract EY-76-S-02-1199, 72 p.
- C00-1199-54 Stensland, G. J., 1979: A Comparison of Precipitation Chemistry Data at a Central Illinois Site in 1984 and in 1977. Proc. 71st Annual Meeting of the Air Poll. Cont. Assoc. Houston, Texas, June.
- C00-1199-55 Stensland, G. J., 1979: Precipitation chemistry trends in the northeastern United States. Proc., 12th Annual Rochester International Conf. on Environ. Toxicity. 18 p.
- C00-1199-56 Gatz, D. F., 1979: Spatial variability of aerosol deposition in rain near St. Louis. Proc., American Chem. Soc, Div. of Environ. Chem. 4 p.
- C00-1199-57 Peden, M. E., L. M. Skowron, and F. M. McGurk, 1979: Precipitation sample handling, analysis, and storage procedures. Research ' Report No. 4 to the United States Department of Energy, Pollutant Characterization and Safety Research Division, Office of Health and Environmental Research. 71 p.
- C00-1199-58 Semonin, R. G., J. Bartlett, D. F. Gatz, M. E. Peden, L. M. Skowron, and G. J. Stensland, 1979: Study of Atmospheric Pollution Scavenging. Seventeenth Progress Report to the U.S. Department of Energy, Pollutant Characterization and Safety Research Division, Contract EY-76-S-02-1199, 118 p.
- C00-1199-59 Gatz, D. F., 1979: An Urban Influence on Deposition of Sulfate and Soluble Metals in Summer Rains. Symposium on Environmental and Health Effects of Sulfur Deposition, October 14-18, 1979, Gatlinburg, Tennessee. 32 p.
- C00-1199-60 Semonin, R. G., J. D. Bartlett, V. C. Bowersox, D. F. Gatz, D. Q. Naiman, M. E. Peden, R. K. Stahlhut, and G. J. Stensland, 1980: Study of Atmospheric Pollution Scavenging. Eighteenth Progress Report to the U.S. Department of Energy, Pollutant Characterization and Safety Research Division, Contract EY-76-S-02-1199.
- C00-1199-61 Gatz, D. F., and D. Q. Naiman, 1980: Spatial Variability of Rain-water Impurities in Mesoscale Events. Symposium on Intermediate Range Atmospheric Transport Processes and Technology Assessment, October 1-3, 1980, Gatlinburg, Tennessee. 10 p.

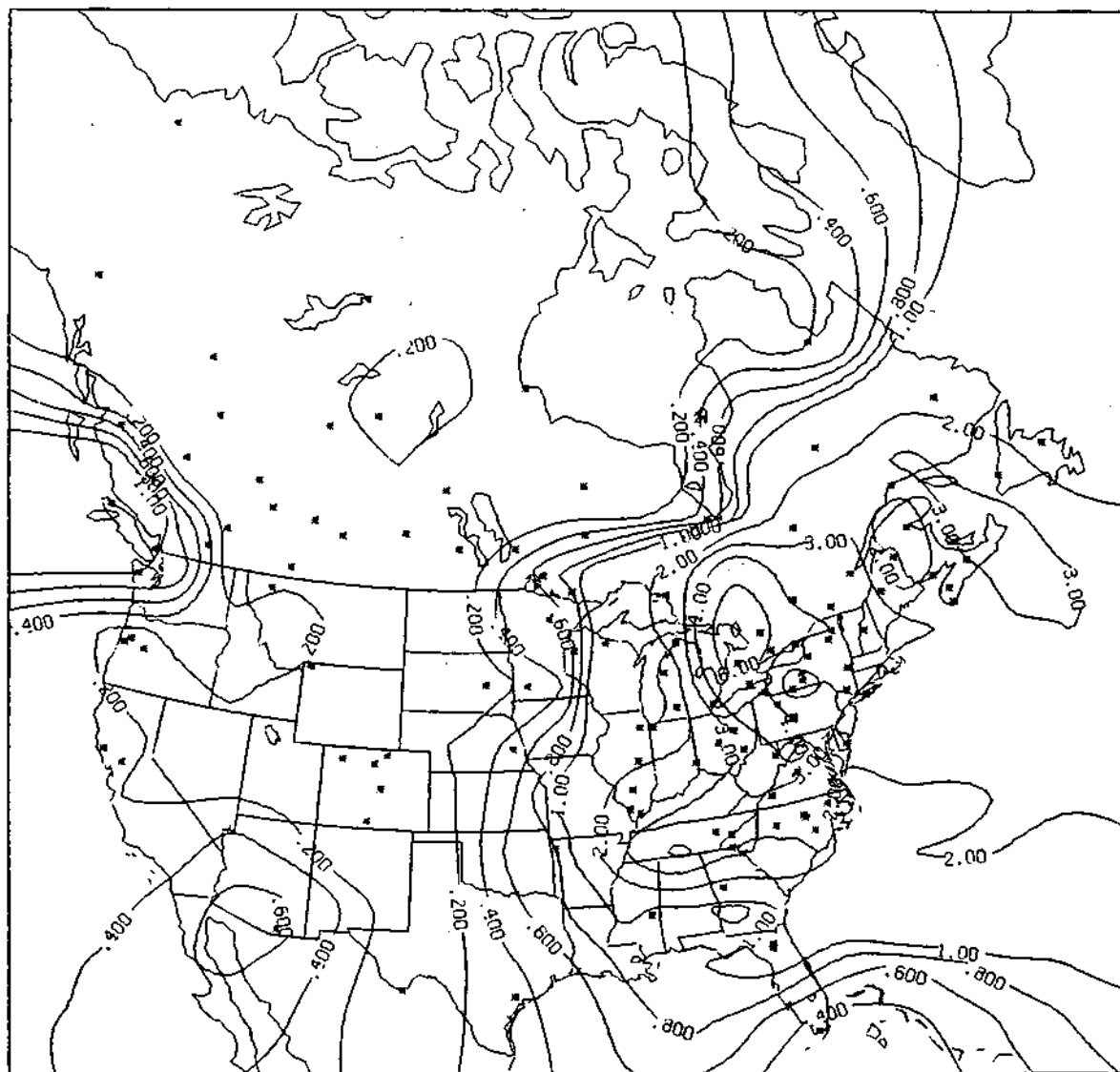
- C00-1199-62 Bowersox, V. C, and G. J. Stensland, 1981: Seasonal Patterns of Sulfate and Nitrate in Precipitation in the United States. Proc. 74th Annual Meeting of the Air Poll. Cont. Assoc. Philadelphia, PA, June.
- C00-1199-63 Semonin, R. G., V. C. Bowesox, D. F. Gatz, M. E. Peden, and G. J. Stensland, 1981: Study of Atmospheric Pollution Scavenging. Nineteenth Progress Report to the U.S. Department of Energy, Pollutant Characterization and Safety Research Division, Contract DE-AC02-76EV01199.

#### CORRIGENDA

The hydrogen ion deposition maps are in error for the four seasons on pages 102-105 (Figs. 37-40) of the report Study of Atmospheric Pollution Scavenging, Nineteenth Progress Report, Contract DE-AC02-76EV01199 by Semonin, et al, May 1981. The attached pages should be inserted in the report to reflect the correct values. This change does not alter the annual pattern of hydrogen ion deposition on page 117 (Fig. 51).

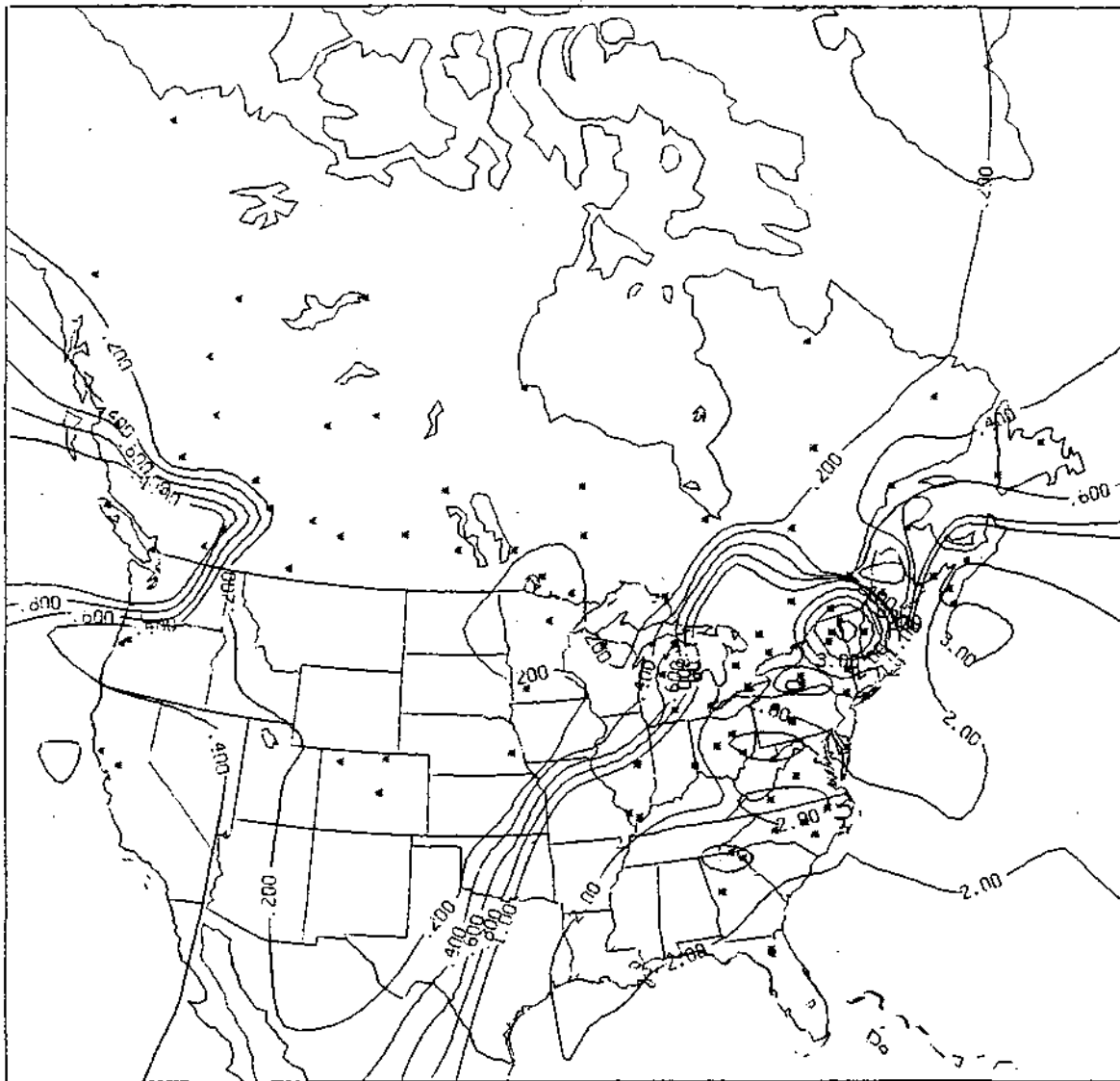
'This error was solely computer generated during the use of the plotting routines. All other maps, while preliminary in nature, are accurate representations of the available data base.

Richard G. Semonin



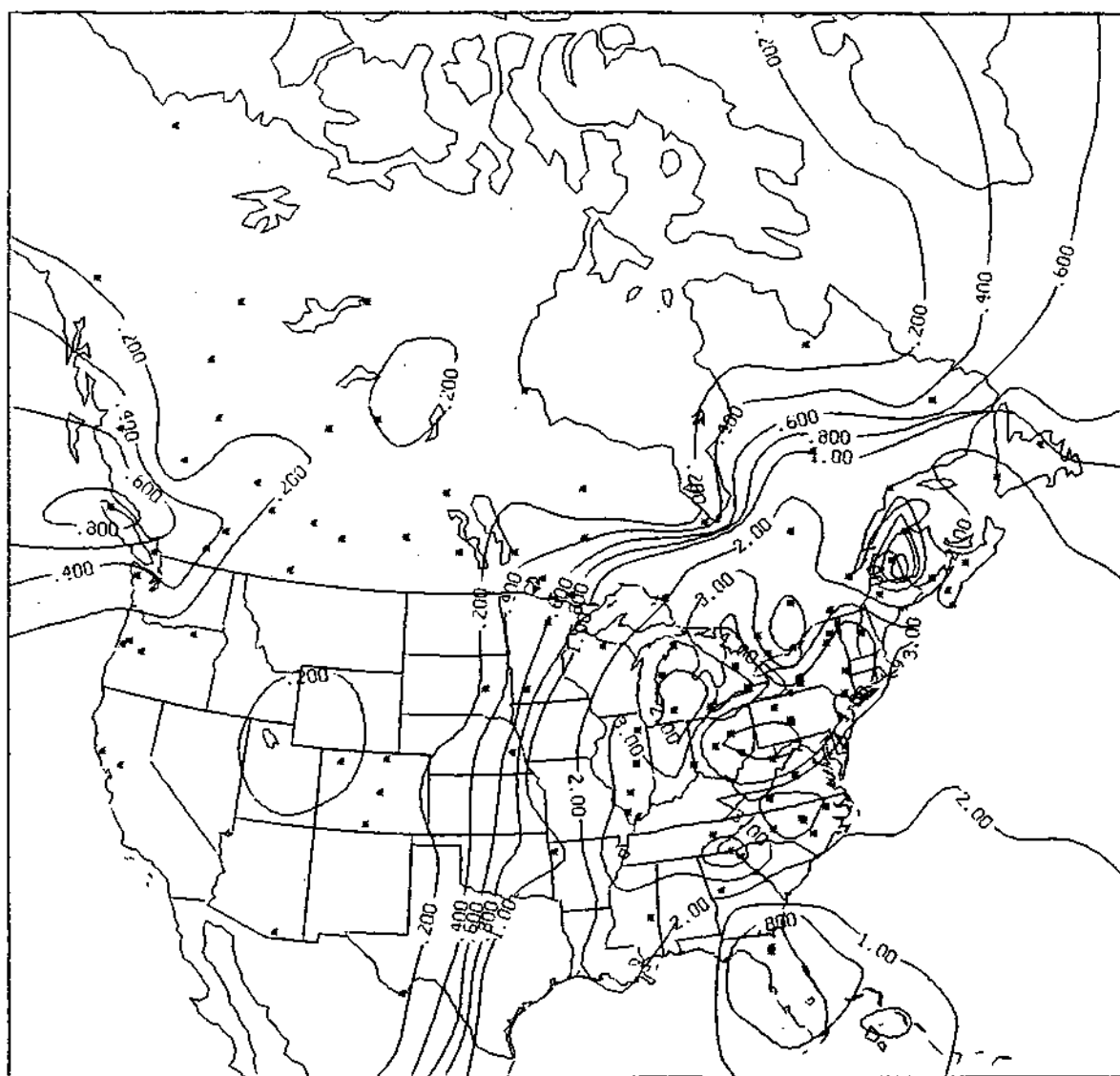
H+ DEPOSITION(UG/M\*\*2)  
NADP-CANSAP-MAP3S FALL

Figure 37. The North American average hydrogen ion deposition ( $\mu\text{g}/\text{m}^2$ ) distribution for the Fall season obtained from the CANSAP and MADP networks.



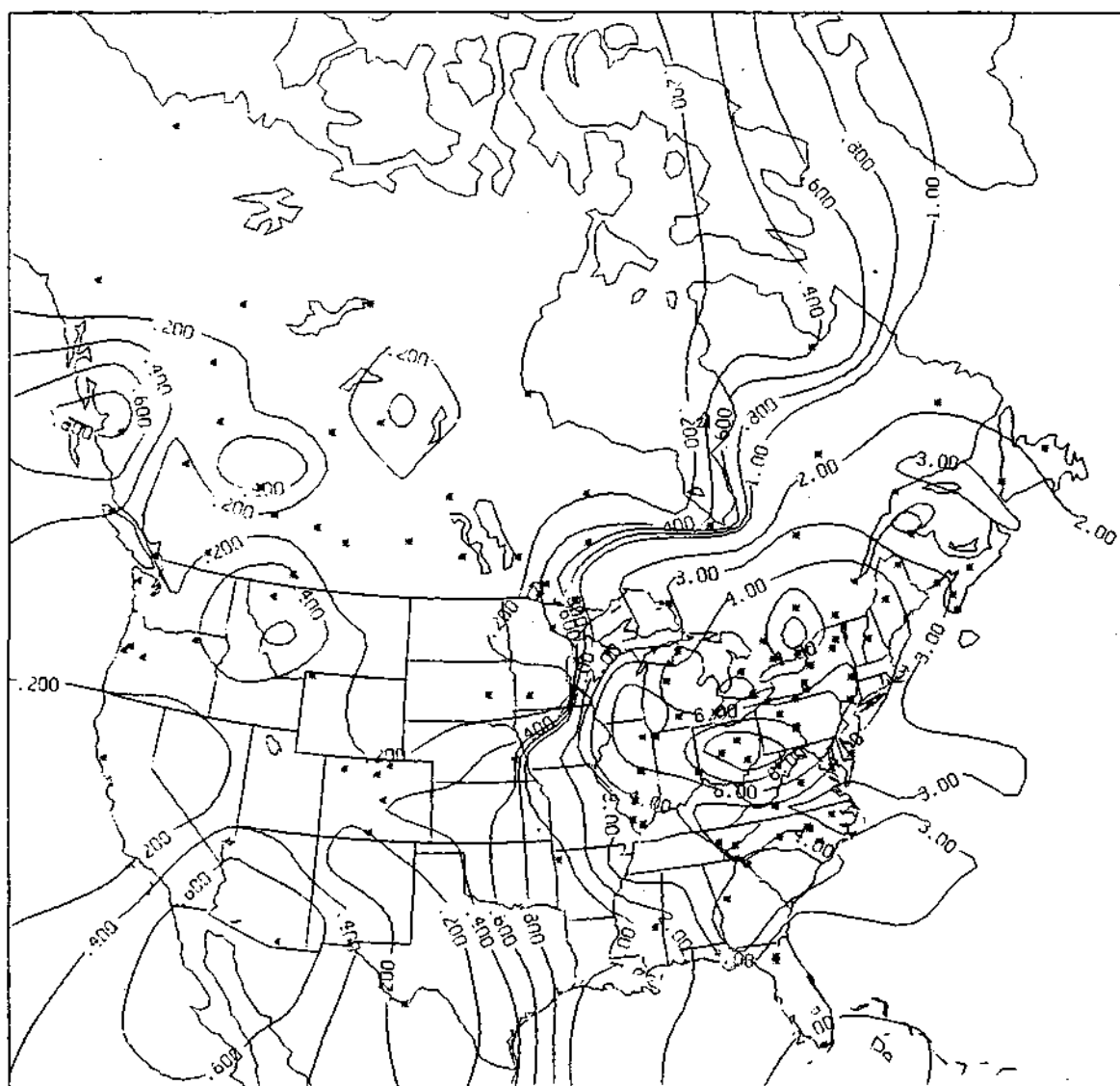
$\text{H}^+$  DEPOSITION ( $\mu\text{g}/\text{m}^2$ )  
NADP-CANSAP-MAP3S WINTER

Figure 38. The North American average hydrogen ion deposition ( $\mu\text{g}/\text{m}^2$ ) distribution for the Winter season obtained from the CANSAP and NADP networks.



H+ DEPOSITION(UG/M\*\*2)  
NADP-CANSAP-MAP3S SPRING

Figure 39. The North American average hydrogen ion deposition ( $\mu\text{g}/\text{m}^2$ ) distribution for the Spring season obtained from the CANSAP and NADP networks.



H+ DEPOSITION(UG/M\*\*2)  
NADP-CANSAP-MAP35 SUMMER

Figure 40. The North American average hydrogen ion deposition ( $\mu\text{g}/\text{m}^2$ ) distribution for the Summer season obtained from the CANSAP and NADP networks.